Rural electrification from local resources: Biomass pyrolysis oil combustion in a direct injection diesel engine

by

Alan Louis Shihadeh

B.S.M.E., University of Texas at Austin, 1989

S.M. Mechanical Engineering, Massachusetts Institute of Technology, 1994
S.M. Technology and Policy, Massachusetts Institute of Technology, 1994

Submitted to the Department of Mechanical Engineering
in partial fulfillment of the requirements for the degree of

Doctor of Science

at the

MASSACHUSETTS INSTITUTE OF TECHNOLOGY

September 1998

Author_____
Department of Mechanical Engineering
July 6, 1997

Certified by_____
Simone Hochgreb
Associate Professor, Department of Mechanical Engineering
Thesis Supervisor

Certified by_____
John B. Heywood
Professor, Department of Mechanical Engineering
Thesis Supervisor

Accepted by_____
Ain A. Sonin
Chairman, Department Graduate Committee

Rural electrification from local resources: Biomass pyrolysis oil combustion in a direct injection diesel engine

by

Alan Louis Shihadeh

Submitted to the Department of Mechanical Engineering
July 6, 1998 in partial fulfillment of the requirements
for the degree of Doctor of Science

ABSTRACT

As the production process continues to be refined, biomass pyrolysis oils are increasingly being considered as potentially feasible renewable fuels. Combustion of pyrolysis oils in diesel engines has been scarcely studied, and the few studies which have been performed indicate that these fuels exhibit excessively long ignition delay, rendering them dependant on auxiliary ignition sources for diesel engine operation. This work focuses on examining what physical and chemical processes may explain poor pyrolysis oil ignition quality, and what can be done to improve it. In addition, biomass oil combustion is characterized in relation to No. 2 diesel fuel combustion.

To investigate linkages between biomass pyrolysis production techniques and the combustion characteristics of the resulting liquids, combustion experiments with pyrolysis oils produced through two differing processes—ENSYN Rapid Thermal Process, and NREL Ablative Vortex Pyrolysis—were examined, with particular attention to the effects of the severity of thermal cracking, volatiles collection and preservation, and extent of feedstock drying. Each of these process parameters was in turn mapped to particular fuel properties, including average molecular weight, volatile species content, water concentration, and physical properties and quantified using various chemico-physical analytic methods. It was found that the NREL oil had considerably lower water content (16.9 versus 26.3 wt %) and average molecular weight (370 versus 550 g/mol) in comparison to the ENSYN oil; little difference in the atomization characteristics and volatile species profile were found.

Using a single cylinder, naturally aspirated direct injection diesel engine, it was found that the NREL pyrolysis oil ignited more readily than the ENSYN oil, though both oils exhibited excessive ignition delay and could not ignite without assistance from combustion air pre-heating. Investigation with a hydrated NREL oil whose water content equaled that of the ENSYN oil revealed that the lower water content only partially accounted for the better ignition quality of the NREL oil, and that the increased thermal cracking severity of the NREL oil accounted for the remainder.

Experimental ignition delay and heat release data were interpreted using a phenomenological spray combustion model. The results showed that the long ignition delay of the pyrolysis oils results from slow chemistry, not slow vaporization, and that pyrolysis oil combustion is predominantly kinetically-controlled, in contrast to the predominantly mixing-controlled diesel combustion. Water was found to account for 15% and 20% of the ignition delay time for the NREL and ENSYN oils, respectively. While the role of water was significant, longer ignition delay and slower combustion rates were found to be inherent to fuel chemical structure, which in turn appears to be upgraded with additional thermal cracking.

Thesis Advisors
Simone Hochgreb, Associate Professor, Department of Mechanical Engineering
John B. Heywood, Professor, Department of Mechanical Engineering

Additional Thesis Committee Members
Wai K. Cheng, Professor, Department of Mechanical Engineering
János M. Beér, Professor, Department of Chemical Engineering

ACKNOWLEDGEMENTS

it was discussed
experiments were performed
jobs were cut
phosphorous was dropped
it was thought
and things were calculated
thatched roofs correctly ignited
as shown by literature cited
the native was disappeared
the child was beaten
the bathroom was cleaned
the earth was planted
the dinner was made
it can be shown

by no one in particular

a flower broke
the hour bloomed
fields hushed
morning dewed
there was no witness and no participant:

i does not appear
we can be neglected

TABLE OF CONTENTS

Chapter 5
Analysis and Modeling

Chapter 6
Summary, Conclusions and Recommendations

Appendices

Chapter 1
Biomass Pyrolysis Oil Production, Properties and Combustion

Communities everywhere have traditionally used biomass—most often wood, but also agricultural residues such as olive pits in Palestine and sugar cane bagasse in Brazil—as fuel for various purposes from cooking to home heating to powering railroad engines. Biomass now accounts for approximately 14% of primary energy use in the world [1,2,3]. One innovation people such as the *Surga* of Senegal made in the use of bio-energy has been the practice of converting the raw material, such as wood logs, into a more convenient form such as charcoal briquettes, which burn more uniformly with less smoke and are more energetically compact [4]. The idea of converting biomass to more convenient fuel forms has taken shape in chemical (e.g. production of grain alcohol), mechanical (e.g. sunflower oil extraction), and thermal processes (e.g. charcoal production), all of which have enabled the use of biomass as fuels in new applications such as gas

---

[1] U.S. President's Committee of Advisors on Science and Technology, "Federal Energy Research and Development for the Challenges of the 21st Century," Report of the Panel on Federal Energy R&D, September 1997.
[2] Carr, E. "Energy: the New Prize," *The Economist*, v331 n7868, June 1994.
[3] Hall, D., Rosillo-Calle, F., and deGroot, P. "Biomass Energy: Lessons from case studies in developing countries," *Energy Policy*, Jan. 1982, 62-73.
[4] Rose, J.W. and Cooper, J.R. *Technical Data on Fuel, Seventh Edition*, World Energy Conference, Scottish Academic Press, 1977.

burners and internal combustion engines. Biomass pyrolysis oil fits into the last category; it is manufactured through a high temperature thermal process in which the biomass feedstock is subjected to rapid heating in the absence of air (pyrolysis), where it vaporizes, cracks, and is condensed after a short residence time.

Usually in the form of producer gas, biomass-derived fuels have often been used to run diesel engine electric power plants. The relatively high thermal efficiency, durability, ease of operation, and fuel versatility have made the diesel engine a preferred technology in many bio-energy applications, including in India, China, and Indonesia—three countries that have made extensive use of integrated biomass gasification-diesel generator systems. On the island of Java, for example, engineers at the Bandung Institute of Technology have developed integrated rice-husk gasification-diesel generators to provide electricity to run the local rice mills and to provide light for households in more than 100 rural villages [5]. While many of these integrated gasification systems have performed as designed, their utility has been hampered by the difficulty of storing or transporting the producer gas, meaning that it must be burned as it is produced [2], whether it is needed or not. This problem motivated this thesis. In particular, since biomass pyrolysis oil can be relatively easily stored and transported, and because it is produced through a process that can accept the same feedstocks as biomass gasification processes, its potential use as a diesel engine fuel was investigated. This thesis explores the possibility of burning biomass pyrolysis oils in diesel engines, with particular focus on linking combustion characteristics to pyrolysis production parameters.

1.1 Pyrolysis Oil Properties and Production

Biomass pyrolysis oil is a dark brown liquid composed of a complex mixture of oxygenated hydrocarbons and typically has a heating value approximately half that of No. 2 fuel oil. It contains significant quantities of moisture, particulates, nitrogen, alkali, and tar, and is more dense and viscous than conventional diesel engine fuels. Whereas petroleum distillates are composed primarily of pure hydrocarbons (paraffins, aromatics, naphthalenes), pyrolysis oils are typically composed of carbohydrates, organic acids, aldehydes,

[5] Interview with Dr. Robert Manurung, Department of Chemical Engineering, Bandung Institute of Technology, Indonesia

and other oxygenated organics [6,7]. Their physical properties and molecular composition vary with the pyrolysis process parameters such as reactor temperature and residence time, as well as the feedstock moisture content and particle size [8]. Table 1.1 lists some properties of sample pyrolysis oils.

A typical pyrolysis plant is depicted in Figure 1.1. After being dried typically to less than 10 wt % water, and ground into particles of typically less than 2 mm, the biomass—which consists mainly of hemicellulose, cellulose, and lignin—is fed into the high temperature, oxygen-lean atmosphere of the pyrolysis reactor, where it decomposes into vapor and char products. The vapor and char are then separated in a cyclone which recycles the char to the reactor to provide process heat. The majority of the vapor phase product exiting the cyclone condenses to form pyrolysis oil, and the remaining non-condensable gases (H_2, CO, CO_2) are re-introduced to the reactor as an additional heat input, or exported for sale. The relative proportion of gas, liquid, and solid products depends on the reaction parameters and pyrolysis method; longer residence time and higher reactor temperature allows greater thermal cracking of the vapor products, resulting in greater production of water, non-condensable gasses, and lower average molecular weight of the condensed product. Therefore slow pyrolysis at low temperature favors char production (30 wt % yield) with moderate amounts of tar by-products, while fast or "flash" pyrolysis maximizes liquid yields up to 80 wt % on a dry feed basis. Characteristic reactor residence times and temperatures of 0.2-1.5 sec and 500-650 °C are typical of high liquid-yield processes. Flash pyrolysis at temperatures above 700 °C maximizes gas yields [9]. Energy efficiencies of conversion from biomass feedstock to pyrolysis oil have been reported from 50-74%, depending on the particular process employed [10,11,12,13].

---

[6] Radlein,D., Piskorz, J., and Scott, D.S. "Lignin derived oils from the fast pyrolysis of poplar wood." *J. Anal. Appl. Pyrolysis*, 12, 51-59.

[7] Evans, R.J., and Milne, T.A. "Molecular characterization of the pyrolysis of biomass. 1. Fundamentals," *Energy & Fuels*, Vol. 1, N. 2, 1987.

[8] Evans, R.J., and Milne, T.A. "Molecular characterization of the pyrolysis of biomass. 2. Applications," *Energy & Fuels*, Vol. 1, N. 2, 1987.

[9] Scott, Donald, Piskorz, J., and Radlein, D. "Liquid Products from the Continuous Flash Pyrolysis of Biomass," *Ind. Eng. Chem. Process Des. Dev.*, 1985, 24, 581-568.

[10] McKeough, P., Nissilä, M., Solantausta, Y., Beckman, D., Östman, A., Bergholm, A., Kannel, A. "Techno-Economic Assessment of Selevted Biomass Liquefaction Processes," IEA Cooperative Project D1, Biomass Liquefaction Test Facility Project, Final Report, #DOE/NBM-1062-Vol. 5, National Technical Information Service, Springfield Virginia, 1988.

In summary, the essential features of the pyrolysis process are a high heating and heat transfer rate requiring a finely ground biomass feed, carefully controlled reactor temperature and residence time, and rapid cooling of the pyrolysis vapors to minimize production of non-condensable gases.

TABLE 1.1 Properties of sample biomass pyrolysis oils. [14]

Manufacturer	No. 2 Fuel Oil	ENSYN	U-Fenosa
Feedstock		Hardwoods	Eucalyptus
pH		2.6-3.0	2.0-2.3
Moisture [wt %]	0.05	19-37	23
HHV [MJ/kg]		13-20	16-18
LHV [MJ/kg]	42	12-18	14-17
Specific Gravity	0.8	1.18 - 1.24	1.26-1.30
Viscosity at 50 °C [cSt]	2	6-108	38-143
Solids [wt %]		0.5-6	0.7-1

1.2 Biodiesel versus biomass pyrolysis oil

In the U.S., "biodiesel" normally refers to oils which are mechanically extracted from vegetables, seeds, or nuts, and thus are distinct from biomass pyrolysis oils. They typically have heating values and Cetane numbers comparable to or better than those of light diesel fuel. They readily atomize and exhibit excellent combustion characteristics in diesel engines, and have been demonstrated in numerous applications [15]. In comparison, biomass pyrolysis oils have half the heating value of diesel fuel, are corrosive, contain suspended solids which can cause abrasive wear, have exhibited poor ignition characteristics [16], and can be highly viscous. Clearly, from a fuel quality perspective, biodiesel fuels are superior to biomass pyrolysis oils at present.

---

[11] Wan, E.I. Proceedings of the 1985 Biomass Thermochemical Conversion Contractors' Meeting, PNL-SA-13571, Pacific Northwest Laboratory, 1986, 167-192.
[12] Blaek, J. "Preliminary Evaluation of the Waterloo Fast Pyrolysis Process," BBC Engineering & Research Ltd., Markham, Ohntario, 1986.
[13] Beckman, D., Elliott, D., Gervert, B., Hörnell, K, Kjellström, B., Östman, A., Solantausta, Y., Tulenheimo, V. "Techno-economic Assessment of Selected Biomass Liquefaction Processes," Technical Research Centre of Finland, Research Reports 697, Espoo, 1990.
[14] Oasmaa, A. and Sipila, K. "Pyrolysis Oil Properties: Use of Pyrolysis Oil as Fuel in Medium-Speed Diesel Engines," *Bio-Oil Production and Utilization*, conference proceedings, 1996.
[15] Ryan, T.W., *et al.*, "The Effects of Vegetable Oil Properties on Injection and Combustion in Two Different Diesel Engines," *JAOCS*, Vol. 61, no. 10 (October 1984).
[16] Solantausta, Y., Nylund, N., Westerholm, M., Koljonen, T. and Oasmaa, A. "Wood Pyrolysis Oil as Fuel in a Diesel-Power Plant," *Bioresource Technology* 46, 1993, 177-188.

From a production standpoint, however, biomass pyrolysis oils offer some distinct advantages. First, pyrolysis oils can be produced from a very wide range of feedstocks: from bagasse to landfill refuse to wood waste from pulp and paper mills to dedicated energy crops such as switchgrass, straw, or short rotation trees [3,17]. As a result, the price of feedstocks are generally much lower than those used for conventional biodiesel such as soybeans, and can even be a "negative" cost if the feedstock is a waste stream that would normally require disposal.

Current cost estimates for soybean-derived biodiesel fuels range from $2.50/gallon to $3.50/gallon, or $19/GJ to $26/GJ [18]. Biomass pyrolysis oil production costs are expected to be many times lower, depending on the price of the feedstock. For example, a detailed study by Bridgewater and Peacocke [19] estimated that wood pyrolysis oil production costs range from $2.4/GJ to $10.8/GJ for corresponding feedstock wood costs of 0 to $120/ton dry. Similarly, Solantausta [20] compared a number of pyrolysis oil cost estimates that assumed a wood cost of $25/ton dry [21, 22, 23, 24, 25] to the Rotterdam spot market price of light fuel oil at the time the estimates were made, and found that the relative product cost of wood pyrolysis oil to light diesel fuel ranged from 0.8 to 2.7, a factor of 2 to 6 cheaper than soybean-derived biodiesel. Thus if the technical challenges to pyrolysis oil utilization can be overcome, pyrolysis oil production can provide a more flexible and economical source of renewable liquid fuels than conventional biodiesel.

---

[17] Pober, K. and Bauer, H. "From garbage—OIL," *CHEMTECH*, March 1977, 164-169.
[18] National Renewable Energy Lab "Existing Technology Options for Production of Biodiesel from Low-Cost Feedstocks," http://www.esd.ornl.gov/BFDP/BFDPMOSAIC/doedocs/94_95sum/biodisl.html
[19] Bridgewater, A.V. and Peacocke, G.V. "Engineering Developments in Fast Pyrolysis for Bio-Oils," *Proceedings Biomass Pyrolysis Oil Properties and Combustion Workshop*, September 27, 1994, Estes Park, Co. National Renewable Energy Lab.
[20] Solantausta, Y., Nylund, N., Westerholm, M., Koljonen, T. and Oasmaa, A. "Wood Pyrolysis Oil as Fuel in a Diesel-Power Plant," *Bioresource Technology* 46, 1993, 177-188.
[21] Scott and Piskorz, 1982
[22] McKeough, P., Nissilä, M., Solantausta, Y., Beckman, D., Östman, A., Bergholm, A., Kannel, A. "Techno-Economic Assessment of Selevted Biomass Liquefaction Processes," IEA Cooperative Project D1, Biomass Liquefaction Test Facility Project, Final Report, #DOE/NBM-1062-Vol. 5, National Technical Information Service, Springfield Virginia, 1988.
[23] IEA 1987
[24] Cottam, M.L. and Bridgewater, A.V. "Techno-economics of bio-oil production and upgrading," *Proceedings of Energy from Biomass Contractors' Meeting*, ed. Bridgewater, A.V. and Grassi, G. Gent, Belgium, 1991.

It should be noted that the above estimates were made for U.S., Canadian, or European industrial contexts, and that the impetus in many societies for using biomass as fuel has often been based not on technical cost estimates, but on making use of what is locally available, living within nature rather than attempting to subordinate it, and long-term ecological considerations [26, 27]. One argument that has been advanced in favor of utilizing biomass fuels is that doing so can in principle close the CO_2 loop, since the carbon released from burning biomass is fixed from the atmosphere by the growing biomass in the first place [28].

1.3 Current understanding of pyrolysis oil combustion

While there is a large body of literature addressing pyrolysis chemistry and bio-oil production spanning two decades of work, there has only recently begun a systematic effort to study the combustion characteristics of biomass pyrolysis oils, owing largely to the fact that flash pyrolysis processes have only lately made oil production for fuel a possibility.

The only published study on biomass pyrolysis oil combustion in an internal combustion engine was made by Solantausta et al in 1993 [29]. Using a naturally aspirated 0.5 liter high-speed, single cylinder, direct injection diesel engine (15.3:1 compression ratio), Solantausta compared ignition delay and burn duration data for diesel fuel, ethanol, and ENSYN wood pyrolysis oil (Table 1.2) with the engine run at a constant load of 2.5 bar brake mean effective pressure (BMEP), and 2000 rpm. It was found that the pyrolysis oil would not auto-ignite without an ignition additive, and therefore a nitrated alcohol was added in various concentrations to the pyrolysis oil. A minimum of 5 vol. % additive was required for stable engine

---

[25] Freel, B., Graham, R., Huffman, D., and Vogiatzis, A. "Rapid Thermal Processing of Biomass: Development, Demonstration, and Commercialization," Paper presented at the Institute of Gas Technology Energy from Biomass and Wastes XVI Conference, Orlando, Florida, 1992.

[26] for an indegenist perspective on 'the environment,' see for example Churchill, W. "False Promises: an Indigenist Examination of Marxist Theory and Practice," in *Since Predator Came: Notes from the Struggle for American Indian Liberation*, Aigis Publications, 1995.

[27] see also "A Basic Call to Consciousness," 1977 Address to the UN in Geneva, Switzerland, by the Haudenosaunee (Iroquois) Peoples, printed in *basic call to consciousness*, Book Publishing Company, 1991.

[28] National Renewable Energy Lab, *Biomass Power Program*, http://www.nrel.gov/research/industrial_tech/biomass2.html.

operation (typical applications for this product range from 0.1-1 vol. %), though even with 9 vol % additive, the ignition delay—the time elapsed from start of injection to start of combustion—of the pyrolysis oil was 9 crank angle degrees (CAD), compared to 6 CAD for the No. 2 fuel oil. In addition to the long ignition delay of the ENSYN pyrolysis oil, it was found to rapidly clog the pintle-type injector nozzle by coking.

The 10-90% cumulative heat release duration of 15 CAD with the ignition enhanced (9 %) pyrolysis oil was considerably shorter than the 25 CAD of the No. 2 fuel, which is partly explained by the longer ignition delay of the pyrolysis oil, which increases the rapid heat release fraction of the heat release profile by allowing more time for pre-mixing of the fuel-air charge during the delay period. CO, NO, and HC emissions were comparable for the pyrolysis and diesel fuels. Because the results were obtained with a large amount of ignition additive, it is difficult to ascertain the combustion characteristics of the pyrolysis oil, though the experiments demonstrated that it is technically possible to burn pyrolysis oil in a diesel engine. Solantausta et al concluded that the ENSYN oil would be appropriate for a pilot-ignited medium speed diesel engine, and VTT Energy and Wartsila Diesel of Finland have proceeded jointly with research in this direction, focussing on developing fuel injection equipment which can handle the corrosive and particle laden pyrolysis oils [30].

TABLE 1.2 Pyrolysis oil properties for references [19] and [22].

Reference		[19]	[22]
Manufacturer		ENSYN	NREL
S.G. at 15 °C		1.22	
Viscosity [cSt]	20 °C	128	
	25		58
	50	13	
	55		11
Ash [wt %]		0.13	
Water [wt%]		20.5	21
Elemental composition, dry [wt%]			
	C	55.5	46.5
	H	6.7	7.2
	N	0.1	0.15
	O (by difference)	37.7	46.1
HHV [MJ/kg]		17.5	18.6

[29] Solantausta, Y., Nylund, N., Westerholm, M., Koljonen, T. and Oasmaa, A. "Wood Pyrolysis Oil as Fuel in a Diesel-Power Plant," *Bioresource Technology* 46, 1993, 177-188.
[30] Gros, S. "Pyrolysis oil as diesel fuel," Wartsila Diesel International, Ltd.

Using a modified version of the Siebers and Dyer combustion bomb [31], Suppes et al [32] measured the ignition delay of several fuels, including an NREL pyrolysis oil (Table 1.2). The bomb simulated diesel engine cylinder pressure and temperature by spark-igniting a mixture of hydrogen, nitrogen, and oxygen to produce a hot gas mixture with a density similar to air (but with an oxygen concentration of 46%) prior to injecting the test fuel. The temperature of the mixture was varied from 670 K to 850 K by allowing the bomb to cool prior to injection. Suppes found that the NREL pyrolysis oil exhibited similar ignition delay to a 27 Cetane reference fuel which was tested in the same set-up.

Other relevant diesel-related experiments reported in the literature include those done with water-fuel oil emulsions, including light and heavy fuel oils. Water-oil emulsions have been investigated primarily as a means of reducing particulate and NOx emissions [33, 34, 35, 36, 37], and have also been found to generally increase thermal efficiency [38, 39, 40]. In all cases, increasing water content was found to increase ignition delay and pre-mixed heat release. Significant for this research is also the micro-explosive behavior induced by the rapid expansion of water in the oil. Because thermal diffusivities of liquids are often much higher than their mass diffusion coefficients, the outer layer of the droplet becomes depleted of lighter compounds and it assumes the boiling temperature of the heavier constituents [41]. Conduction then causes the interior portion of the droplet to approach this higher boiling temperature. If this temperature exceeds the nucleation temperature of the inner mixture, internal vaporization of the droplet

---

[31] Siebers, D.L. and Dyer, T.M. "The autoignition and combustion of coal-water slurry under simulated diesel engine conditions," *ASME Transactions*, Vol. 108, 1986, 654-660.
[32] Suppes, G.J., Rui, Y., and Regehr, E.V. "Hydrophilic Diesel Fuels – Ignition Delay Times of Several Different Blends," *SAE Paper* 971686.
[33] Wilson, R.P. "Emission Study of a Single-Cylinder Diesel Engine," *SAE Paper* 740123, 1974.
[34] Greeves, G., Khan, I., and Onion, G. "Effects of Water Introduction on Diesel Engine Combustion and Emissions," *Sixteenth Symposium (International) on Combustion*, 1976, 321-326.
[35] Andrews, G.E., Bartle, K.D., Pang, S.W., Nurein, A.M., and Williams, P.T. "The reduction in diesel particulate emissions using emulsified fuels," *SAE Paper* 880348, 1988.
[36] DeVita, A. "Multi-cylinder DI diesel engine tests with unstabilized emulsion of water and ethanol in diesel fuel," *SAE Paper* 890450, 1989.
[37] Lawson, A., and Last, A.J. "Modified fuels for diesel engines by application of unstabilized emulsions," *SAE Paper* 790925, 1979.
[38] Murayama, T., and Tsukahara, M. "Experimental reduction of NOx, Smoke, and BSFC in a Diesel Engine Using Uniquely Produced Water (0-80%) to Fuel Emulsion," *SAE Paper* 780224, 1978.
[39] Hsu, B.D., "Combustion of water-in-diesel emulsion in an experimental medium speed diesel engine," *SAE Paper* 860300, 1986.
[40] DeVita, A. "Multi-cylinder DI diesel engine tests with unstabilized emulsion of water and ethanol in diesel fuel," *SAE Paper* 890450, 1989.

can cause it to swell or, if the surface tension forces are exceeded, to rupture. Gollahalli et al [42] used high-speed photography to observe microexplosions of water-oil emulsion sprays under diesel engine conditions, results that have been observed by others using a number of methods for both emulsions and multicomponent miscible fuels [43,44,45]. Given the greater water content, expected droplet size, the wide range of component volatilities, and the presence of char particles which can act as heterogeneous nucleation sites (lowering the superheat limit [46]) in the pyrolysis oils, it entirely possible that they will also exhibit micro-explosive behavior in a diesel engine.

The most extensive combustion studies with biomass pyrolysis oils have been conducted in the Sandia single droplet, atmospheric pressure laminar entrained flow reactor [47, 48, 49, 50]. The experimental set-up employed a shear-flow droplet generator to create a stream of uniformly sized droplets (varied from 300-500 μm) which flow with the oxygen-enriched hot gases (24 mole % O_2, ~1600 K) produced by a flat flame diffusion burner located at the top of the reactor. The walls of the reactor were made of quartz to provide optical access for a high-resolution video imaging system.

Using seven different wood pyrolysis oils made by NREL under varying pyrolysis reactor conditions, and one made by ENSYN, investigators found that the droplets invariably underwent disruptions which varied

---

[41] Williams, F.A. *Combustion Theory,* 2nd edition. Benjamin/Cummings Publishing Company, 1985, p69.
[42] Gollahalli, S.R., Rasmussen, M.L., and Moussavi, S.J. "Combustion of drops and sprays of No.2 diesel oil and its emulsions with water," *Eighteenth Symposium (International) on Combustion*, The Combustion Institute, 1978, 349-360.
[43] Greeves, G., Khan, I., and Onion, G. "Effects of Water Introduction on Diesel Engine Combustion and Emissions," *Sixteenth Symposium (International) on Combustion*, 1976, 321-326.
[44] Wang, C.H., and Law, C.K. "Microexplosions of fuel droplets under high pressure," *Combustion and Flame*, V.59, N.1, 1985.
[45] Sheng, H., Chen, L., and Wu, C. "The droplet group micro-explosions in W/O diesel fuel emulsion sprays," *SAE Paper* 950855, 1995.
[46] Blander, M. and Katz, J.L. *AIChE Journal*, 21, 1975, 833-848.
[47] Wornat, M.J., Porter, B.G., and Yang, Y.C. "Single Droplet Combustion of Biomass Pyrolysis Oils," *Energy & Fuels* 8, 1994, 1131-1142.
[48] Shaddix, C.R. and Huey, S.P. "Combustion Characteristics of Pyrolysis Oils Derived from Hybrid Poplar," *Developments in Thermochemical Biomass conversion*, Conference proceedings, Banff, Canada, 1996. Conference Proceedings
[49] Shaddix, C.R., Huey, S.P., Wornat, M.J., and Davis, K.A. "Fundamental Aspects of Combustion of Biomass Pyrolysis Oils," *Biomass Usage for Utility and Industrial Power*, Conference proceedings, Snowbird, UT, 1996.
[50] Shaddix, C.R. and Tennison, P.J. "Effects of Char Content and Simple Additives on Biomass Pyrolysis Oil Droplet Combustion," *27th Symposium (International) on Combustion*, The Combustion Institute, 1998.

in intensity and timing depending on the particular fuel. In contrast, the No. 2 fuel oil drops burned quiescently throughout their lifetime. Among the NREL oils, it was found that the oils that had undergone the most severe thermal cracking in the pyrolysis process exhibited the most violent microexplosions which completely atomized the parent droplet, resulting in slightly more rapid burnout than the No. 2 fuel oil. The less severely cracked oils were found to exhibit an earlier (~40 ms vs. ~100ms) but less effective micro-explosion phase characterized as an "eruption," resulting in a partial fragmentation of the parent drop and significantly longer burnout times than with No. 2 fuel oil (~180 ms vs. 110 ms).

Because the more severely cracked oils contained more water (30 wt % vs. 21 wt %, due to secondary reactions in the pyrolysis unit), water was added to the less severely cracked oils to determine whether the water content could alone account for the difference in microexplosion severity. It was found that water addition did increase the intensity, though not enough to reproduce the violent microexplosions of the more severely cracked oils. The investigators concluded that the combination of high water content and a significant concentration of low-volatility components produced in the more severe cracking process was responsible for the more intense explosion. This is significant for the current work, because the two oils investigated have undergone different residence times in the high-temperature vapor phase, as discussed in Chapter 2. It should be noted however that because the experiments were conducted at atmospheric pressure, and with droplets that are an order of magnitude larger than expected in a diesel spray, the effects noted above will be attenuated under diesel conditions.

In summary, the literature reveals a picture of pyrolysis oil combustion which is complicated by long ignition delays, more or less rapid burn rates and varying microexplosive behavior across oils with varying impacts of water, char, and volatiles. Furthermore, it shows that considerable practical problems, including corrosivity, coking, and high viscosity, make pyrolysis oil utilization in a diesel engine problematic at present. This thesis addresses a piece of the problem, namely long ignition delay (and combustion in general), and places it in the context of what in the pyrolysis process can be changed to improve the oils from a diesel engine utilization perspective. Chapter 2 presents this task in more detail.

1.4 Nomenclature

For convenience many terms are abbreviated throughout the thesis. They are listed below.

BMEP	brake mean effective pressure
CAD	crank angle degrees
DATC	crank angle degrees after top center
DSOC	crank angle degrees after start of combustion
DSOI	crank angle degrees after start of injection
EOC	end of combustion
EOI	end of injection
Φ	fuel equivalence ratio
ID	ignition delay
IMEP	indicated mean effective pressure
IVC	inlet valve closed timing
LHV	lower heating value
PM	pre-mixed
SOC	start of combustion
SOI	start of injection
TDC	top dead center

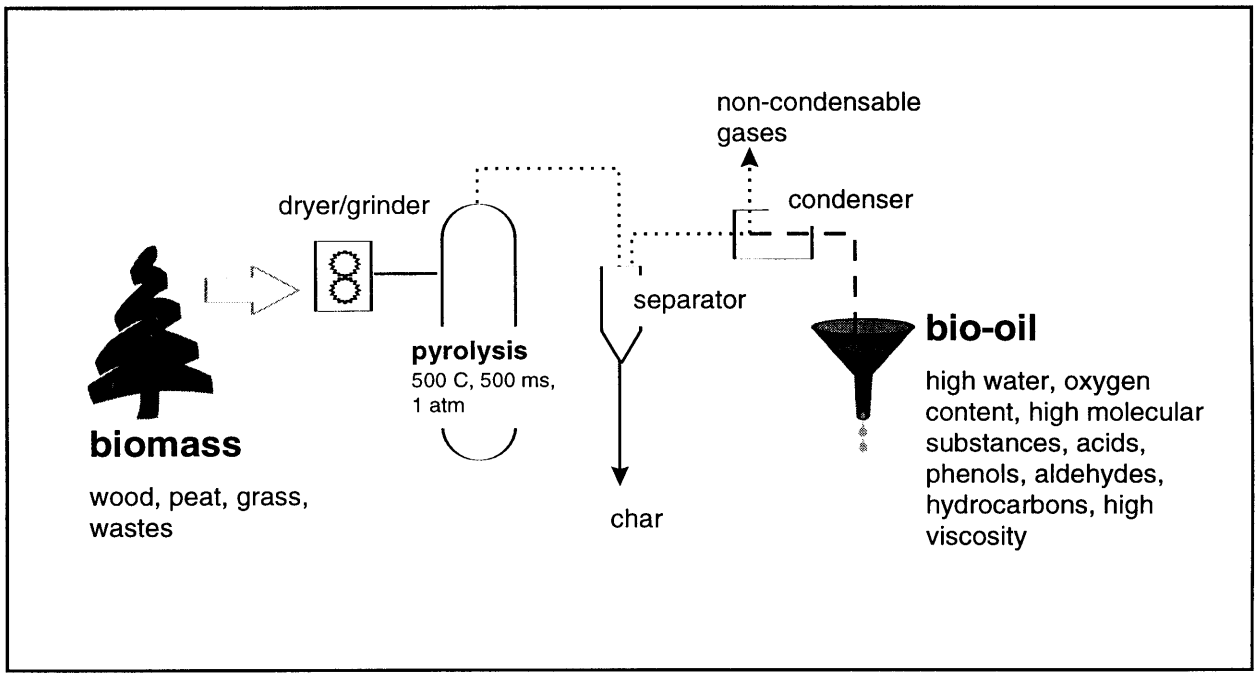

Figure 1.1 Schematic of biomass pyrolysis oil production.

Chapter 2
Research Objectives and Strategy

The purpose of this work is to characterize how the combustion of biomass oils in a high speed direct injection diesel engine differs from that of No. 2 fuel oil, and to elucidate the impact of various pyrolysis process parameters on the ignition delay of the resulting oils.

2.1 Research approach

This question was pursued by comparing the ignition delay and burn rate of diesel fuel and wood pyrolysis oils made through two widely differing processes: ENSYN Rapid Thermal Process, and NREL Vortex Ablative Pyrolysis. The ENSYN process represents the most widely implemented commercial pyrolysis technology at present. It utilizes a thermal mixer in which a high-temperature solid particulate contacts and rapidly heats the biomass feed, after which both are fed into a residence time and temperature controlled tubular transport reactor [1]. The NREL process utilizes an ablative vortex reactor in which the biomass feed is forced to slide in a helical path on the hot cylindrical wall of the reactor. The sliding contact of the biomass particles results in an ablative process in which char buildup on the particle surface is constantly

[1] Elliot, D.C., Beckman, D., Bridgwater, A.V., Diebold, J.P., Gevert, S.B., Solantausta, Y. "Developments in Direct Thermochemical Liquefaction of Biomass: 1983-1990," *Energy & Fuels*, 5, 1991, 399-410.

scraped, continually exposing fresh biomass material to the reducing atmosphere [1]. The NREL process represents a more complex experimental system which produces a low char content oil, but with lower liquid yields.

Because the NREL process employs a filtration stage prior to pyrolysis vapor condensation ("hot gas filtration") the additional residence time at the elevated temperature results in more severe cracking of the cellulosic materials, resulting in greater production of non-condensable gases (i.e. CO, H_2) and lower oil yields, but potentially an oil composed of smaller, more readily burned compounds [2]; in contrast, the ENSYN process filters the product after it has been condensed. In addition, the NREL process employs a condensation temperature of near 0 °C, in comparison to near 100 °C for the ENSYN process [3]. As a result, the NREL process may capture more volatile species. Because of these process differences, and because the initial drying of the biomass feedstock may be different, the oils can also contain different amounts of water, and exhibit differing physical properties.

Thus a comparison of the ignition delay and burn rate of the two types of oils enables a study of the diesel combustion relevance of four pyrolysis process variables, each of which maps to some quantifiable fuel 'property,' as listed in Table 2.1.

TABLE 2.1 Mapping process parameters and fuel properties

Pyrolysis process parameter	Corresponding fuel property
Severity of vapor thermal cracking	Average molecular weight
Collection of volatile species	GC Volatiles
Extent of feedstock drying	Water content
Derivative physical properties	Viscosity, surface tension, density

In sum, by comparing the ignition delay and heat release characteristics of oils produced by two widely differing pyrolysis processes, the importance of several pyrolysis process parameters can be assessed.

[2] Diebold, J.P., Scahill, J.W., Czernik, S., Phillips, S.D., and Feik, C.J. "Hot-Gas Filtration to Remove Char from Pyrolysis Vapors Produced in the Vortex Reactor at NREL," Proceedings of Specialists Workshop on Biomass Oil Properties and Combustion, Estes Park, Co., 1994, 90-109.

2.2 Research program

The overall research program evolved with the work. Following the initial set of experiments to determine how the combustion of the two oils differed with respect to one another and to diesel fuel, attention was turned to investigating what particular fuel properties (and therefore pyrolysis process parameters) could account for the observed differences. Thus the four oil properties identified above—average molecular weight, GC volatiles, water content, and physical properties—were investigated for both oil types, using chemical and physical analysis techniques described in Chapter 3. A set of experiments then followed to confirm or negate the importance of any measured differences. The overall scheme, which couples chemical analysis and combustion experiments, is given in Figure 2.1 and is discussed below.

2.2.1 Determining the significance of differences in volatile fractions

One possible reason for one pyrolysis oil igniting more readily than another is that the composition of the volatile fractions vary. For example, acetaldehyde—which has a reported autoignition temperature of 175 °C at atmospheric pressure [4]—was found by Scott & Piskorz [5] to vary in concentration from 1 to 8.5 wt % in the pre-condensed pyrolysis vapors of Poplar wood which were produced by differing methods. Furthermore, since acetaldehyde has a boiling temperature of 20 °C, even if it were produced in significant quantities, the ENSYN process would not capture it since it employs a condenser temperature close to 100 °C, in contrast to the NREL process which condenses the pyrolysis vapors close to 0 °C.

Thus using liquid and gas chromatography as described in Chapter 3, the volatile fraction of the two oils were analyzed. If the results showed that there were significant differences, a combustion experiment (Experiment B in Figure 2.1) would be carried out in which the volatile fraction of the better performing pyrolysis oil would be mixed as an "additive," or substituted altogether for the volatile fraction of the poorer performing oil. In this way, the importance of any measured volatiles differences with respect to combustion behavior could be determined directly.

---

[3] Diebold, J.P. Personal communication, January 1997.
[4] Reid, R.C., Prausnitz, J.M. and Poling, B.E. *The Properties of Gases and Liquids*, fourth edition, McGraw Hill, 1987.

2.2.2 Importance of water content

Because water affects the vaporization rate (both by increasing the heat of vaporization and potentially by affecting the microexplosive behavior, as discussed in Chapter 1), as well as the local gas temperature and specific heat, its impact on both ignition delay (and burn rate) can be significant, as will be shown in Chapter 5. Since the water content of the pyrolysis oil is affected by the extent to which the biomass feed is dried as well as the extent of thermal cracking, it was quite possible that the NREL and ENSYN oils contained different amounts of water, and that this might therefore explain combustion differences between them. Thus water was added to the lower water content oil and its impact on ignition delay and heat release recorded (Experiment C in Figure 2.1) to determine a) whether water could account for the differing combustion behavior of the two oils, and b) the impact of water in general.

2.2.3 Average molecular weight

Because pyrolysis chemistry is complex and the impact of the extent of thermal cracking on the resulting compositional profile of the oils is not well characterized, the detailed mechanisms by which this process parameter affects combustion characteristics cannot yet be determined. It is nonetheless useful to study in an aggregate fashion the impact of the degree of thermal cracking, using average molecular weight as the quantifiable surrogate. Thus by comparing the average molecular weights of the ENSYN and NREL oils, it is possible to determine whether they in fact have undergone significantly different degrees of thermal cracking (lower MW indicates greater cracking). If so, an experiment would be carried out in which the other variables were held constant or accounted for, and the combustion differences ascertained. This experiment (Experiment D) thus entailed comparing the ignition delay of the two oils whose water content was equalized by adding water to the lower water content fuel, while taking into account any residual differences in fuel properties, such as the physical properties, as discussed in Chapter 3. Any unaccounted for difference in ignition delay could then be attributed to the differences implied by the differing molecular weights.

---

[5] Scott, D.S. and Piskorz, J. "The Flash Pyrolysis of Aspen-Poplar Wood," Canadian Journal of Chemical

2.2.4 Physical properties

The surface tension and viscosity of the oils largely determine their atomization characteristics, and therefore impact the vaporization related aspects of ignition and combustion. While adding water to a particular oil reduces its viscosity (as will be shown in Chapter 3), Meier and Scholze [6] found that oils with greater molecular weight had greater viscosity, even if they had greater water content than the lower molecular weight pyrolysis oils. Therefore physical properties a) must be taken into account when water is added to an oil in the above experiments, and b) are in and of themselves important variables that are likely to vary from one oil to another. It is also possible that the high reported viscosity of pyrolysis oils in general can explain via poor atomization the longer ignition delays observed by Solantausta [7]. Thus the physical properties of the oils, in particular the viscosity and surface tension, were measured to determine whether they could account for observed combustion differences across oils, and between the oils and No. 2 diesel fuel. If the differences were found to be significant, their relevance to combustion could be assessed by varying the injected fuel temperature, since viscosity of the pyrolysis oils is steeply dependant on temperature, as shown in Figure 2.2 for a particular NREL oil [8].

Engineering, 60, 1982, 666-674.

[6] Meier, D. and Scholze, B. "Fast Pyrolysis Liquid Characteristics," EU-JOULE Program, Contract JOR3-CT95-0025.

[7] Solantausta, Y., Nylund, N., Westerholm, M., Koljonen, T. and Oasmaa, A. "Wood Pyrolysis Oil as Fuel in a Diesel-Power Plant," *Bioresource Technology* 46, 1993, 177-188.

[8] Diebold, J.P., Scahill, J.W., Czernik, S., Phillips, S.D., and Feik, C.J. "Progress in the Production of Hot-Gas Filtered Biocrude Oil at NREL," NREL document TP-431-7971, presented at 2nd EC-Canada Workshop on Bio-oil, 1995.

2.3 Research questions

In summary, the research process consisted of investigating how and why ignition delay and burn rate varied across pyrolysis oils produced by two widely differing methods, and also how they differed from diesel fuel. This was pursued by investigating whether there were differences in volatiles, water content, molecular weight, and physical properties, and whether these differences were significant from a combustion standpoint. Thus the following questions were addressed in the research:

1. How does pyrolysis oil combustion differ from that of diesel fuel?
2. Can pyrolysis process parameters significantly impact the ignition and combustion characteristics of pyrolysis oils?
    2.1. How much and through what mechanisms does water impact the ignition delay and burn rate?
    2.2. How does the pyrolysis severity impact the ignition delay and burn rate?

In the process of pursuing these guiding questions, additional ones were derived and addressed:

1. Can slow vaporization relative to diesel fuel soleley underlie the longer observed ignition delay with pyrolysis oils?
2. How do the pyrolysis oils' ignition and combustion traits compare to one another and to diesel fuel when the effect of water is removed? In particular, what are the differences in ignition chemistry and vaporization rates of the 'parent oils'?
3. Can water alone account for the slower observed heat release of the pyrolysis oils?

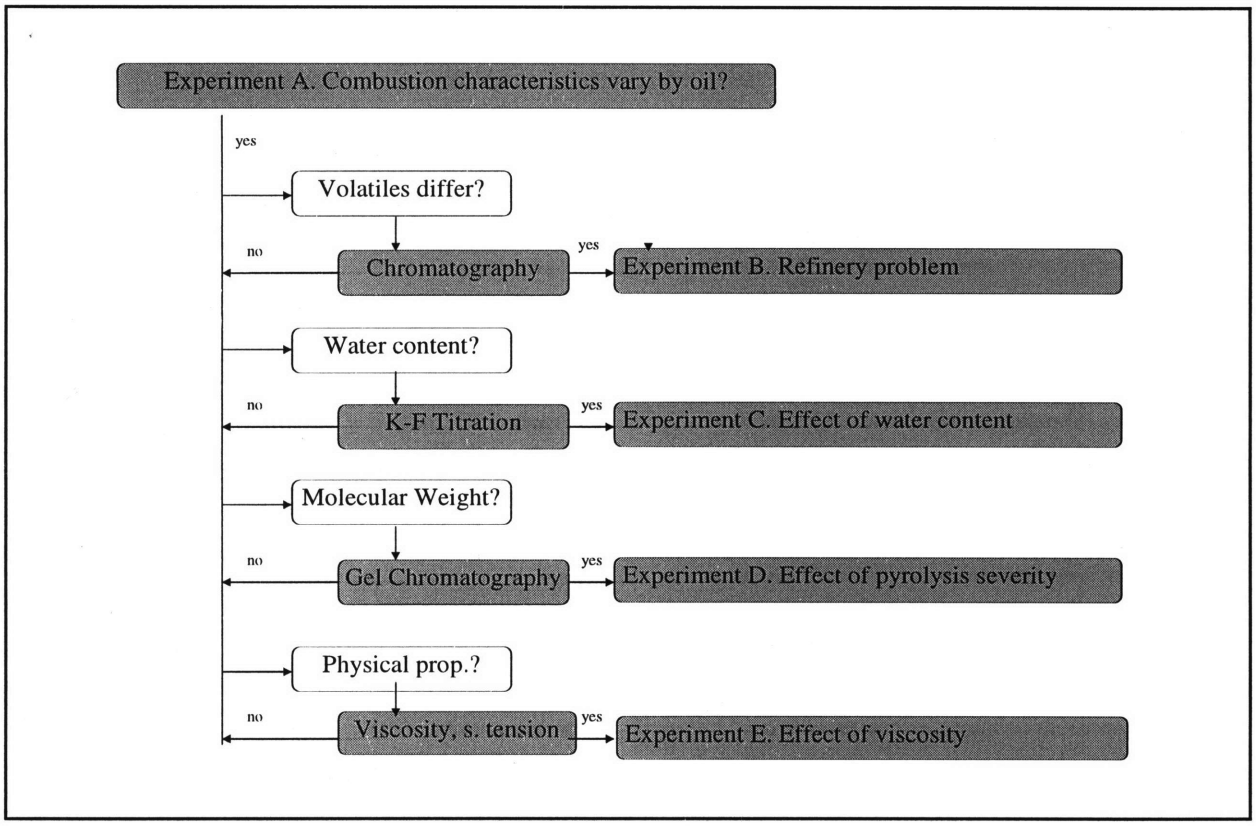

Figure 2.1 Schematic of experimental plan. Each experiment is coupled with a chemical or physical analytic test to determine whether the variable under question actually differs across oils and could therefore explain the results of Experiment A.

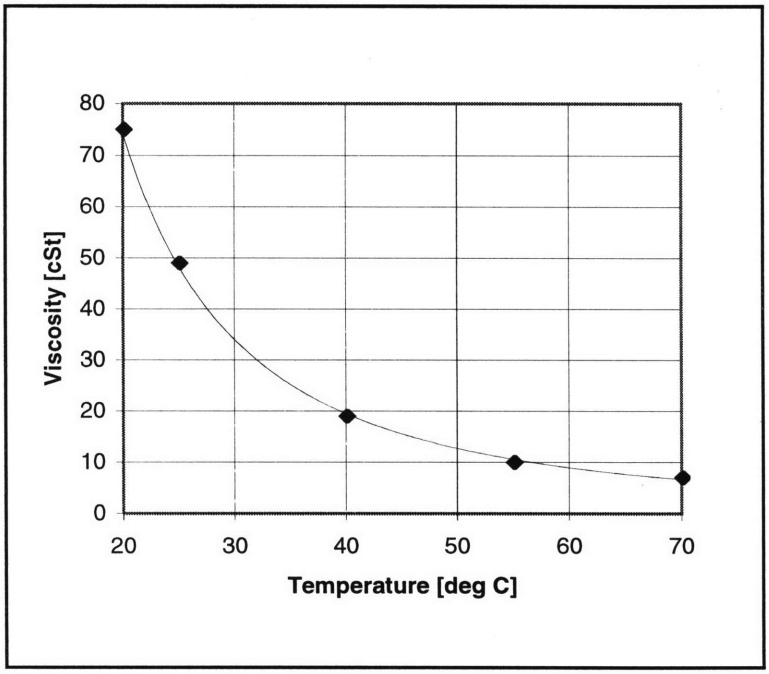

Figure 2.2 Impact of temperature on viscosity of an NREL pyrolysis oil [8]

Chapter 3
Fuel Analysis and Experimental Procedures

3.1 Fuel Analysis

3.1.1 Volatiles

Pyrolysis oils can be separated into aqueous and organic phases, of which the later—known commonly as 'pyrolytic lignin'—consists of a brown tar containing the high molecular weight compounds derived from lignin, while the aqueous fraction (accounting for 60-70 wt % of the whole oil) contains the lower molecular weight substances [1]. To facilitate analysis of the oils in conventional LC and GC equipment, it is typical to analyze the aqueous fraction alone; the phase separation is achieved by adding water to the oil.

To determine whether the lower condensation temperature of the NREL process significantly impacted the capture of volatile species, the aqueous fractions were analyzed by RTI, Ltd. of Waterloo, Ontario, Canada using liquid and gas chromatography. The liquid chromatography (HPLC) was performed to obtain quantitative data for select volatile species, while the gas chromatography (GC) was used to provide a

[1] Piskorz, J., Scott, D.S. and Radlein, D. "Composition of Oils Obtained by Fast Pyrolysis of Different Woods," in *Pyrolysis Oils from Biomass: Producing, Analyzing and Upgrading*, ed. Soltes, E.J. and Milne, T.A., ACS Symposium, 1988, 156-166.

qualitative overall comparison of the volatiles. Specifications for the HPLC and GC procedures, as well as the obtained gas chromatograms are given in Appendix A.

Table 3.1 shows the concentrations of compounds that could be identified and quantified using HPLC. More than 50% of the water solubles did not elute from the HPLC column because the molecules were too large. The higher concentrations of cellobiosan, levoglucosan, and glyoxal in the ENSYN oil indicates that it has undergone less severe thermal cracking than the NREL oil, as these are the most unstable components at high temperatures [2]. The cracking of these compounds produces mostly CO and H_2, part of the reason that increased pyrolysis reduces liquid yields. With regard, however, to the efficiency of volatiles collection in the condensation train, Table 3.1 indicates no measurable advantage of the low-temperature NREL process, particularly considering that glyoxal is the most volatile of the species recorded, and appears in higher concentration in the ENSYN oil. This is also true of the GC chromatograms which show no significant differences in volatile species across the two oils. The main peaks in the GC analysis were hydroxacetaldehyde, acetic acid, acetol, levoglucosan and a variety of phenolics (the greatest peaks were of the order of 1%).

TABLE 3.1 Species quantified using HPLC on aqueous fractions, ultimate analysis of whole oils.

Concentration [wt% dry]	NREL M2	ENSYN
Cellobiosan	0.85	1.74
Glyoxal	0.51	3.28
Levoglucosan	3.43	6.04
Hydroxacetaldehyde	5.90	7.41
Acetic Acid	7.71	7.46
Acetol	5.97	3.84

3.1.2 Water content

Water content of the oils was determined by RTI, Ltd. using Karl-Fischer titration, a technique in which a titrate is added to the sample until all of the water has been consumed, as determined by a potentiometer. Since the titrate:water proportion is fixed, the amount of titrate added is directly proportional to the amount

[2] Piskorz, J., RTI, Ltd., personal communication, April 1997.

of water in the sample. It was found that the NREL oil had considerably less water than the ENSYN oil, as shown in Table 3.2. This indicates that water content may be an important factor in explaining differences in ignition and combustion between the two fuels, as discussed below.

TABLE 3.2 Water, aqueous, pyrolytic lignin fractionation.

Fraction [wt%]	Water content	Aqueous fraction	Pyrolytic lignin
NREL M2	16.9	49.7	33.4
ENSYN	26.3	47.1	26.6

3.1.3 Molecular weight

The average molecular weight of the oils was determined through the use of gel permeation chromatography (GPC) by NREL. GPC is a size exclusion technique in which the sample solution flows through a column packed with a porous media. Components of the sample are eluted in the descending order of molecular size, and are detected using a differential refractometer.

The results showed that the NREL oil had an average molecular weight of 370 g/mol compared to 550 g/mol for the ENSYN oil, indicating that the NREL oil had undergone significantly greater thermal cracking, consistent with the HPLC results presented above. For comparison, a typical average molecular weight of No. 2 diesel fuel is 170 g/mol. These results are consistent with a recent study by Meier and Scholze [3] in which they found average molecular weights of the pyrolytic lignin fraction of an ENSYN and NREL oil to be 1637 and 896, respectively.

3.1.4 Physical properties

Surface tension and viscosity were measured in order to estimate the relative atomization quality of the pyrolysis oils with respect to diesel fuel, and to determine whether differing atomization could account for differences in ignition delay across oils and with respect to diesel fuel.

[3] Meier,D. and Scholze, B. "Fast Pyrolysis Liquid Characteristics," Federal Research Center for Forestry and Forest Products Report, 1997.

Viscosity

Kinematic viscosity measurements were taken for both pyrolysis oils, over a range of temperatures and with varying water content using a Cannon-Fenske routine type viscometer, in accordance with ASTM D 445-61. The procedure entails measuring the time taken for a given volume of liquid to flow under the force of gravity through a constricted passage from one reservoir to another. The measurements were taken with the viscometer immersed in a constant temperature oil bath, where the temperature was varied from 23 to 50 C. Water was added to the NREL oil to examine its impact on viscosity, and to examine the difference in viscosity when both the NREL and ENSYN oils had the same amount of water.

The results shown in Figure 3.1 indicated that the base NREL oil had somewhat lower viscosity than the ENSYN oil, and that water addition drastically reduced the viscosity at lower temperatures, as reported previously by Diebold et al [4]. It is important also that the viscosity of the base oils decreases rapidly with increasing temperature, resulting in diminishing differences across the tested oils. The fact that the NREL oil has lower viscosity even though it contains less water than the ENSYN oil is consistent with Meier's [5] findings that the molecular weight correlates with pyrolysis oil viscosity.

For the purpose of extrapolating viscosity beyond the measured temperature range, the data were fit to an exponential of the form $\mu = Ae^{B/T}$ where μ is viscosity, T is temperature, and A and B are empirical constants [6]. As shown in Figure 3.2, the data follow an exponential fit quite well.

Surface Tension

Surface tension was measured using a ring tensiometer, which measures the force taken to break the liquid surface into which a ring of known diameter has been submerged. The technique was verified by measuring the surface tension of distilled water. The results are given in Table 3.3, where it can be seen that diesel fuel exhibits the least and the ENSYN oil the greatest surface tension, though the differences are not great across oils.

---

[4] Diebold, J.P., Scahill, J.W., Czernik, S., Phillips, S.D., and Feik, C.J. "Progress in the Production of Hot-Gas Filtered Biocrude Oil at NREL," presented at 2nd EC-Canada Workshop on Bio-oil, 1995.
[5] Meier, 1997.

TABLE 3.3 Measured surface tension at 20 C.

Liquid	Surface Tension [mN/m]
distilled water	74.0
No. 2 diesel	29.3
NREL M2/16.9 % water	34.7
NREL M2/26.3 % water	32.2
ENSYN/26.3 % water	40.0

Atomization quality

Spray atomization is typically characterized by the Sauter Mean Diameter (SMD), which physically represents the ratio of fluid volume to surface area in a given spray, and for which have been developed a number of empirical correlations for diesel fuel injection [7]. Generally, SMD is a function of fuel viscosity, surface tension, density, injection pressure, and cylinder air density. Thus to examine the importance of the measured viscosity and surface tension differences across oils and diesel fuel, the normalized SMD with respect to diesel fuel properties was calculated for the two pyrolysis oils using the following empirically derived relation adapted from [8]

$$\frac{D_{32}}{D_{32}^*} = \left(\frac{\nu}{\nu^*}\right)^{0.385}\left(\frac{\sigma}{\sigma^*}\right)^{0.737}\left(\frac{\rho}{\rho^*}\right)^{0.737} \qquad [3.2]$$

where ν, σ, ρ, are fuel viscosity, surface tension, and density, respectively, and * indicates diesel fuel properties. Density was assumed constant at 840 and 1200 kg/m^3 for the diesel fuel and pyrolysis oils, respectively, while the viscosity was allowed to vary in accordance with the empirical fits shown in Figure 3.2. Surface tension was assumed to vary linearly with temperature [9] from the measured value at 20 C to zero at the critical temperature (assumed at 620 K, the value for decane).

As shown in Figure 3.3, the difference in predicted SMD between the base NREL and ENSYN fuels is only 5% at 24 C and decreases with increasing temperature. Also, the impact of water addition to the NREL oil (to 26.3 wt %) reduces the predicted SMD by a maximum of approximately 15% at 24 C, though the difference also diminishes with increasing temperature. The predicted normalized SMD decreases with

[6] Fox, R.W. and McDonald, A.T. *Introduction to Fluid Mechanics*, Wiley and Sons, 1985, 685-688.
[7] For a compilation, see Hiroyasu, H. "Diesel Engine Combustion and Its Modeling," *in Diagnostics and Modeling of Combustion in Reciprocating Engines*, COMODIA, 1985, 53-75.
[8] Elkotb, M.M. "Fuel Atomization for Spray Modeling," *Prog. Energy Comb. Sci*, 8, 1982, 61.

temperature because the viscosity of the pyrolysis oils is more steeply dependent on temperature than is diesel fuel, as shown above.

To estimate the temperature of the fuel in the nozzle, and therefore the expected SMD*, the heat transfer from the nozzle to the fuel was calculated (Appendix B), showing that the fuel would exit the nozzle at the same temperature as the nozzle itself. (To determine the average residence time of the fuel in the nozzle, the volume of the flow passages were measured from a machined nozzle cross-section.) The nozzle temperature is usually assumed to be the same as that of the head surface [10], which for a 13.5 CR DI diesel engine operating at 2400 rpm with 85 C coolant temperature has been measured to vary from an average of 195 to 250 C, depending on the location of the measurement and the engine load [11]. Other related references to nozzle or fuel temperature include Bosch [12], which lists the maximum nozzle temperature as 270 C, and the SAE literature which refers to fuel exiting the diesel injector nozzle at temperatures greater than 100 C [13]. Finally, using Frank's [14] formulation for effective cylinder temperature based on piston temperature measurements for varying load and speed with a DISC engine, an effective wall temperature of 200 C is calculated for the current experimental conditions. Taken together, the available data indicate that the temperature of the fuel exiting the nozzle will likely be well above 100 C, which means that the differences in SMD between the ENSYN and NREL oils will be negligible, as shown to Figure 3.3, and both oils with exhibit an SMD of no more than 1.3 times that of diesel fuel.

3.1.5 Conclusions and experimental plan

Table 3.4 provides a summary of the results given in the preceding sections. As discussed, it has been found that a) the volatile fraction is not measurably affected by the differing condensation methods of the NREL and ENSYN processes, b) that the water content of the two oils is significantly different, c) that the

---

[9] Fox and McDonald, 1985.
[10] Akinyemi, O.C., Cummins Engine Company, personal communication.
[11] Hoag, K.L. "Measurement and Analysis of the Effect of Wall Temperature on Instantaneous Heat Flux," SAE Paper 860312, 1986.
[12] *Diesel Fuel Injection*, Robert Bosch GmbH, 1994.
[13] Kesling, H.S., Liotta, F.J., and Nandi, M. "The thermal stability of a peroxide-based cetane improvement additive," SAE Paper 941017, 1994.
[14] Frank, 1989.

molecular weight (and therefore extent of thermal cracking) differs substantially, and d) that the predicted Sauter Mean Diameter does not significantly differ by oil at the relevant injection temperatures.

TABLE 3.4 Summary of fuel analysis. SMD normalized by diesel fuel value at same conditions.

Fuel property	NREL M2	ENSYN	Diesel fuel
Water content [wt %]	16.9	26.3	-
Average MW [g/mol]	370	550	170
SMD* at 140 C	1.2	1.2	1
LHV [MJ/kg]	17.0	16.3	44
LHV stoich mixture [MJ/kg]	2.28	2.46	2.79
A/F stoich	6.45	5.62	14.5
Whole oil ultimate analysis [wt% dry]			
C	58.25	57.95	87
H	7.40	7.23	13
N	1.52	1.64	-
O (by difference)	32.83	33.19	-
Aqueous fraction composition [wt % dry]			
Cellobiosan	0.85	1.74	
Glyoxal	0.51	3.28	
Levoglucosan	3.43	6.04	
Hydroxacetaldehyde	5.90	7.41	
Acetic Acid	7.71	7.46	
Acetol	5.97	3.84	

Thus of the four hypotheses examined, only two—water content and molecular weight—remained plausible with respect to variations in ignition delay and heat release. It should be noted that molecular weight is actually a lumped parameter which includes molecular composition and all the derivative thermo-chemical properties, and is therefore not a parameter with unique implications. It does, however, serve well as an index of the sum of effects which derive from varying thermal cracking in the pyrolysis plant; if it is found that the extent of thermal cracking leads to important combustion differences, the underlying phenomena can be investigated in more detail. For this thesis, however, it is only important to determine to what extent variations in thermal cracking (within expected limits) affects the ignition delay.

Given the results, engine experiments were performed with a) diesel fuel to establish a baseline, b) NREL pyrolysis oil (M2-10), c) ENSYN pyrolysis oil (RTP 15TPD), and d) hydrated NREL oil (M2-10+) such that its water content equaled that of the ENSYN oil. Apart from comparing the combustion

characteristics of the base oils, the hydrated NREL runs allowed an assessment of a) the importance of water content for a given oil, and b) the role of molecular weight, all else (volatiles, atomization, water content) being equal. Table 3.5 summarizes the experimental plan which emerged from the fuel analysis findings. Maximum break torque (MBT) injection timing was used for all cases, which means that the injection timing was varied by fuel type and operating condition such that the maximum torque was obtained for a given fuel flow rate, as would be done in a real application. The relatively high speed of 2400 RPM was chosen because it represents the more difficult operating condition which would be required of automotive and truck applications, and because it is a synchronous speed for AC power generation. Lower engine speeds are generally easier to attain with low quality fuels because of the greater residence time available for ignition and combustion. Ideally, it would be best to examine the pyrolysis oils under a range of engine speeds, though, because of the difficulties caused by the severe erosive and deposit forming tendencies of the oils, tests for more than one operating speed would have been excessively onerous. The following section presents the combustion experiments and analysis methods in more detail.

TABLE 3.5 Experimental matrix.

Fuel	IMEP [bar]	Air Temp [C]	Speed [rpm]	Timing
No. 2 Diesel	5.0	25-120	2400	MBT
ENSYN	5.0	25-120	2400	MBT
NREL	5.0	25-120	2400	MBT
NREL + water	5.0	25-120	2400	MBT

3.2 Combustion Experiments

3.2.1 Engine

Table 3.6 shows the relevant characteristics of the single cylinder, direct injection diesel engine used in this study. The engine employs a toroidal bowl in the piston to achieve rapid fuel air mixing and is naturally aspirated. Its bore/stroke ratio and operating speed range is typical of modern light-duty diesel engines, which generally require more stringent fuel specifications than medium or low-speed diesel engines because there is less time available to complete the combustion event. The fuel injection system utilizes a Bosch Type A in-line fuel pump and a hole-type injector nozzle which opens at 250 bar; the fuel pump delivers a maximum pressure of 600 bar. The injector timing is varied by rotating the fuel pump relative to the crank shaft through the use of a remote controlled electric actuator. The combustion air inlet temperature can be pre-heated up to 130 C through the use of an inline electric heater, which allows experimentation with fuels that have long ignition delay without relying on any ignition additives. The engine was coupled to a load and speed controlled dynamometer for motoring and load provision.

TABLE 3.6 Engine specifications.

Model	Ricardo Hydra Mark 4
Cylinders	1
Bore [mm]	80.26
Stroke [mm]	88.9
Swept volume [liters]	0.4498
Compression ratio	19.8
Aspiration	natural
Rated speed [rpm]	4500
Water outlet temperature [C]	85
Oil outlet temperature [C]	85
IVO/IVC [DATC]	-10/221
EVO/EVC [DATC]	122/11
Injector nozzle	4 hole x 0.21mm dia x 155 deg cone angle
Opening pressure [bar]	250

All experiments were performed at 5.0 bar IMEP and 2400 rpm, while the combustion air temperature was varied to obtain the ignition delay dependence. This load condition was chosen such that experiments with low LHV fuels could operate at the same load (and approximately the same chemical energy input per

cycle) as diesel fuel without increasing the fuel injection system capacity. This is realistic in a real application where pyrolysis oil is being substituted for diesel fuel.

3.2.2 Special considerations

Because the pyrolysis oils contain significant amounts of char and are known to polymerize when exposed to high temperatures [15], several modifications to the fuel injection system were necessary to obtain reliable engine operation during the experimental runs. The primary hindrance to continuous operation was the abrasive wear of the fuel pump plunger-barrel assembly and injector nozzle caused by the char, as well as the apparent *in situ* growth of solid particles larger than could be traced to the parent fuel. As is typical with in-line diesel injection pumps, the fuel is continuously cycled through the pump to provide cooling, while a small fraction of the internal flow is delivered to the injector. Stainless steel mesh filters (40 micron) were installed in the circulation loop to capture particles formed within the system, in addition to pre-filtering the oils in a batch method with a separate pressurized filtration rig employing a 10 micron paper element automotive type oil filter. As a further measure, the fuel injector spill return, which is normally reintroduced to the fuel pump, was diverted to an external reservoir, since it was thought that much of the particulate formation occurred within the hot environment of the fuel injector body.

In addition to these modifications, the fuel system was configured to allow on-line switching between diesel, nitrate-enriched ethanol, and the pyrolysis oils, so that the fuel pump and injector could be flushed with ethanol between data collection (typically every 15 minutes) to prevent gumming, and also to reduce scaling of the combustion chamber surfaces, since alcohol is an effective detergent for pyrolysis oil. Furthermore, since diesel fuel and pyrolysis oil are not miscible, ethanol, which is miscible in both, was used as an intermediary when switching from diesel fuel (which was used to warm the engine) to pyrolysis oil. At the end of each experiment, the engine was run for 30 minutes with ethanol, and then switched to diesel fuel for an additional 20 minutes before shut-down. Because ethanol has poor lubrication and ignition properties, Lubrizol 9520A additive was used (0.1 vol %) for lubricity, and di-ethylhexylnitrate

[15] Czernik, S. "Storage of Biomass Pyrolysis Oils," proceedings *of Biomass Pyrolysis Oils Properties and Combustion Meeting*, NREL, September 1994.

was added (15 vol %) to ensure good ignition at all operating conditions. The Lubrizol additive was also used with the pyrolysis oils.

This operational procedure and fuel filtering scheme was chosen after several design iterations and pump failures. Even with these measures however, engine operation could only be sustained with reasonable performance for approximately 6 hours, after which the pump required over-hauling, and the nozzle required replacement. Thus to ensure consistent data and engine performance across tests, the pump was overhauled and the nozzle replaced after each day's runs (typically less than 3 hours on pyrolysis oils). A schematic of the fuel delivery system is shown in Figure 3.4.

Compounding the fuel injection problems was the buildup of carbon deposits in the combustion chamber and exhaust valve and port, as shown in the photographs in Figures 3.5 and 3.6, which were taken after approximately 14 hours of running on the NREL and ENSYN pyrolysis oils, after which the intake valve seized in the valve guide and was struck by the piston. Thereafter, the head, valves, and piston were removed and cleaned, the cylinder wall scraped clean, and the valves re-seated at the end of each day's experiments. Clearly, this is not a desirable mode of operation in any practical situation, though it did allow repeatable combustion measurements to be taken. It was noted that the ENSYN oil built up deposits much more rapidly than the NREL oil, though neither oil would be acceptable in a real application.

3.2.3 Cylinder pressure and needle lift measurement

Cylinder pressure was measured using a flush-mounted Kistler 6125 piezo-electric transducer located near the center of the head. The transducer was connected to a Kistler model 504 dual mode charge amplifier. The voltage output of the amplifier was sampled using a PC based data acquisition system using a Data Translation A/D card at a rate of 2.5 points per crank-angle degree. The pressure signal was indexed to bottom center with a 2 volt spike inserted into the signal at the appropriate time by a 360 pulse-per-revolution optical shaft encoder. Normally cylinder pressure and all other instantaneous data are taken using the shaft encoder as the clock, yielding an accurately crank-angle-indexed measurement. In this case, however, it was found that the 1 CAD resolution of the shaft encoder was not sufficient to capture the

details of the cylinder pressure traces, and therefore the internal computer clock was used to trigger the data acquisition; the data was indexed to crank angle by assuming constant engine speed between BDC marks for each cycle. The reference pressure was chosen at BDC to equal 1 atmosphere, since the diesel engine is not throttled and the piston velocity near BDC is small.

To check the validity of pressure measurement, it is standard to examine log-P versus log-V plots of motored traces to ensure linearity of the compression and expansion strokes, that they meet at a sharp point at TDC, and that the polytropic compression exponent falls between 1.24 and 1.35 [16, 17]. Curvature in the compression or expansion strokes near TDC normally indicates erroneous clearance volume, while near BDC curvature indicates erroneous reference pressure. Curvature in the center portion of the compression and expansion usually indicates that the pressure data itself is faulty (charge leakage, thermal effects, or a faulty amplifier). If the data is not properly phased, this will be indicated by either the compression and expansion strokes crossing before TDC (if pressure is retarded with respect to volume), or coming together in a curve rather than a sharp point (if the pressure is advanced) [18]. A log-log plot of a motored pressure trace taken with the experimental set-up is shown in Figure 3.7. Its polytropic compression exponent is 1.30, and the linearity of the compression and expansion strokes, and their sharp intersection indicates that the measurement method is correct. It should be noted that earlier runs with a Kistler type 6121 transducer gave erroneous data due to the build-up of carbon deposits in a clearance groove between the transducer tip and body during experiments, resulting in thermal and mechanical interference in its operation. The tip and body of the model 6125 transducer are seamless, and therefore it does not have this problem.

Injector needle lift was measured using a Hall-effect proximity sensor which was designed and machined into the fuel injector by Wolff Controls Corp. The sensor was connected to a signal conditioner, also provided by Wolff Controls, which delivers a differential voltage signal proportional to needle lift. Needle

---

[16] Lancaster, D.R., Krieger, R.B., and Lienesch "Measurement and Analysis of Engine Pressure Data," SAE Paper 750026, 1975.
[17] "Acquisition and Analysis of Cylinder Pressure Data Recommended Procedures," Ford Motor Company Standard, 1992.
[18] Lancaster, 1975.

lift data was recorded simultaneously with cylinder pressure using the same acquisition system; an example needle lift and cylinder pressure trace is shown in Figure 3.8.

3.2.4 Heat release and ignition delay analysis

The heat release analysis used in this study was adapted for diesel combustion from the SI code developed by Cheung [19], and originally formulated by Gatowski [20], Chun and Heywood [21] and Stenderowicz [22]. The program utilizes a First Law single-zone treatment of the combustion chamber contents assuming perfect gas relations, as given in Equation 3.1, which has been simplified here by ignoring the effect of crevices:

$$\frac{dQ_{rel}}{d\theta} = \frac{\gamma}{\gamma - 1} p \frac{dV}{d\theta} + \frac{1}{\gamma - 1} V \frac{dp}{d\theta} + \frac{dQ_{ht}}{d\theta} \qquad [3.1]$$

where Q_{rel} and Q_{ht} are the energy release by combustion, and the heat transfer to the chamber walls, respectively. p and V are cylinder pressure and volume, respectively, while γ is the effective ratio of specific heats. The program uses semi-empirical relations for determining heat transfer, residual fraction, effective wall temperature and crevice gas losses. Before and after combustion, the effective specific heat ratio is a linear function of average cylinder temperature, and a look-up table based on fuel equivalence ratio and fuel type is used to determine the appropriate empirically derived constants. During combustion the specific heat ratio is assumed to remain constant, and is also determined from an empirical look-up table. A transition period of 10 CAD at the beginning and end of combustion allows the value of the specific heat to change from one phase to the next without discontinuities. See Cheung [19] for error analysis.

---

[19] Cheung, H.M. *A Practical Burn Rate Analysis for Use in Engine Development and Design*, S.M. Thesis, M.I.T., 1993.
[20] Gatowski, J.A., Balles, E.N., Chun, K.M., Nelson, F.E., Ekchian, J.A. and Heywood, J.B. "Heat Release Analysis of Engine Pressure Data," SAE Paper 841359, 1984.
[21] Chun, K.M. and Heywood, J.B. "Estimating Heat-Release and Mass of Mixture Burned from Spark Ignition Pressure Data," *Combustion Science and Technology*, 54, 1987, 133-144.
[22] Stenderowicz, M.L. and Heywood, J.B. "Cycle-to-Cycle IMEP Fluctuations in a Stoichiometrically-Fueled SI Engine at Low Speed and Load," SAE Paper 902143, 1990.

Several changes were made in the program for the purposes of this study. First, since with a diesel engine the fuel and air are not pre-mixed during compression, the compression phase γ was assumed to be that of air, as formulated by Frank [23]. Fuel injection was accounted for by allowing the cylinder mass to increase incrementally during each time step from SOI to EOI, which are determined internally from the needle lift traces as the times at which the needle lift reaches 10% of the maximum. During combustion, γ was specified as 1.28, which corresponds to the value found by Chun and Heywood [24] for gasoline combustion at stoichiometric conditions. Frank [25] showed that the calculated heat release was not greatly impacted by varying the combustion specific heat ratio from 1.28 to 1.32, a range covering a fuel equivalence ratio range from 0.4 to 1.2, and, assuming that combustion in a diffusion flame occurs predominantly at an equivalence ratio close to 1, chose a value of 1.28 for his investigation of a stratified charge engine. After combustion, γ was specified as a function of cylinder temperature and fuel equivalence ratio based on Chun and Heywood's published constants for lean mixtures, as formulated by Frank. Finally, ignition delay was calculated in the program as the time elapsed from SOI to the time at which the instantaneous heat release rate reached a value of 5% of the peak release.

[23] Frank, R. *Sources of Unburned Hydrocarbon Emissions from a Direct-Injection Stratified Charge Engine*, PhD Thesis, MIT Department of Mechanical Engineering, 1989.
[24] Chun and Heywood, 1989.
[25] Frank, 1989.

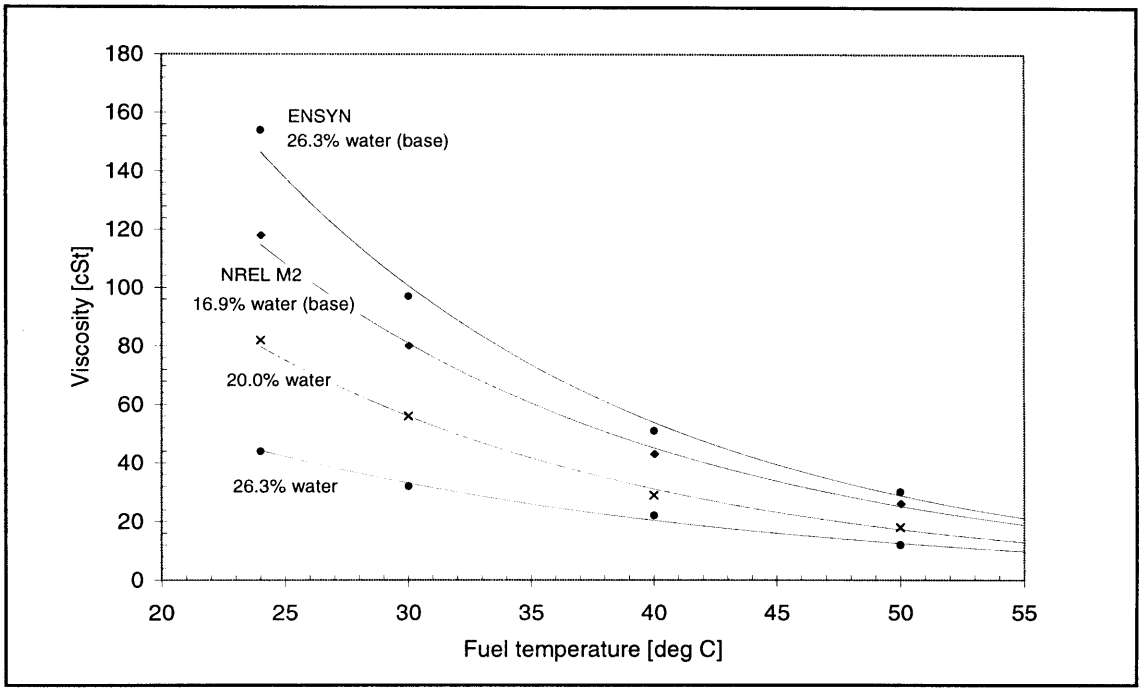

Figure 3.1 Measured kinematic viscosity for ENSYN and NREL oils. Impact of water content examined with NREL oil by adding water to base oil. Results reported are average of 5 points at each temperature, repeatable to +/- 5%.

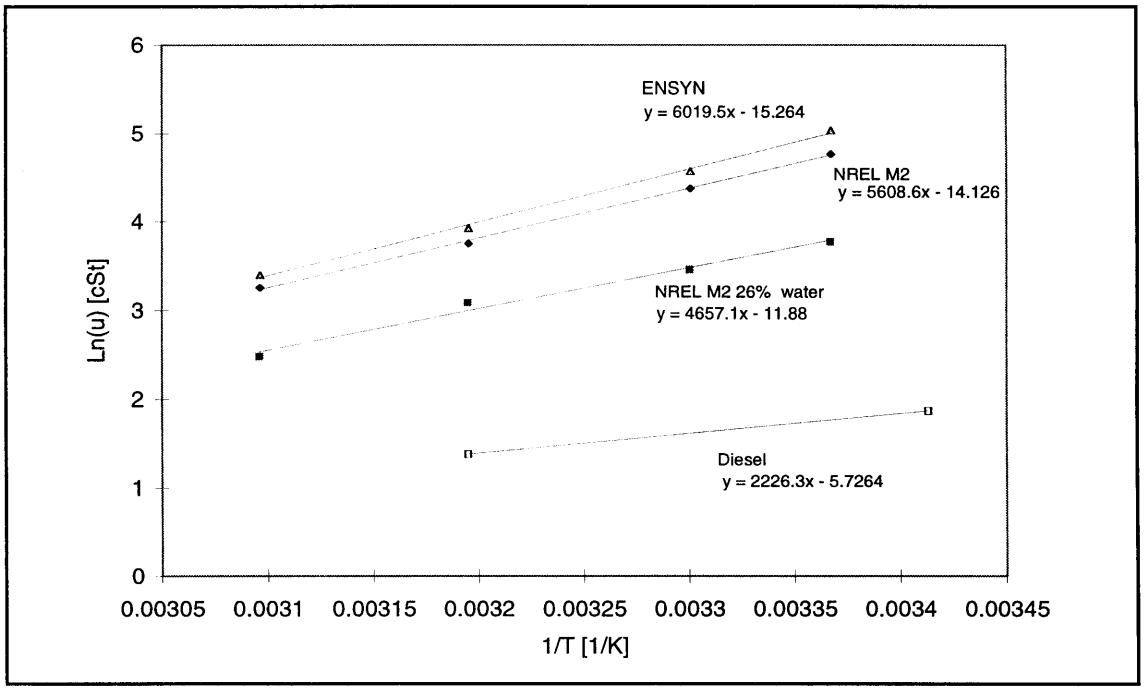

Figure 3.2 Natural log of viscosity versus 1/T.

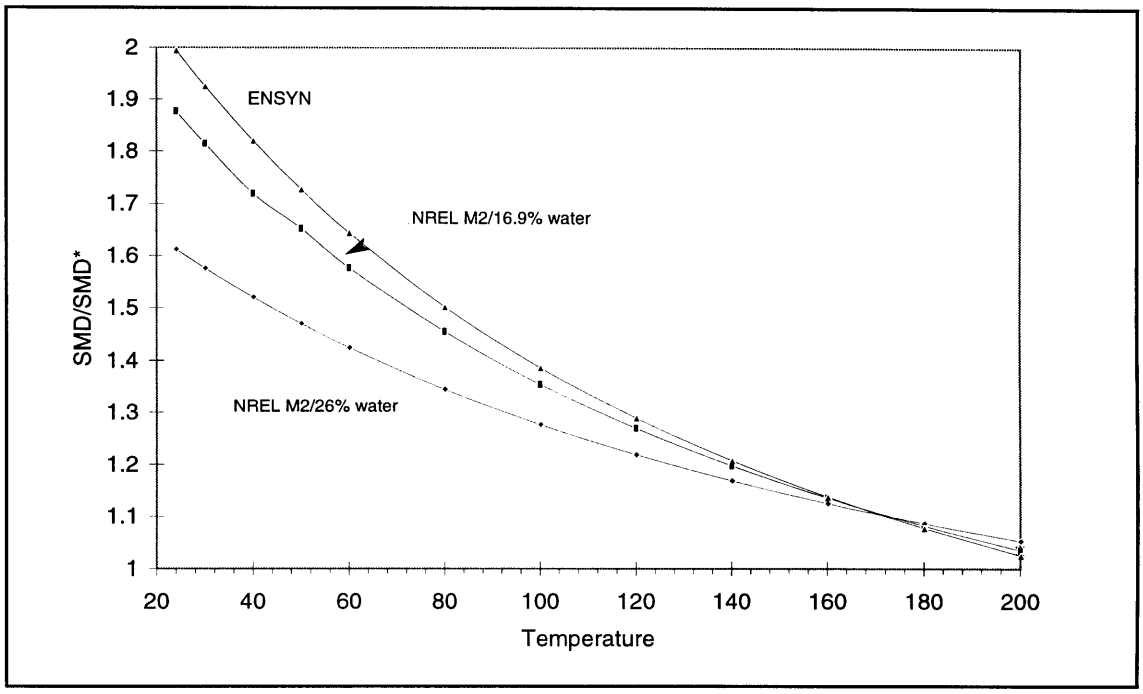

Figure 3.3 Predicted Sauter Mean Diameter versus oil temperature. Values normalized by predicted diesel fuel SMD at the same temperature.

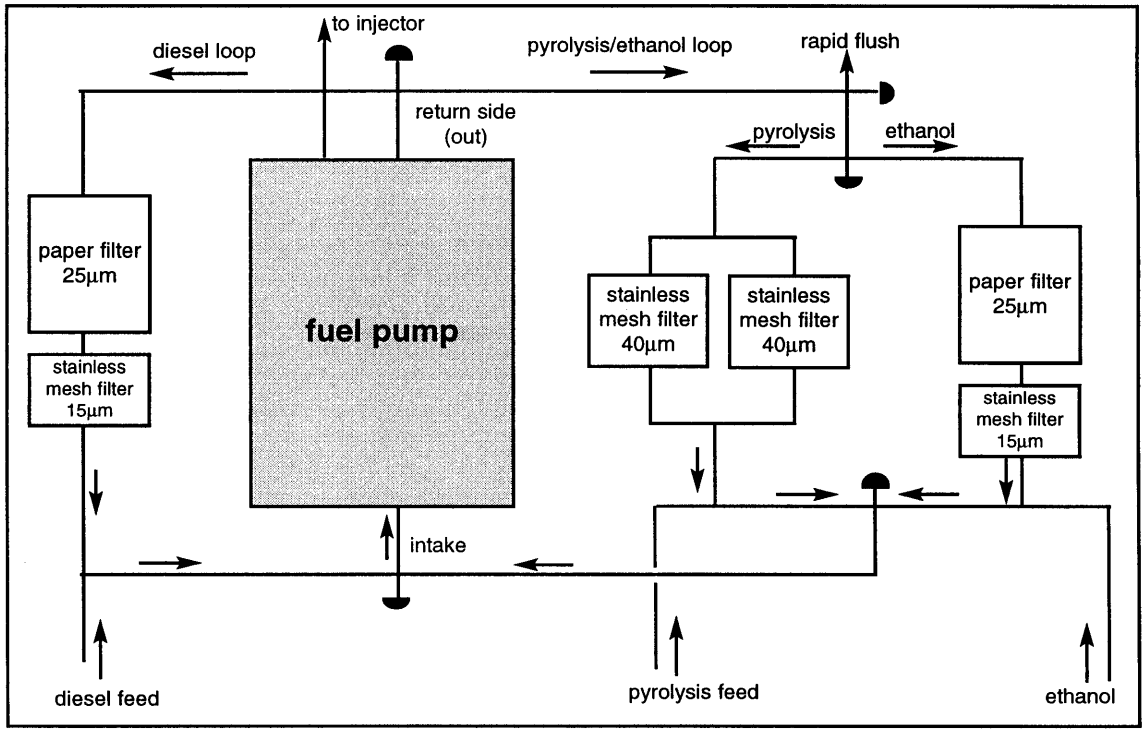

Figure 3.4 Schematic of experimental fuel delivery system.

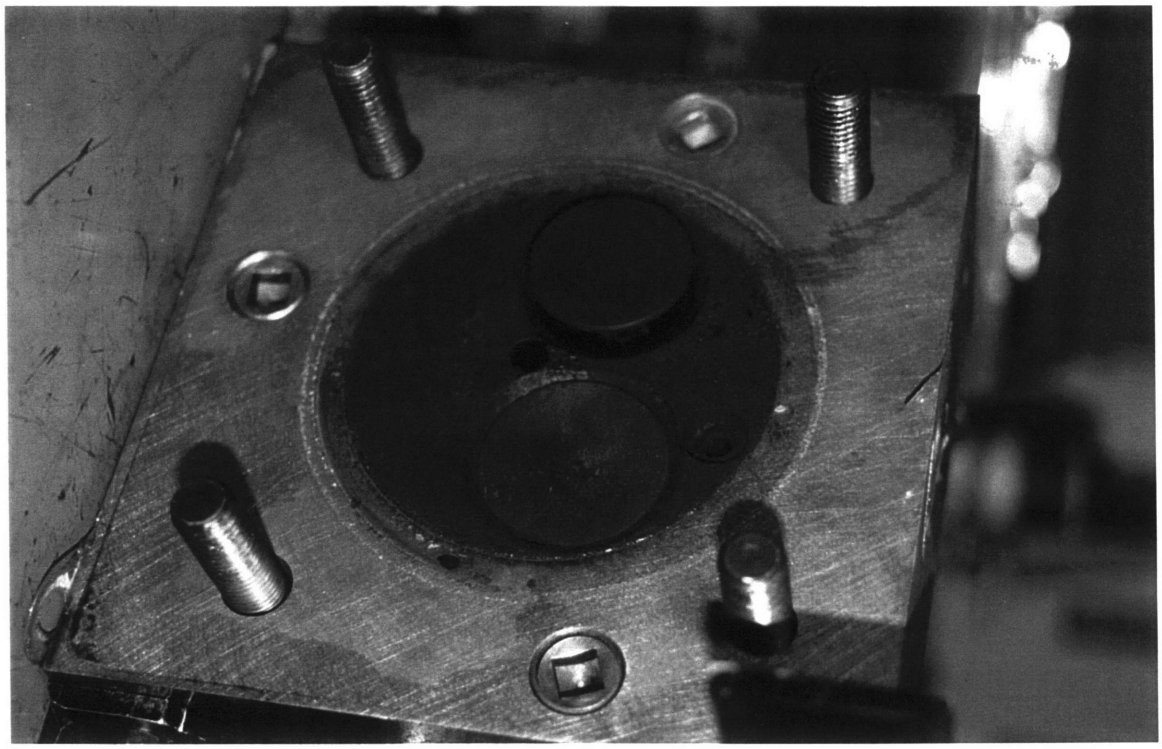

Figure 3.5 Deposits on cylinder head after 14 hours of pyrolysis oil operation.

Figure 3.6 Deposits on piston and cylinder liner after 14 hours of pyrolysis oil operation.

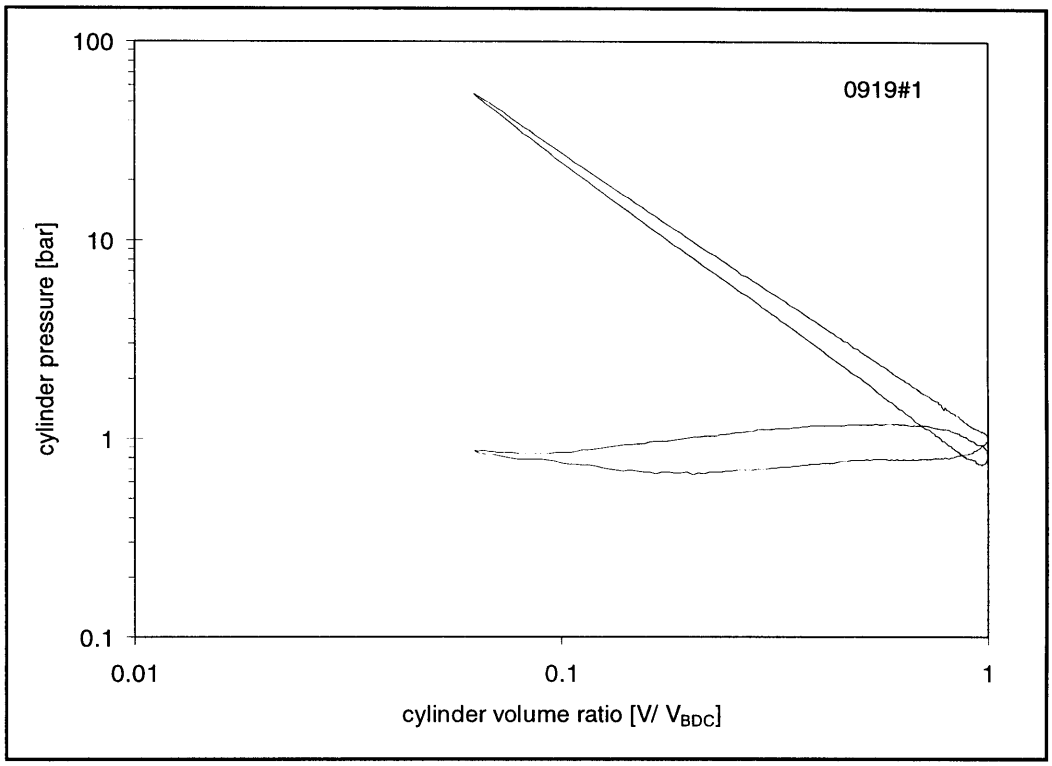

Figure 3.7 Log-P versus Log V plot of a motored pressure trace. Polytropic compression exponent equals 1.30. Data taken at 2400 RPM.

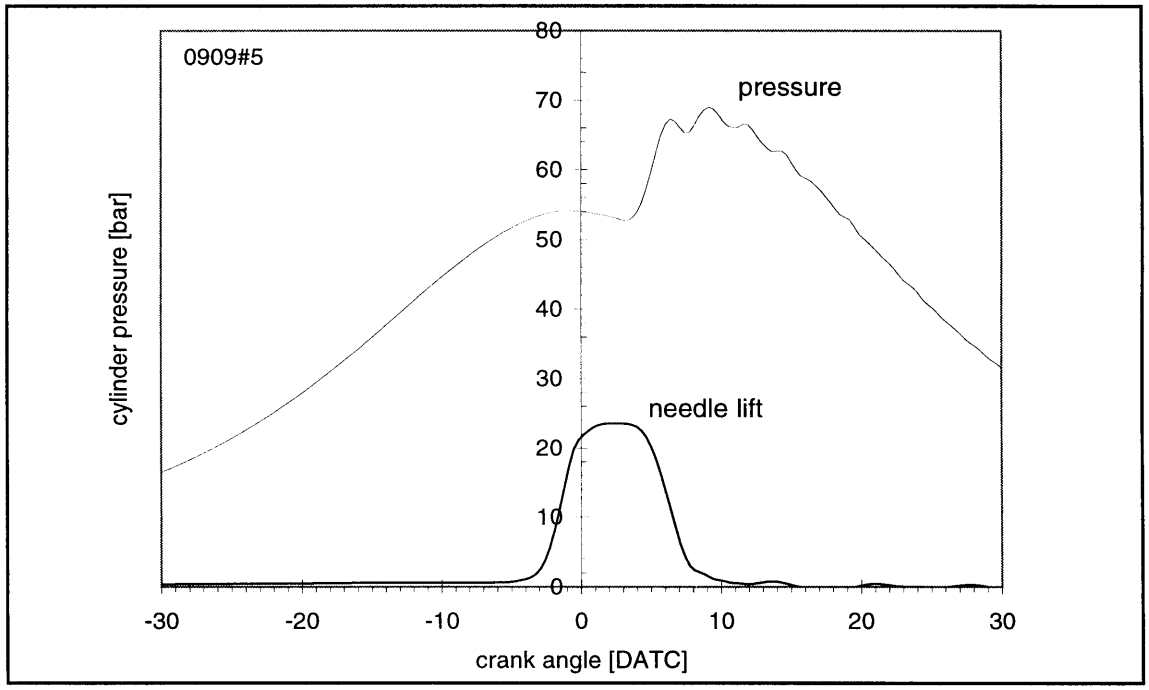

Figure 3.8 Typical injector needle lift and cylinder pressure traces for a diesel fuel case. Needle lift in arbitrary units.

Chapter 4
Experimental Results

This chapter examines the ignition delay and heat release data of the ENSYN and NREL pyrolysis oils and diesel fuel in order to characterize combustion differences between them. It also examines the impact of water on combustion, and whether differing water content can account for observed ignition delay and heat release differences between the two pyrolysis oils. As discussed in Chapter 3, combustion experiments were performed with the NREL, ENSYN, and diesel fuels, as well as a hydrated NREL oil whose water content equaled that of the base ENSYN oil (26.3 wt %). The engine speed and load were maintained constant at 2400 rpm and 5.0 bar IMEP (ϕ ~0.4), and the air inlet temperature varied.

4.1 General observations

Some observations regarding the differences of pyrolysis oil and diesel fuel combustion can be made directly from the (typical) cylinder pressure traces shown in Figures 4.1-4.3, for NREL, ENSYN, and diesel fuels, respectively. First, while the three cases exhibit the same peak pressure timing of 9.5 DATC, the peak pressure of the pyrolysis oils is approximately 15% greater than that of diesel fuel. Second, the qualitative shape of the pressure trace during the bulk of the combustion is significantly different; the pyrolysis oils do not exhibit the period of almost constant pressure volume expansion following the initial

rapid pressure rise, as exhibited by the diesel case. Third, as shown in Figure 4.4, the rate of cylinder pressure rise of the diesel fuel is some 30-70% greater than that of the pyrolysis oils, even when the ignition delay of the pyrolysis oils is significantly greater. Normally, long ignition delay fuels (low Cetane number) are associated with great pressure rise rates, resulting in diesel knock in extreme cases.

As will be shown in Chapter 5, these qualities together imply that pyrolysis combustion is predominantly kinetically controlled, a fundamental difference from the predominantly mixing-controlled diesel fuel combustion. It is noteworthy, however that despite these differences, the gross indicated thermal efficiency was approximately equal for the pyrolysis oils and diesel fuel, as shown in Figure 4.5. Finally, the engine was found to operate as smoothly with pyrolysis oils as it did with diesel fuel, even when the ignition delay was long; the IMEP coefficient of variation remained within an acceptable range in all cases from 1 to 3%, and did not correlate with fuel type.

4.2 Ignition delay

4.2.1 Comparison of base ENSYN, NREL, and diesel fuels

Ignition delays for the pyrolysis oils are plotted versus charge temperature at the start of injection in Figures 4.6 and 4.7. The data fall within typical ignition delay ranges for high speed DI diesel engines of 0.4 to 1 ms, corresponding to 6 to 14 CAD at 2400 rpm [1]. Corroborating the earlier cited work, it was found that neither pyrolysis oil would auto-ignite below a charge temperature of 870 K, which corresponded to an air inlet temperature of 55 °C for the experimental engine; no corresponding lower temperature limit was observed with the diesel fuel. It should be noted that preliminary experiments with another NREL fuel (NREL #175) indicated that it may ignite with no air preheating, though the data were found to be flawed by a faulty pressure transducer and the experiments could not be re-run due to insufficient oil supply.

Because the ignition chemistry is exponential with temperature, usually expressed as $\tau_{ID} = Ap^{-n} \exp\left[\frac{E_A}{\tilde{R}T}\right]$

[1] Heywood, J.B. *Fundamentals of Internal Combustion Engines*, McGraw Hill, 1988.

where T is temperature, E_A is the apparent activation energy, p is pressure, and A and n are constants, the natural log of the ignition delay is often plotted against 1/T (where T is charge temperature at start of injection), as shown in Figure 4.8 for the pyrolysis and diesel fuels. When plotted this way the apparent activation temperature (E_A/R) is given by the slope of the linear regression through the data. Greater activation energy implies that chemistry is relatively more important relative to mixing and evaporation processes [2], as chemical kinetics are exponential with temperature whereas mixing processes are at best linear with temperature. As shown in the figure, and tabulated below, the apparent activation energies of the pyrolysis oils are more than two times greater than that of the diesel fuel. It should be noted that when calculated this way the apparent activation energy is not a true chemical property of the fuel, as it lumps physical (vaporization and mixing) and chemical processes together.

TABLE 4.1 Apparent activation energy by fuel.

	E_A/R [K]
ENSYN	7300
NREL	7600
diesel	3200

It can also be seen that the NREL oil ignition delay is significantly less than that of the ENSYN oil, though both exhibit approximately the same temperature dependence. It is also noteworthy that at the higher temperatures, the ignition delay of the pyrolysis oils approaches that of diesel fuel, which is consistent with the explanation that the longer ignition delay is predominantly due to slow chemical kinetics, not poor atomization, vaporization, or mixing. If mixing rates with pyrolysis oils were significantly slower than with diesel fuel (to the point that ignition were mixing-limited), the ignition delay would remain greater even at high temperatures. This hypothesis is explored further in Chapter 5.

4.2.2 Effect of water and comparison of ENSYN and hydrated NREL oils

The impact of water addition is shown in Figure 4.9, where it can be seen that the hydrated NREL oil exhibited increased ignition delay at the lower temperatures (approximately 15% at T_{SOI} = 870 K), accounting for approximately half the difference in ignition delay between the base NREL and ENSYN oils at 870 K. The importance of water diminishes however as the temperature is increased; beyond 920 K, the

[2] Heywood, 1988.

hydrated and base curves merge. Thus while the water content difference between the base oils can account for part of the difference in ignition delay at the lower temperatures, the data shows that the oils behave differently even when the water content is the same.

The ignition delay picture is summarized in Figure 4.10, in which simple exponential fits to the data of the form $y = Ae^{B/T}$ are plotted for each fuel.

4.3 Heat release

4.3.1 Comparison of base ENSYN, NREL, and diesel fuels

Calculated instantaneous heat release data for 3 conditions corresponding to T_{SOI} = 870, 920, and 950 K are plotted for the NREL, ENSYN, and diesel fuels in Figures 4.11 through 4.19. The diesel cases consistently exhibited the greatest peak heat release, followed by the NREL and ENSYN oils, respectively. The intense fluctuations characteristic of the diesel cases are due to pressure oscillations recorded by the pressure transducer, and whose frequency (circa 4000 Hz) was found to correspond to the characteristic acoustic frequency of the cylinder chamber. This acoustic phenomenon was reported by the engine manufacturer as inherent to the design, and has been widely reported in the literature. The intensity of the oscillations can be seen to attenuate as the charge temperature was increased, likely due to the fact that the ignition delay decreased, resulting in a less steep pressure rise and smaller pre-mixed heat release spike as shown. Because the oscillations are less intense with the 950K diesel case (Figure 4.13), the pre-mixed versus diffusion controlled stages of combustion can be delineated in accordance with classical descriptions of diesel combustion.

In contrast, the pyrolysis oil heat release traces shown in Figures 4.14–4.19 do not exhibit any qualitative shift from one combustion mode to another. While the peak heat release occurs almost immediately after SOC with the diesel cases, the pyrolysis oils' peaks occur significantly later, as shown in Figure 4.20 where the peak heat release timing for the pyrolysis oil cases is shown to occur more than 50% later relative to SOC than with diesel fuel. As a result, by the time the peak heat release is reached, more than 40% of the fuel has been consumed, in contrast to the diesel cases in which less than 20% has burned, as shown in

Figure 4.21. It should be noted that Figures 4.20 and 4.21 correspond to typical cases at 950K, at which the ignition delays across the three fuels are approximately equal. Thus the combustion process differs markedly between pyrolysis oil and diesel fuel, quite apart from ignition delay.

The heat release profiles are qualitatively consistent with those obtained with the rapid compression machine experiments by Collela et al [3] of diesel combustion, in which long ignition delay and slow combustion chemistry induced by low charge temperatures yielded purely premixed combustion with relatively low heat release rates. It was found that in addition to reducing the peak heat release, slower chemical kinetics resulted in reduced rate of instantaneous heat release (the slope of the instantaneous heat release curve) in the early combustion phase, resulting in delayed peak heat release timing relative to SOC. The physics underlying the heat release profiles reported here will be explored in detail in Chapter 5.

Figure 4.22 shows the characteristic burn duration for the three fuels versus charge temperature at SOI. The characteristic burn duration is defined as the time elapsed from SOC to the point at which the cumulative heat release fraction (normalized by the lower heating value of the injected fuel) reaches a value of $(1\text{-}e^{-1}) = 0.632$, corresponding to the characteristic time of the integral of an exponential decay (see §5.2.3 for details). As shown in the figure, the burn duration is generally shorter for the pyrolysis oils than for diesel fuel, which is partly explained by the fact that they also have longer ignition delay, allowing more fuel and air to mix prior to SOC; when the ignition delays are equal—above approximately 920K T_{SOI}—there is no significant difference in burn duration. This is consistent with published data which show that pre-mixed burn fraction is proportional to ignition delay [4]. It is noteworthy, however that the NREL fuel consistently burns more rapidly than the ENSYN fuel, even though it exhibits shorter ignition delay.

[3] Colella, K.J., Balles, E.N., Ekchian, J.A., Cheng, W.K., and Heywood, J.B. "A Rapid Compression Machine Study of the Influence of Charge Temperature on Diesel Combustion," SAE Paper 870587, 1987.
[4] Watson, N., Pilley, A.D., and Marzouk, M. "A Combustion Correlation for Diesel Engine Simulation," SAE Paper 800029, 1980..

4.3.2 Effect of water and comparison of ENSYN and hydrated NREL oils

Figures 4.23—4.25 show typical heat release profiles for the hydrated NREL oil for T_{SOI} = 870, 920, 950 K. When compared to those of the base NREL oil (shown in gray), it can be seen that increasing water generally attenuated the instantaneous heat release and initial slope, and increased the time elapsed from SOC to peak heat release, as tabulated in Figure 4.26. While these effects made the heat release profiles more like those of the ENSYN cases, there remained significant differences which could not be accounted for by water alone. Figures 4.27 and 4.28 shows heat release profiles of ENSYN and hydrated NREL cases plotted together (where the curves have been aligned with respect to SOC for comparison) for the 920K and 950K case, for which the ignition delay was equal for both oils. As shown in Figure 4.28, the hydrated NREL case exhibits approximately 70% greater peak heat release than the ENSYN case, though both have the same peak heat release timing, and prior to the second heat release burst exhibit approximately equal slopes.

The characteristic burn duration is also impacted by water, as indicated in Figure 4.29 which shows that the hydrated cases burn duration is 20-30% greater than the base cases. Figure 4.30 shows that the hydrated NREL cases exhibit the same burn duration as the ENSYN fuel, indicating that water can account fully for the difference in burn duration between the base NREL and ENSYN oils.

4.4 Summary of experimental results

It was found that while the pyrolysis oils exhibit similar indicated thermal efficiencies to diesel fuel, they were characterized by much greater ignition activation energies and longer delays, and despite that, lower peak heat release and pressure rise rates. The oils would not ignite without combustion air pre-heating. Furthermore, whereas the diesel heat release profiles were consistent with the classical two-phase combustion description, the pyrolysis heat release traces did not exhibit any perceptible qualitative shift from kinetic- to mixing-controlled phases, and also gave 50% later peak heat release timing relative to SOC. As a result, nearly 40% of the fuel burned prior to the peak, in comparison to less than 20% for diesel cases, even when the ignition delays were equal. The heat release profiles were consistent with previous research on diesel combustion in which chemical kinetics had been suppressed by low

temperatures, suggesting that slow chemistry may underlie the observed heat release profiles, and—because of the high apparent activation energies of ignition—may also underlie the long ignition delays.

With respect to combustion differences between pyrolysis oils, the NREL oil ignited significantly more readily than the ENSYN oil, though they exhibited similar sensitivities to charge temperature. Water addition to the NREL oil increased its delay, but it remained significantly lower than that of the ENSYN oil, indicating that the difference in water content between the base oils could only partially account for their differing ignition quality. It was also found that the NREL oil consistently exhibited shorter characteristic burn duration than the ENSYN oil, though both were comparable to one another and to diesel fuel at charge temperatures greater than 920K. Water addition to the NREL oil increased its burn duration by 20-30%, equaling that of the ENSYN oil. This indicated that the difference in burn duration could be fully accounted for by the differing water content of the base oils, though the resulting heat release profiles were significantly different, with the peak heat release of the hydrated NREL oil approximately 70% greater than that of the ENSYN oil for the same ignition delay.

In summary, the pyrolysis oils exhibited behavior characteristic of slow chemistry in comparison to diesel fuel, both with regard to ignition and combustion. Also, the NREL oil ignited more readily and burned more rapidly than the ENSYN oil. While the difference in water content accounted partially for combustion and ignition differences between the pyrolysis oils, substantial differences remained between the ENSYN and hydrated NREL cases, indicating that *both* water content and extent of thermal cracking are overlapping and important variables with regard to combustion. In Chapter 5, these effects are quantitatively deconvolved, and physical explanations derived for the observations reported above.

Figures 4.1-4.3

Cylinder pressure and needle lift traces. Needle lift in arbitrary units. Average of 100 cycles. 5.0 bar IMEP, 2400 RPM, T_{SOI}= 920 K

4.1 NREL

SOI = -4 DATC, ID = 6.2 CAD.

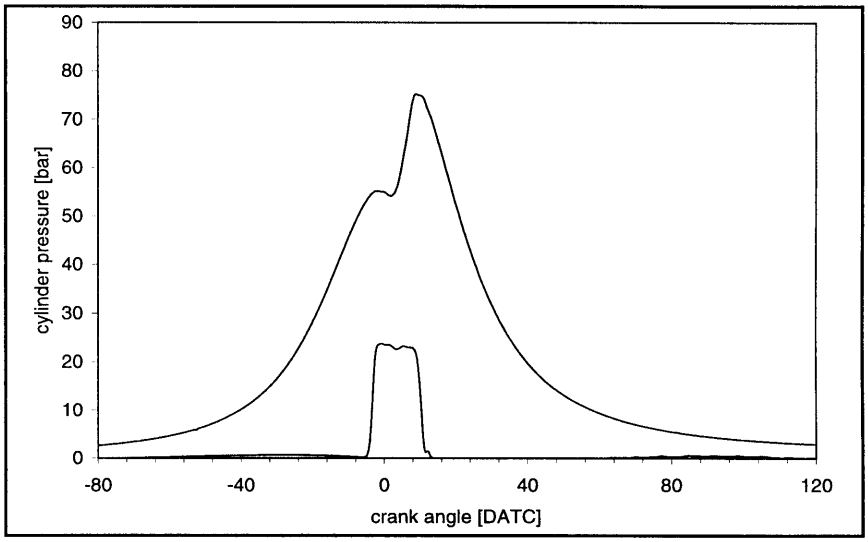

4.2 ENSYN

SOI = -7 DATC, ID = 7.9 CAD.

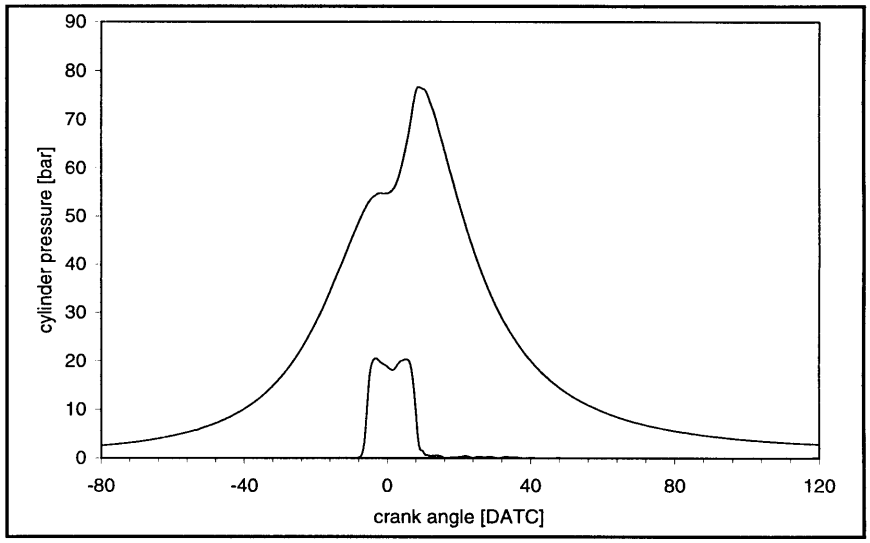

4.3 No. 2 diesel

SOI = -3 DATC, ID = 6.3 CAD.

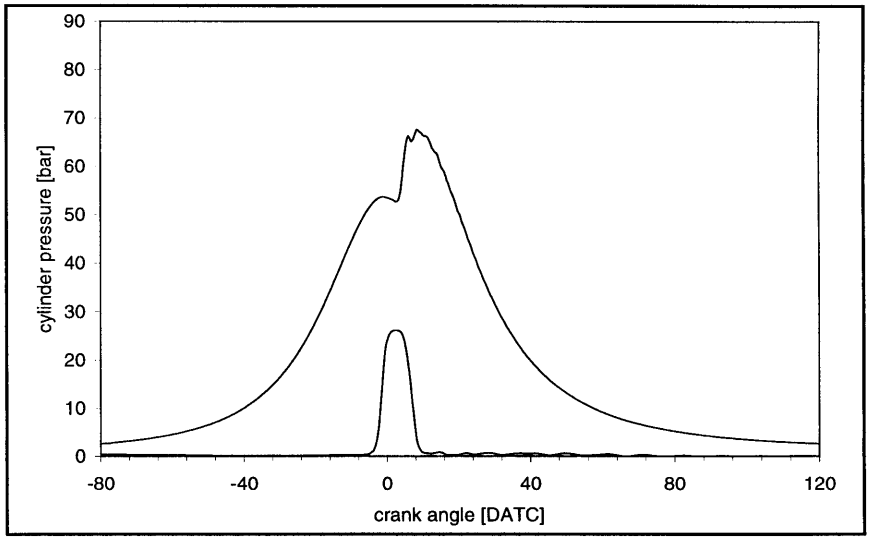

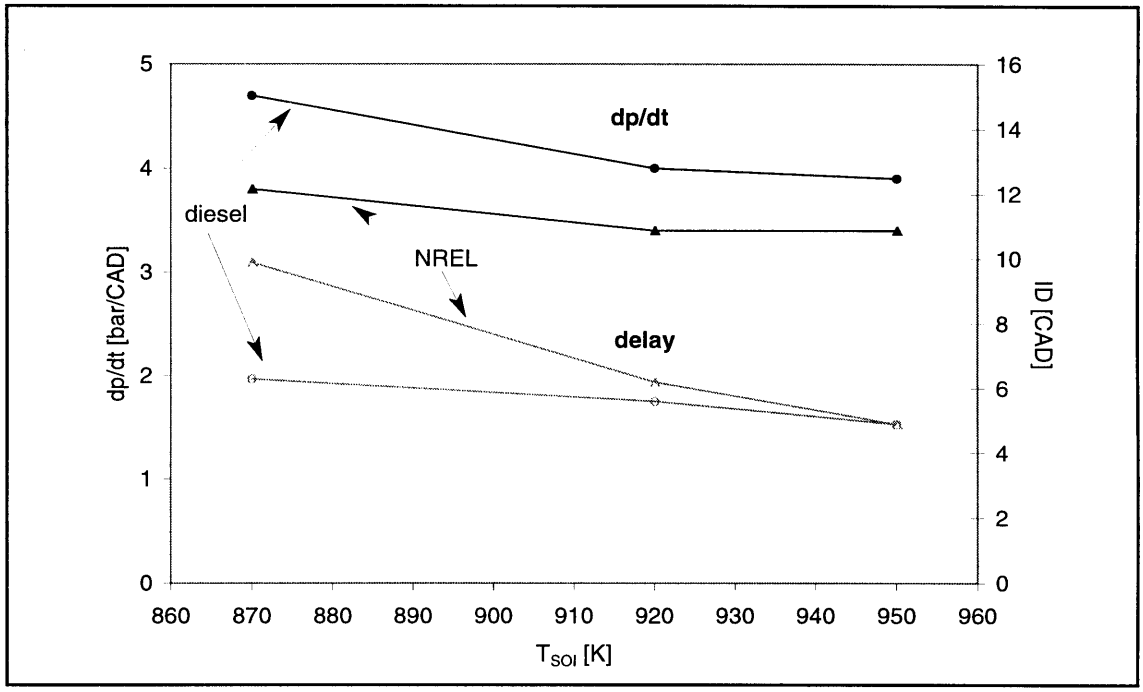

Figure 4.4 NREL and diesel fuels average rate of pressure rise rate during rapid rise period following SOC. Ignition delay shown in gray. 100 cycle average, 2400 RPM, 5.0 bar IMEP.

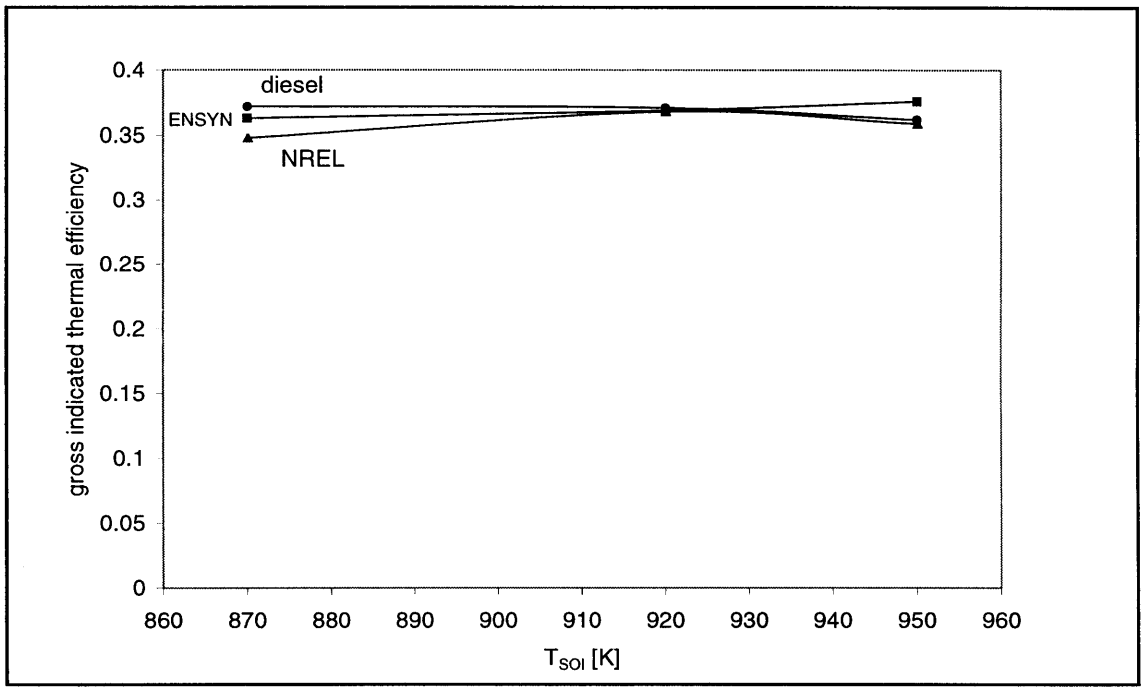

Figure 4.5 Gross indicated thermal efficiency with NREL, ENSYN, and diesel fuels. 2400 RPM, 5.0 bar IMEP.

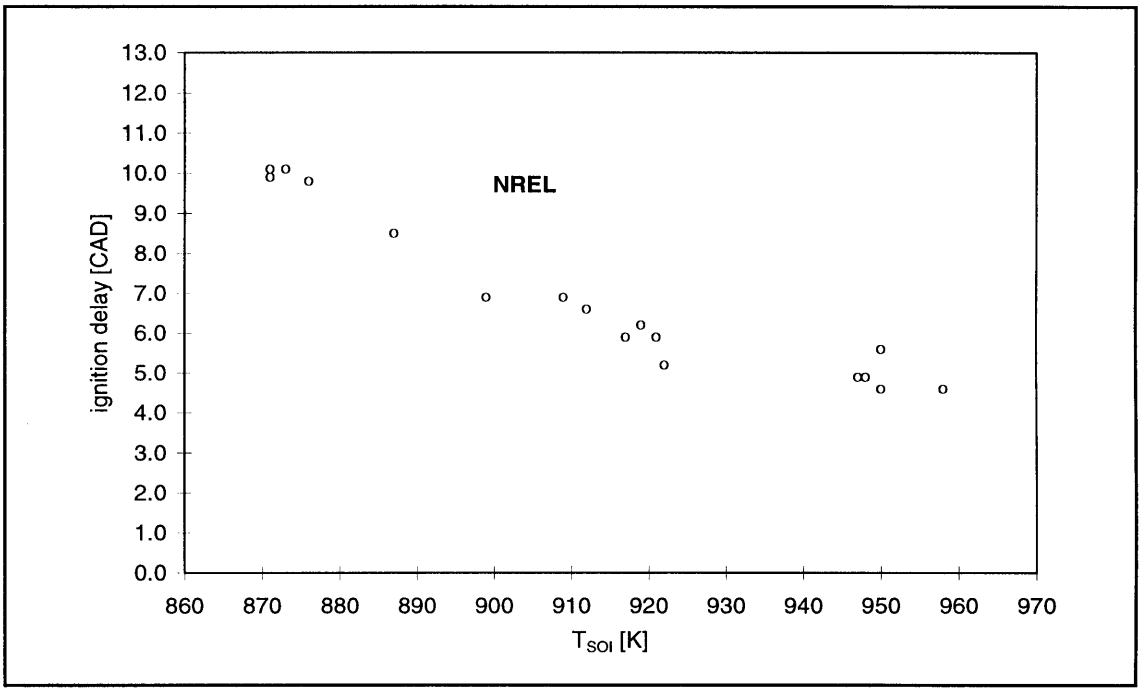

Figure 4.6 NREL oil ignition delay versus charge temperature at SOI. 2400 RPM, 5.0 bar IMEP, 100 cycle average.

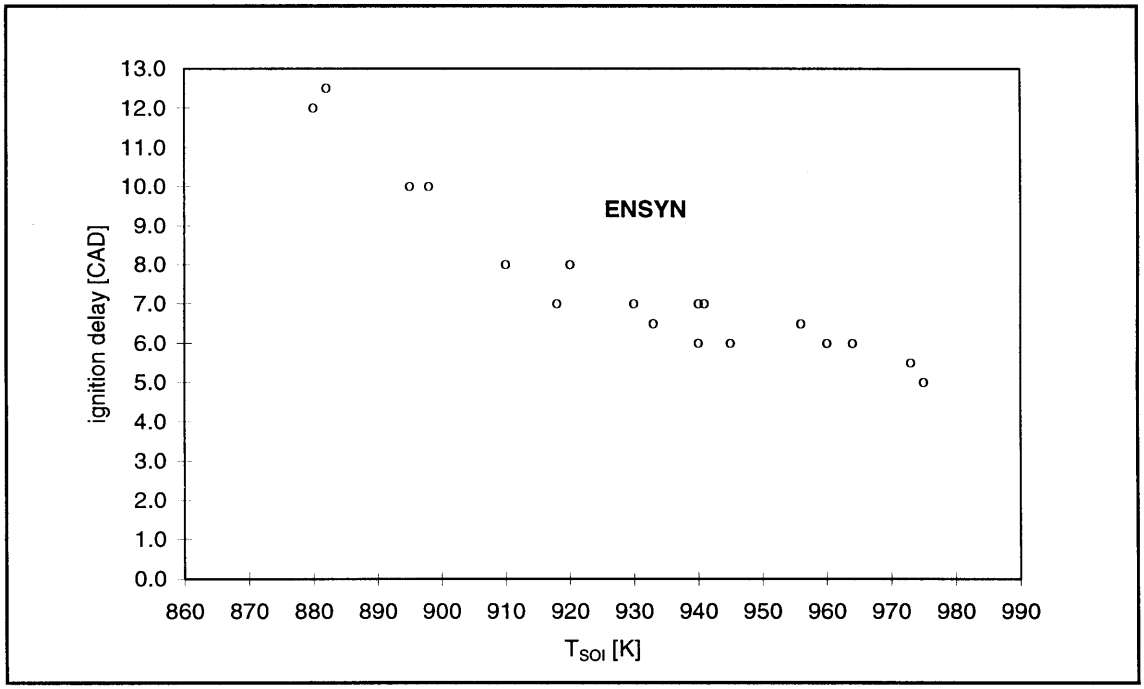

Figure 4.7 ENSYN oil ignition delay versus charge temperature at SOI. 2400 RPM, 5.0 bar IMEP, 100 cycle average.

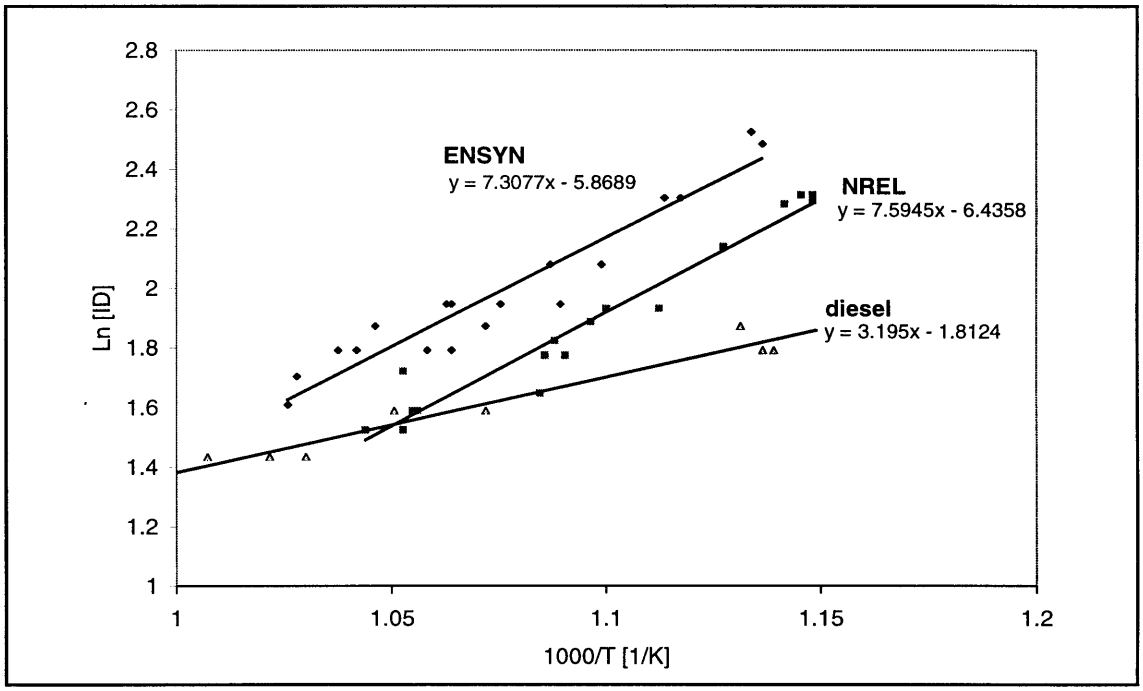

Figure 4.8 Comparison of apparent activation energies for ENSYN, NREL, and diesel fuels. 2400 RPM, 5.0 bar IMEP, 100 cycle average. ($R^2 > 0.9$ in all cases.)

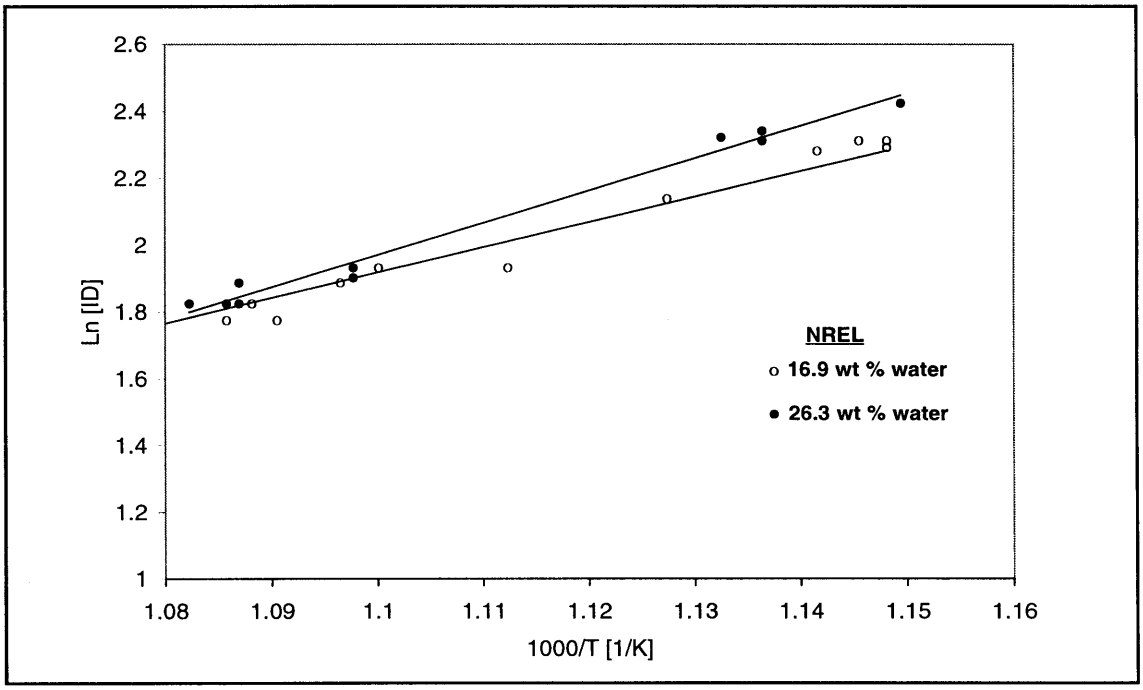

Figure 4.9 Effect of water on ignition delay; hydrated and base NREL oils ignition delay versus charge temperature. 2400 RPM, 5.0 bar IMEP, 100 cycle average.

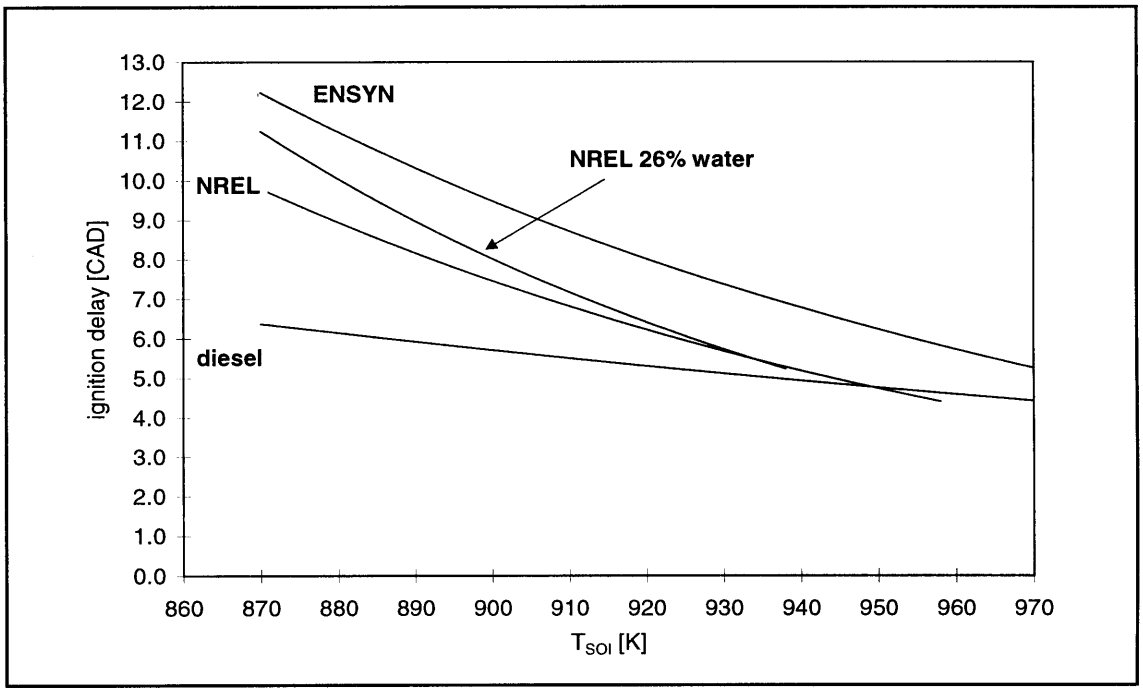

Figure 4.10 Summary of ignition delay data. Curves obtained by exponential fit to experimental data. 2400 RPM, 5.0 bar IMEP. (R^2 > 0.9 in all cases)

Figures 4.11-4.13 (Diesel)

Instantaneous heat release normalized by heat input per cycle, averaged over 100 cycles. 2400 RPM, 5 bar IMEP. Charge temperature at SOI indicated.

4.11 T_{SOI} = 870 K

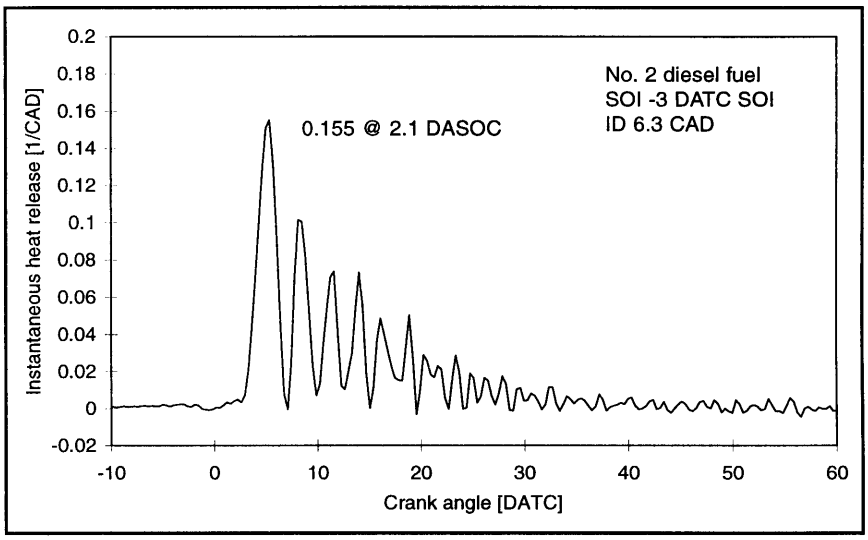

4.12 T_{SOI} = 920 K

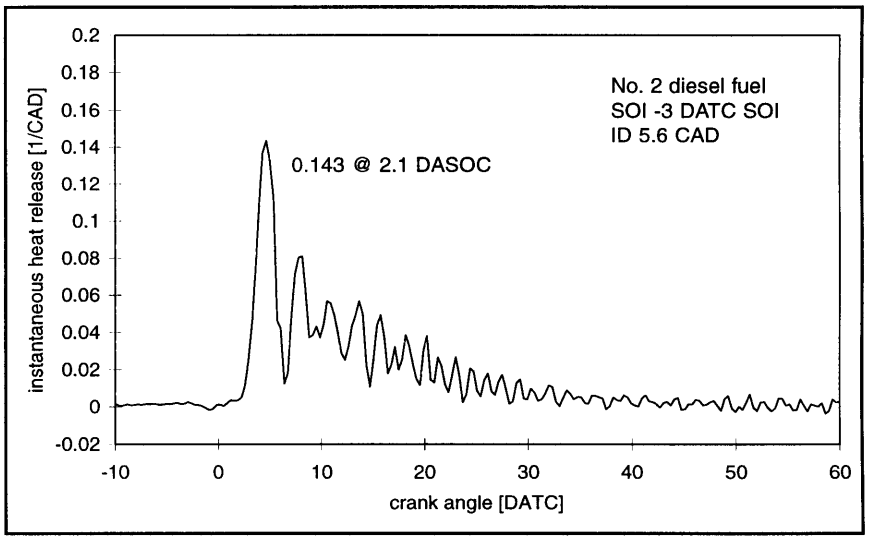

4.13 T_{SOI} = 950 K

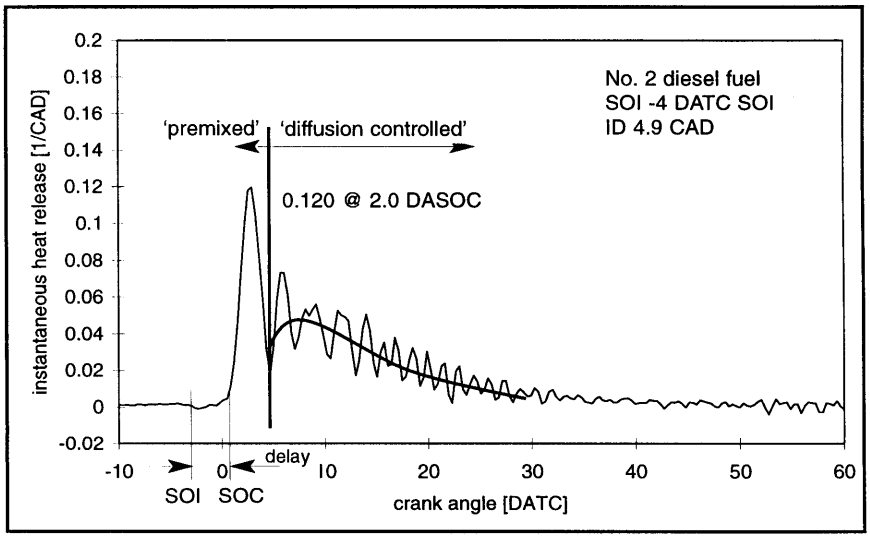

Figures 4.14-4.16 NREL oil

Instantaneous heat release normalized by heat input per cycle, averaged over 100 cycles. 2400 RPM, 5.0 bar IMEP. Charge temperature at SOI indicated.

4.14 T_{SOI} = 870 K

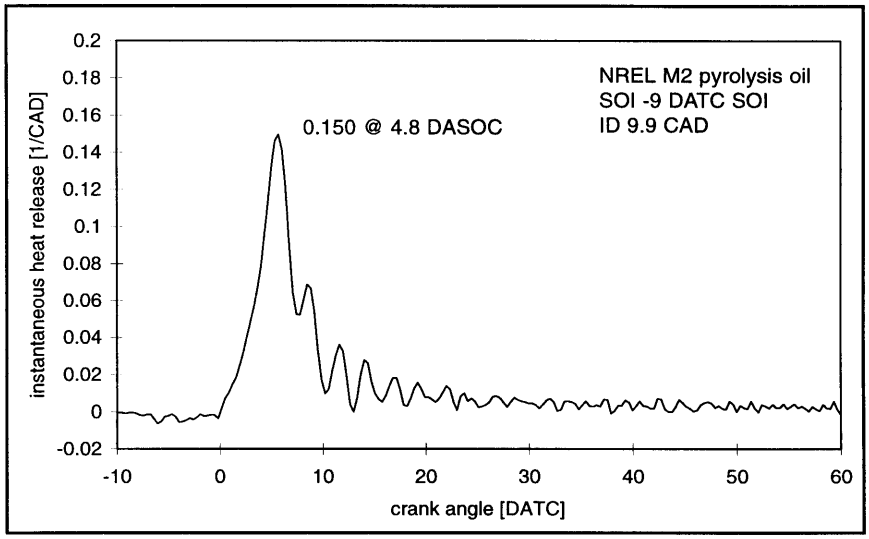

4.13 T_{SOI} = 920 K

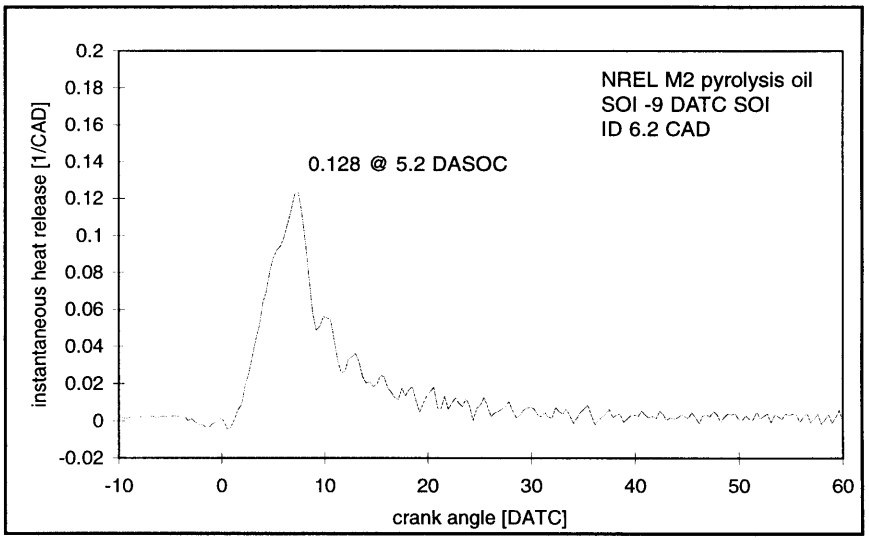

4.16 T_{SOI} = 950 K

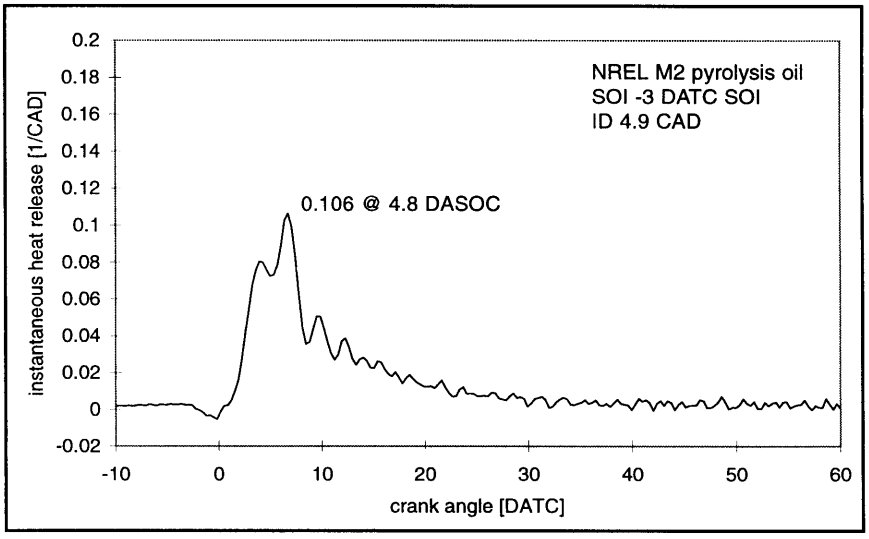

Figures 4.17-4.18 ENSYN oil

Instantaneous heat release normalized by heat input per cycle, averaged over 100 cycles. 2400 RPM, 5 bar IMEP. Charge temperature at SOI indicated.

4.17 T_{SOI} = 870 K

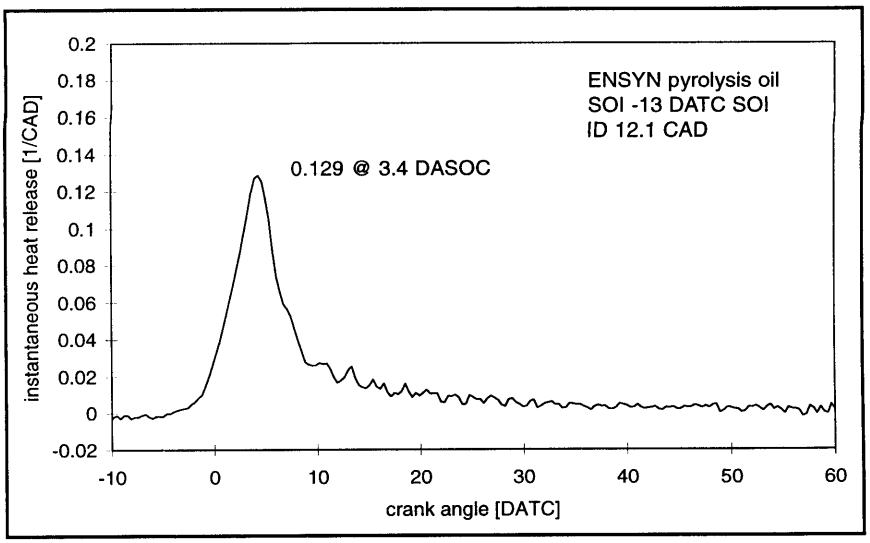

4.18 T_{SOI} = 920 K

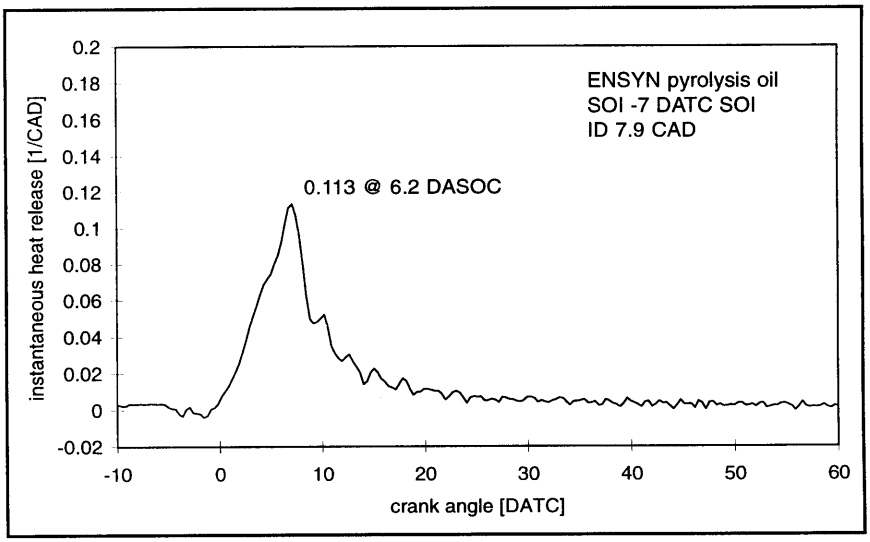

4.19 T_{SOI} = 950 K

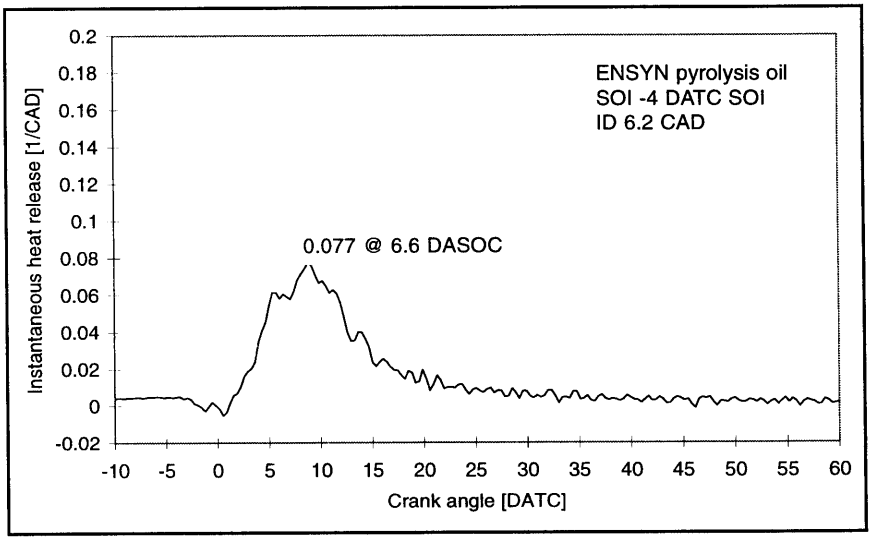

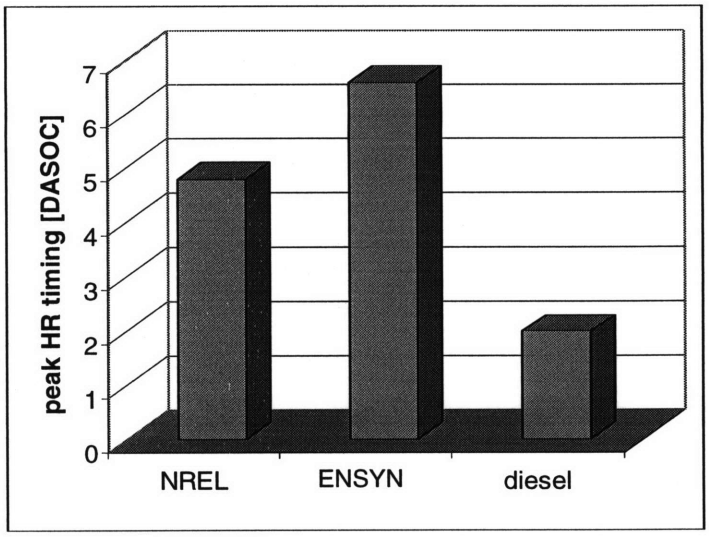

Figure 4.20
Peak heat release timing relative to SOC. T_{SOI} = 950 K, 2400 RPM, 5.0 bar IMEP.

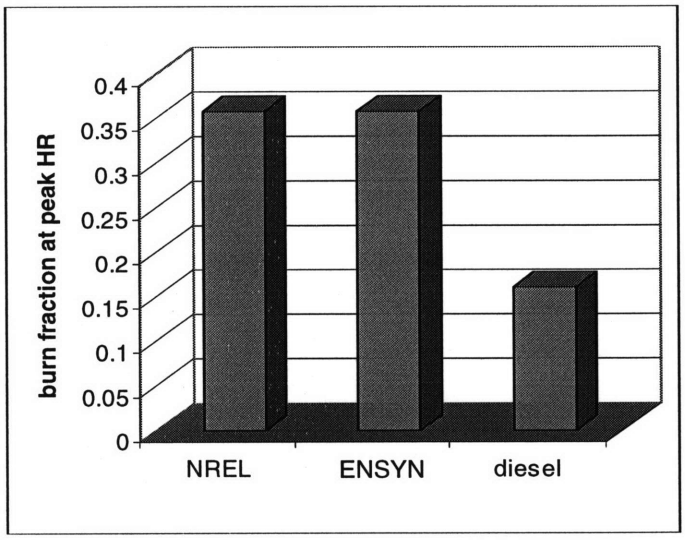

Figure 4.21
Corresponding cumulative burn fraction at peak heat release. T_{SOI} = 950 K, 2400 RPM, 5.0 bar IMEP.

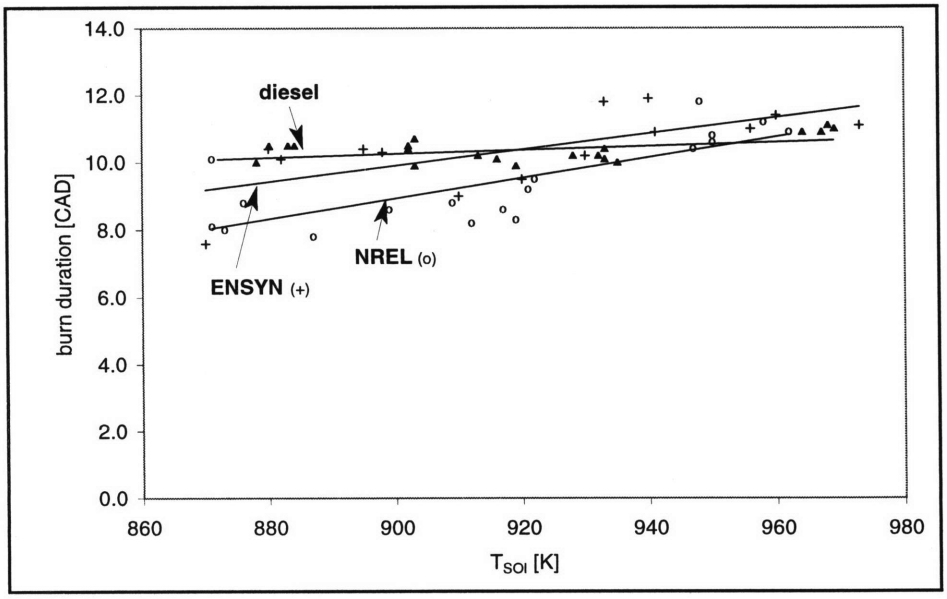

Figure 4.22
Characteristic burn duration versus charge temperature. 2400 RPM, 5.0 bar IMEP, 100 cycle average.

Figures 4.23-4.25
NREL- 26.3 wt% water

Instantaneous heat release normalized by heat input per cycle, averaged over 100 cycles. 2400 RPM, 5 bar IMEP. Charge temperature at SOI indicated. Base NREL oil shown in gray.

4.23 T_{SOI} = 870 K

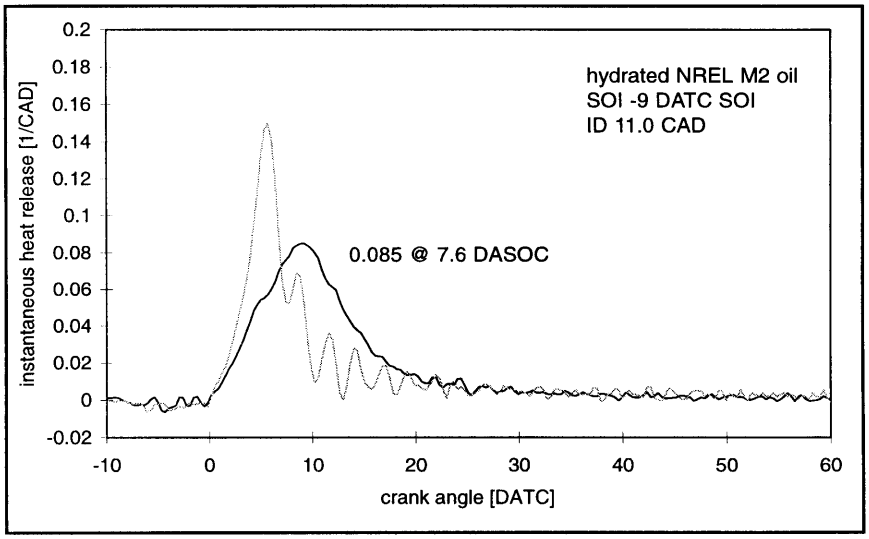

4.24 T_{SOI} = 920 K

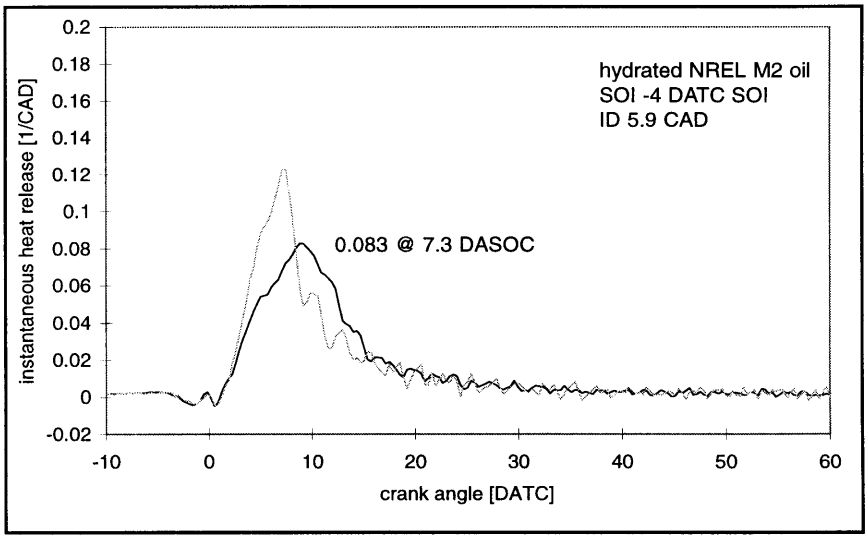

4.25 T_{SOI} = 950 K

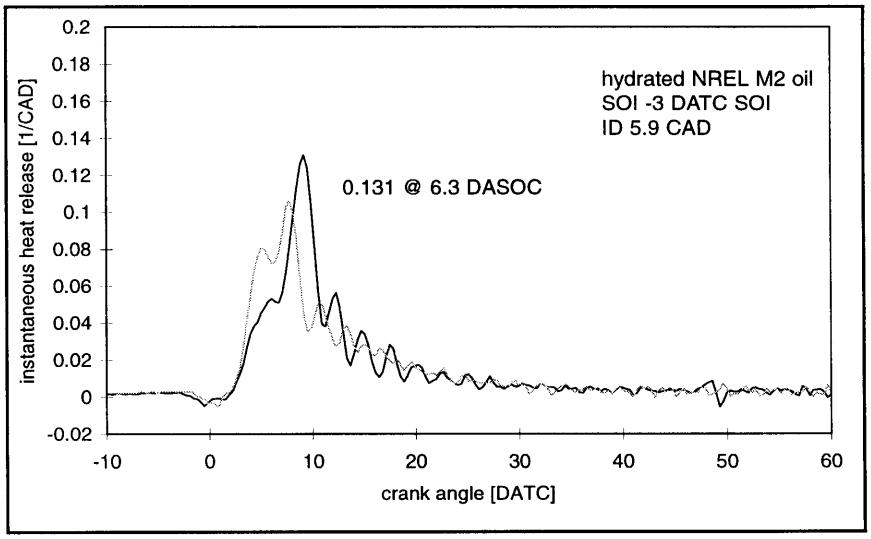

Figure 4.26

Impact of water on peak heat release timing relative to SOC for NREL oil. 2400 RPM, 5.0 bar IMEP.

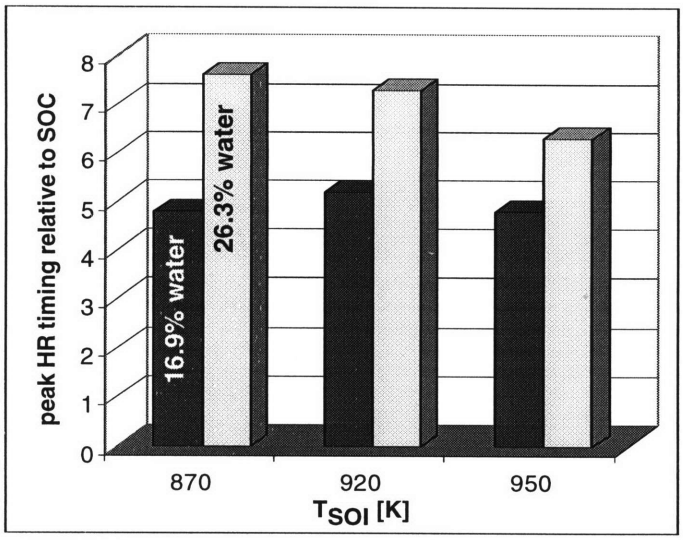

Figures 4.27-4.28

Comparison of ENSYN and hydrated NREL heat release rates. ENSYN shown in gray. X-axis shifted such that SOC's align.

4.27 T_{SOI} = 920 K

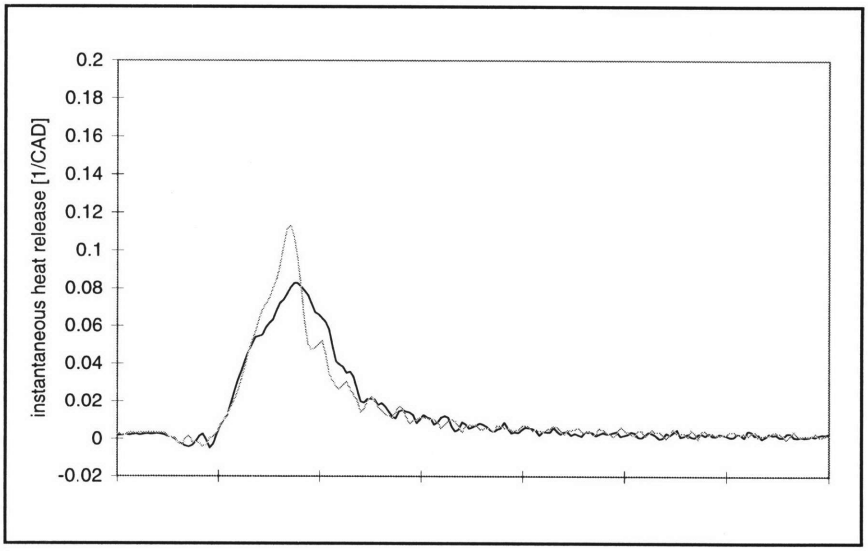

4.28 T_{SOI} = 950 K

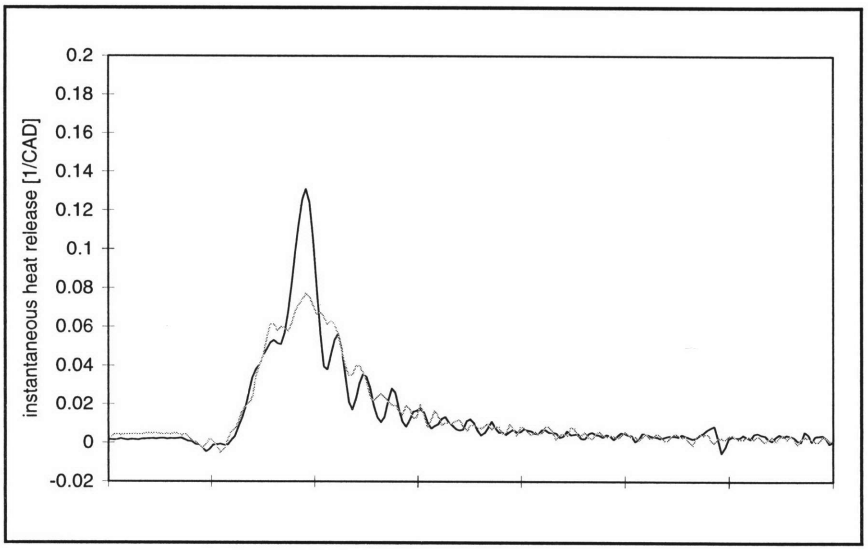

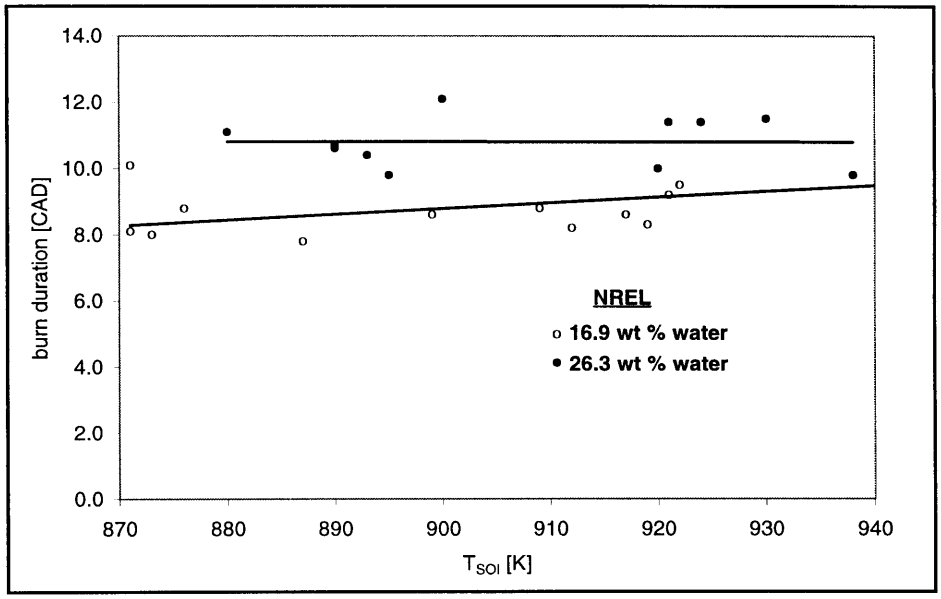

Figure 4.29 Impact of water on characteristic burn duration. 2400 RPM, 5.0 bar IMEP, 100 cycle average.

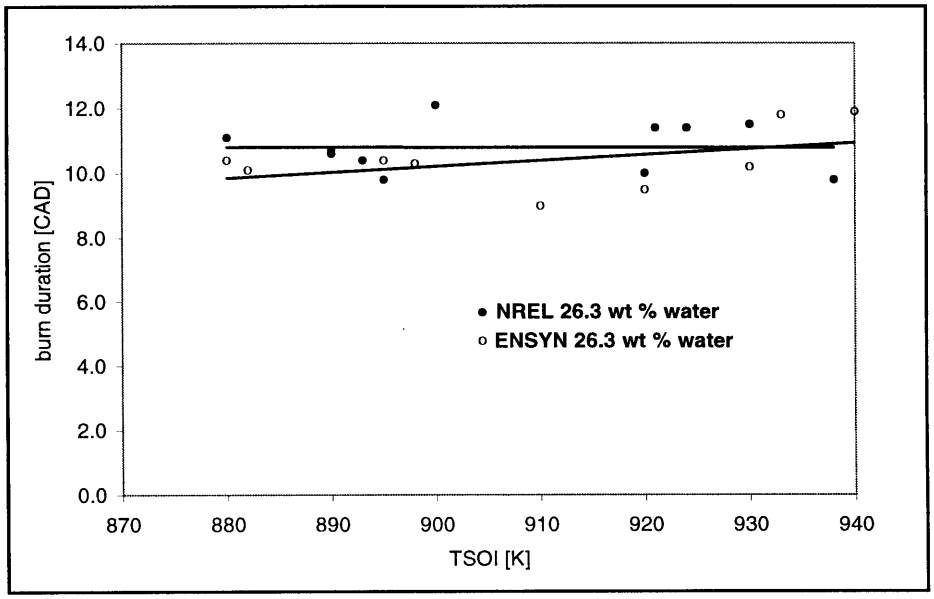

Figure 4.30 Comparison of ENSYN and hydrated NREL oil chracteristic burn duration. 2400 RPM, 5.0 bar IMEP, 100 cycle average.

Chapter 5 Analysis and Modeling

Heat release profiles contain information about the mixing and chemical processes prior to and during combustion. For example, a relatively large heat release spike in the early combustion stage suggests that a significant amount of fuel has pre-mixed with air prior to the start of combustion. If this condition is observed even when there is a relatively short ignition delay, it would suggest a relatively more rapid fuel-air mixing process during the ignition delay period. On the other hand, if the ignition delay is relatively long, one would expect a greater peak heat release rate due simply to the fact that the fuel had more time to mix with air. Thus with a combustion model relating fuel properties, ignition delay, and heat release, one could predict, for example, what sort of heat release profile would be expected in a case where long ignition delay results from slow fuel-air mixing (as opposed to slow chemistry), and compare this to experimental data to determine whether the observed heat release and ignition delay are consistent with this picture. This chapter, then, presents results obtained with a combustion model implemented to interpret the heat release and ignition delay data and some conclusions regarding the nature of biomass oil combustion based on comparisons between experimental data and model predictions.

5.1 Modeling goals

To recapitulate the results presented so far, it has been shown that the pyrolysis oils exhibit longer ignition delay than diesel fuel, and that the NREL oil exhibits better ignition characteristics than the ENSYN oil. It has been shown that the lower water content of the NREL oil accounts for part of the difference between its ignition delay and that of the ENSYN fuel, suggesting that the difference in thermal cracking also plays a role in the ignition delay. Since increasing the water content was shown to have an adverse effect on the ignition delay, the question was posed whether simply reducing the water content could improve the ignition delay sufficiently without relying on other modifications to the pyrolysis process. Answering this question requires in effect requires deriving the ignition and combustion characteristics of the underlying "parent" fuel without water. Thus one goal of modeling the combustion of the pyrolysis oils was to separate the impact of water from other fuel variables.

More generally, an analytic framework was needed to interpret the heat release/ignition delay data in a way which connected the data to particular physical or chemical processes. For example, what do the heat release data suggest with regard to the combustion kinetics and vaporization of pyrolysis oils in comparison to diesel fuel? Thus the modeling task focused on two goals: to determine what physical and chemical processes explained the different combustion behavior of pyrolysis and diesel fuels, and secondly, to relate these processes to particular fuel properties (and to infer from the model the fuel properties which were not known at the outset – such as the apparent activation energy of ignition – which would give agreement between the model and the experimental data.) This strategy is depicted in Figure 5.1 below.

The following questions were pursued:

1. Can slow vaporization relative to diesel fuel cause the longer observed ignition delay with pyrolysis oils?
2. What is the nature of the impact of water on ignition delay? How much does it affect vaporization (via latent heat effects) versus chemical processes (through local temperature effects)?
3. How do the ignition and combustion traits of pyrolysis oils compare to one another and to diesel fuel when the effect of water is accounted for? In particular, what are the differences in ignition chemistry and vaporization rates of the "parent oils?"

4. Can water alone account for the slower observed heat release of the pyrolysis oils? What interpretations can be given to the differences once water content is accounted for?

5.2 Model formulation

A phenomenological spray combustion model formulated by Hiroyasu et al [[1] and later updated and commercially packaged by GTI, Inc. was adopted for this work. The model accounts for the in-cylinder processes of fuel-jet formation, its breakup into droplets, entrainment of air, evaporation of fuel droplets, mixing of air with fuel vapor, ignition, and combustion [2].

In the model, the spray issuing from the nozzle is discretized into hundreds of packets in the axial and radial directions (Figure 5.2). For simplicity, it is assumed that no intermixing among the packets occurs. Each packet entrains air as it travels through the combustion chamber, at a rate determined from the momentum conservation equation which is solved using an empirically prescribed ordinary differential equation for fuel jet penetration as a function of time (i.e. spray velocity as a function of radial and axial distance from the nozzle).

As each packet (initially containing only liquid fuel) travels through the cylinder entraining air, fuel is assumed to vaporize according to single droplet evaporation equations (after an initial jet column breakup time), and the vapor mixes instantly with the air in the packet. The local equivalence ratio is calculated from the fuel vapor and air in each package. When a fuel-air mixture in a packet is within the combustion limits, the prepared fuel-air charge is allowed to burn – at a rate depending on the local temperature and fuel equivalence ratio – after some ignition delay period which is calculated using an Arrhenius rate expression. (Therefore as the combustion proceeds, and the temperature increases, the significance of the chemical delay for each packet decreases, and the combustion approaches a "mixing-controlled" process.) Thus each package consists of 3 subzones: liquid droplets, vaporized fuel plus entrained air, and products. At every time step, the heat released from each package is summed, and the overall cylinder temperature and

[1] Hiroyasu, H., Kadota, T., and Arai, M. "Development and Use of Spray Combustion Modeling to Predict Diesel Engine Efficiency and Pollutant Emission," paper 213-12, Bull. JSME, vol. 26, no. 214, 1983, 569-575.
[2] Morel, T. and Wahiduzzaman, S. "Modeling of Diesel Combustion and Emissions," Gamma Technologies Report, 1996.

pressure are updated according to the energy conservation equation, which is solved at each time step for the individual sub-zones and the cylinder as a whole. Each package has a different temperature, which varies with time and space, and is different from the mass average temperature calculated from the cylinder pressure. The thermodynamic properties of the air and eleven individual species (N2, O2, CO2, H2O, CO, OH, NO, H2, O, H, and N) are described by JANAF polynomial fits, and during combustion the mixture is treated on the basis of kinetic equilibrium between them.

This formulation of diesel spray combustion allows detailed descriptions of the physics which are most affected by varying fuel properties (volatility, viscosity, surface tension, autoignition characteristics), while relying on empirical information for spray dynamics. As a result, the program can be executed rapidly on a PC.

5.2.1 Governing Equations

The detailed equations governing the various processes can be found in [1]. It is useful for the ensuing discussion however to present the rate governing equations for fuel vaporization, ignition delay, and combustion below.

Droplet vaporization

The droplets in each fuel package are assumed to vaporize according to the 1-D single droplet diffusion and continuity equations. Thus the evaporation rate per droplet is given by

$$dm_v / dt = M_v G \pi D_d^2 \qquad [5.1]$$

where M_v is a user-input "vaporization multiplier," and D_d is the instantaneous droplet diameter. In the case of diffusion-limited evaporation, G, the mass flux is given by

$$G = \rho \ Sh \ \alpha \ln(1+\beta) / D_d \qquad [5.2]$$

where ρ is the droplet density, α is the mass diffusion coefficient, and β is the mass transfer number, defined as $\beta = (Y_o - Y_\infty)/(1 - Y_\infty)$. The Sherwood number is given by $Sh = 2 + 0.57 Sc^{1/3} Re^{1/2}$. In the case

of boiling-limited evaporation, the vaporization rate is proportional to the heat transfer rate and thus G becomes

$$G = Q / h_{fg} \qquad [5.3]$$

where Q is the heat flux to the droplet and h_{fg} is the latent heat of vaporization (which is treated as a constant during the droplet lifetime). The heat flux is calculated assuming convective transfer only, and follows the well known Nusselt number correlation of Ranz and Marshall [3]. The evaporation regime is determined by calculating the fuel vapor pressure at the droplet surface. If it exceeds the cylinder pressure, the evaporation is switched to the boiling-limited mode.

Ignition

The ignition delay is calculated separately for each packet using an Arrhenius type expression

$$\tau = M_i A_i / [\phi(3-\phi)^2] p^{B_i} \exp(C_i / T) \qquad [5.4]$$

where M_i is a user-input "ignition delay multiplier," ϕ is the local vapor phase fuel equivalence ratio, and T and p are the local temperature and pressure. The constants A_i, B_i, and C_i are input to the program, and assume default values based on correlation with published data. Note that C_i is the activation energy divided by the gas constant, yielding an "activation Temperature."

Because cylinder and local conditions (p, T, ϕ) are changing continually, the ignition delay calculated at each time step from Equation 5.4 for a given fuel packet is different. To circumvent this problem, this model calculates the ignition delay by integrating the kinetic rate expression and assumes that ignition occurs when the value of the ignition integral, *I*, equals one:

$$I = \int \frac{1}{\tau} dt \qquad [5.5]$$

Combustion

Under normal diesel engine conditions, combustion proceeds at a rate determined by the availability of fuel vapor and air mixed at the molecular level to combustible proportions, and the combustion kinetics provide

[3] Ranz,W.E., and Marshall, W.R., "Evaporation of Drops," *Chemical Engineering Progress*, Vol. 48, 1952.

no additional limit on the rate of combustion. However, when the local temperature is sufficiently low, or the mixture sufficiently fuel lean, chemical kinetics can become the rate limiting step. In this case the rate of combustion is determined by Equation 5.6

$$dm_k / dt = M_c A_c \phi (3.0 - \phi)^2 p^{B_c} \exp(-C_c / T) \qquad [5.6]$$

where m_k is the mass of fuel in a given packet. M_c can be input as a "combustion rate multiplier." The constants B_c and C_c are fixed at values of 2.5 and 400 K, respectively. The model transfers the calculated mass of fuel which burns in a given time step along with a mass of air proportional to the local fuel/air ratio from the unburned to the burned subzone of a given packet. Energy will continue to be released due to the oxidation of partial combustion products from the burned zone as it entrains air.

5.2.2 Inputs

Inputs to the program include engine geometry, fuel injection profile, fuel properties, and cylinder initial conditions. A sample of the more important inputs are listed below, while a detailed sample input file can be found in Appendix C.

TABLE 5.1 Model inputs.

Engine Data	Fuel Injection	Fuel Properties
compression ratio	mass of fuel injected/cycle	LHV
Bore	number of nozzle holes	C/H/O content
stroke	nozzle diameter	liquid density
connecting rod length	injection timing, duration	heat of vaporization
piston cup diameter and depth		10, 50, 75 % distillation temp
piston TDC clearance height		ignition activation energy
wall, head temperatures		
cylinder P and T at IVC		

5.2.3 Verification

The model was verified using measured engine data for a number of test conditions in which the injection timing or air inlet temperature were adjusted over a range of typical experimental conditions. The cases modeled are described in Table 5.2 below. Detailed data input to the model can be found in Appendix C,

while the assumed fuel properties (defaults in the model) are given in Table 5.3. The primary diagnostics used for comparing the model to the data were the ignition delay, cylinder pressure, and heat release traces.[4]

TABLE 5.2 Diesel fuel cases used to verify model. Air inlet temperature varied from 55 to 89 °C, SOI varied from -3 to -8 DATC. Engine run at 2400 rpm at constant load. IVC temperature calculated from cylinder pressure using ideal gas law.

Case	IMEP [bar]	Fueling [mg/cyc]	SOI [DATC]	EOI [DATC]	Air flow [g/s]	Air temp [K]	P@IVC [bar]	T@IVC [K]
1	4.8	12	-3	8	9.5	55	1.14	361
2	4.9	12.3	-3	9	9.2	67	1.12	373
3	4.8	12.8	-4	8	8.7	89	1.13	395
4	4.8	12.5	-5	7	9.2	67	1.16	373
5	4.8	12.5	-8	3	9.2	67	1.14	373

TABLE 5.3 Default diesel fuel properties in model.

Lower heating value	42.5	MJ/kg
Heat of vaporization	0.25	MJ/kg
Liquid density	830	kg/m^3
Ignition delay activation temperature	3500	K
Ignition delay pressure exponent	-1.25	
Distillation temperature	490 K	10 wt%
	542 K	50 wt%
	562 K	75 wt%

Ignition delay and cylinder pressure

As shown in Figures 5.3, the predicted delay agrees very well with the experimental data (with all multipliers equal to unity). The peak cylinder pressure and timing for the 5 cases tested are given in Figure 5.4, and, as shown, are slightly over predicted by the model. The average error in peak cylinder pressure and timing relative to SOI over the five cases is 6.6 and 2.0 percent, respectively. The error partly derives from the fact that the experimental cylinder pressure oscillations can not be predicted by the model, though this does not diminish its utility for the present purposes. Figures 5.5 and 5.6 show the predicted and experimental cylinder pressure and heat release profiles for Case 1.

[4] It should be noted that because the model as received had been calibrated for use with modern injection equipment (i.e. with injection pressures upward of 1500 bar, in comparison to 550 bar for the Ricardo engine), two adjustments were necessary to simulate the current setup. In consultation with GTI, Inc. the Sauter Mean Diameter correlation was multiplied by a factor of 0.7, and the jet breakup length by a factor of 0.8.

Heat Release

While the predicted ignition delay and cylinder pressure agree closely with the experimental data, the heat release is more difficult to compare due to the experimentally recorded pressure oscillations during combustion, which are reflected in the $dp/d\theta$ term in the heat release calculation (see §3.2.4) by the oscillations shown in Figures 5.6. In addition, because the instantaneous slope of the recorded cylinder pressure trace during these oscillations is very different from that of the mean cylinder pressure, the resulting heat release rate calculation can yield unrealistically large positive and negative values. Thus rather than attempting to compare particular features (e.g. the peak heat release and timing) of the experimental and calculated heat release rate, the characteristic burn duration (the integrated, or cumulative heat release) were compared. Because the heat release profile resembles an exponential decay, the characteristic burn duration for the comparison was specified as the time elapsed from SOI to the point at which the cumulative normalized heat release reached a value of $(1-e^{-1}) = 0.632$. This is shown schematically in Figure 5.7. When compared this way the predicted and experimental data agree well (2% average error for the 5 cases, max error = 4.5%), as shown in Figure 5.8.

Taken together, the ignition delay, cylinder pressure, and heat release data demonstrate that the model provides a good representation of the mean physical processes leading up to and during combustion.

5.2.4 Comparison to State of the Art Description of Diesel Combustion

Recent experimental work by Dec [5] has clarified the process of diesel jet combustion in modern high-injection pressure diesel engines. Using laser sheet imaging of the cylinder contents during the injection event, Dec found that fuel vaporized rapidly, producing a surprisingly homogeneous, strictly vapor-phase fuel-rich zone at the end of the fuel spray (Figure 5.9) which remained throughout the injection event. Almost from the first appearance of the fuel vapor region, and well before the premixed heat release spike, chemiluminescent emissions were observed throughout it, likely as a volumetric rather than surface phenomenon. During most of the premixed spike, the vast majority of the combustion occurred within this

fuel rich vapor-phase zone. Thus, rather than ignition occurring in a few locations within a nearly stoichiometric zone and then spreading, Dec found that ignition actually occurred throughout a fuel rich (ϕ = 2 to 4) vapor phase zone, and that the subsequent consumption of air within it provided the bulk of the heat release during the premixed spike. The near stoichiometric or fuel lean zone during ignition delay and the early premixed burning was found to be negligibly thin.

Shortly (~1.5 CAD) after the onset of the premixed heat release phase, and near the peak heat release, a diffusion flame fed by the products of the incomplete fuel-rich premixed combustion forms around the periphery of the fuel jet (Figure 5.10). The diffusion flame remains throughout the remainder of the life of the fuel jet (i.e. during injection), and the liquid fuel penetration remains short and all the fuel in the main combustion zone is in the vapor phase.

Thus Dec deduced three primary observations about the nature of modern diesel combustion. First, rapid entrainment of hot cylinder air upstream of the diffusion flame zone promotes rapid vaporization of the liquid fuel and results in a rich combustible vapor phase mixture downstream of the liquid containing region. Second, as a result of high mixing rates, this rich vapor phase zone is relatively uniform. Third, the gradients characterizing the fuel jet equivalence ratio, liquid fraction, and other variables are much steeper than originally deduced from averaged images which tended to produce Gaussian distributions across the fuel jet.

In order to determine how well the model used in this study qualitatively agreed with these new findings, Dec's experiments were modeled. Engine and fuel data for the experimental condition modeled are given in Table 5.4. The primary measures for comparison were whether:

1. a purely vapor phase fuel rich zone forms at the end of the fuel spray;
2. ignition occurs in multiple locations and in a fuel-rich mixture;
3. premixed combustion takes place under fuel rich conditions;

---

[5] Dec, J. "A Conceptual Model of DI Diesel Combustion Based on Laser-Sheet Imaging," *SAE Paper* 970873.

4. the liquid penetration depth is short relative to the overall jet plume, and therefore all fuel in the combustion zone is in the vapor phase;

5. diffusion flame is stationed at jet the periphery.

TABLE 5.4 Case modeled [4].

Bore	139.7 mm	
Stroke	152.4 mm	
Combustion chamber diameter	97.8 mm	
Connecting rod length	304.8 mm	
Compression ratio	10:1	
Intake valve closing	195 DATC	
Exhaust valve opening	235 DBTC	
Number of injector nozzle holes	8	
Hole diameter	0.194	
Start of injection	-11.5 DATC	
Fuel injected per cycle	67.5 mg	
Fuel density	881.2 kg/m^3	
Fuel distillation temperature	493 K	10 wt%
	513 K	50 wt%
	513 K	75 wt%
Motored TDC pressure	5.0 MPa	
Motored TDC temperature	992 K	

Heat release

As shown in Figures 5.11 and 5.12, the predicted and experimental heat release profiles match reasonably well. The calculated peak instantaneous heat release of 176 J/CA at -7 DATC compares to the experimental 175 J/CA at -4 DATC, while the calculated ID (based on heat release) of 3 CAD compares to the experimental 4 CAD. The "mixing controlled" calculated peak heat release of 113 J/CA at 3.5 DATC compares to the experimental peak of 110 J/CA at 2 DATC. The results could be improved by calibrating the model to the engine characteristics if more data were available, but for the present mostly qualitative purposes, the model provides an adequate representation of the experimental case.

Jet penetration

Typical contours of liquid fuel fraction (liquid/total fuel) are plotted in Figure 5.13, where it can be seen that the qualitative shape of the liquid-containing region is quite different from that shown by Dec (Figure 5.10) in that liquid fuel persists considerably longer at the centerline than at the jet periphery, yielding a cone-shaped rather than rounded tip. This feature results from the fact that the model applies a particular empirical sauter mean diameter distribution over the jet cross section which renders the centerline SMD a

factor of 1.35 greater than the average. For the present purposes, then, the SMD distribution function was turned off so that all droplets have the same initial diameter (i.e. a SMD factor multiplier of 1) regardless of their radial distance from the jet centerline. As shown in Figure 5.11, this did not greatly impact the heat release profile, though it did reduce the liquid penetration depth, as shown in Figure 5.14, in which the experimental and calculated maximum liquid penetration depth is plotted. While the liquid penetration was still over predicted, the overall jet plume (liquid + vapor fuel, air, products) penetration into the cylinder was well represented by the model (Figure 5.15).

Ignition

At -8.75 ATC, the first incidence of heat release is recorded (to within $1/10^{th}$ of a crank angle degree, according to the model resolution used in this calculation). Figures 5.17 – 5.18 show contours of calculated temperature, liquid fuel fraction, and fuel equivalence ratio at this crank angle. As indicated by the temperature contour, ignition occurs diffusely in a thin layer at the jet periphery, corresponding to a fuel-rich region in which the fuel equivalence ratio varies from 5 to 1.5. This qualitatively agrees with Dec's experimental observation that ignition occurs simultaneously throughout a fuel rich zone located at the periphery of the jet. The model differs, though, in the fact that the fuel in this zone is only partially vaporized (60 to 80% vaporized), as shown in the liquid fuel fraction contour, whereas Dec found no liquid fuel in this zone.

Early premixed heat release

Figures 5.16-5.18 also illustrate simulations of typical conditions during the beginning stage of the premixed heat release spike (-7.5 CAD). As shown, the greater portion of the high temperature zone, which roughly corresponds to the reaction zone (since individual packets do not thermally communicate in the model), occurs in a near stoichiometric to fuel-lean region. The rapid heat release phase thus largely consists of the consumption of this premixed fuel *lean* charge, while during the later combustion phases, the fuel-rich fraction of the reaction zone grows considerably, yielding a slower heat release rate determined by the entrainment of additional air. This picture differs considerably from the experimental data, in which the rapid heat release phase is characterized by premixed combustion in the fuel-rich, purely vapor phase

region, followed by the onset of a diffusion flame at the jet periphery in which the products of the premixed fuel rich combustion burn to completion as they meet additional air (Figure 5.10). In addition, unlike the experimental data, the model predicts that a considerable fraction of the fuel (up to ~ 75 %) survives in the liquid phase well into the reaction zone, as shown in the liquid fraction contour plot.

Later premixed and mixing controlled stages

The remainder of the combustion event up to the end of injection is represented by the -1.25 DATC simulation profiles in Figures 5.16-18, which differ from the previous figures in the fact that the fuel rich region has extended considerably from the (liquid) fuel spray, accounting for roughly 75% of the vapor containing portion of the jet by -1.25 CAD. This is phenomenologically in agreement with the experimental data. Note that the slower characteristic heat release rate results from the time needed to entrain air into the burning jet. To the extent that a diffusion flame can be represented in the model and distinguished from the remainder of the reaction zone, it would correspond roughly to the thin fuel-lean sheath surrounding the fuel-rich region, in which the remaining combustible species will burn since by this stage of combustion the chemical kinetics are fast.

Overall comparison

The model qualitatively captures the ignition process shown by the experimental data, particularly the fact that ignition occurs diffusely throughout a fuel rich zone. The model differs during ignition by the fact that liquid fuel is present throughout the reacting zone, a difference between the model and experimental data that persists throughout the early part of the combustion event. In addition, the simulated premixed combustion takes place under largely fuel-lean conditions, whereas the experimental data showed that the early part of the premixed heat release is entirely within the fuel-rich vapor phase region. However, as combustion progresses the model correctly predicts a progressive build up of a fuel-rich vapor phase zone downstream of the spray, though it begins significantly further downstream than the experimental data indicate; i.e. the fuel takes longer to vaporize in the model than in reality.

TABLE 5.5 Comparison of key combustion phenomena.

Phenomenon	Description	Dec [4]	Classical [4]	Model
Ignition	Occurs in multiple locations	Yes	No	Yes
	Fuel Equivalence Ratio	2-4	1	1.5-5
	Liquid fuel present in ignition zone	No	Yes	Yes
'Premixed' phase	Fuel equivalence ratio	2-4	~1	~1
	Liquid fuel present in premixed charge	No	Yes	Yes
'Mixing controlled' phase	Liquid penetrates into or near combustion zone	No	Yes	Partially

It should be noted that the above results were obtained using the model's default constants (e.g. for entrainment rate), which could be adjusted to give better agreement with Dec's findings, particularly with regard to the rapid vaporization of the fuel droplets. One possible reason for the under predicted vaporization is that the model does not account for heat transfer between adjacent fuel packets (including radiation). As a result, the only heat transfer to the fuel spray occurs via convection with entrained cylinder air, whose average temperature will be significantly lower than the local temperatures of a reacting zone. Given, however, that the vaporization is slower even before ignition occurs, it is likely that other factors, such as a possible over prediction of the Sauter Mean Diameter, are at work. A systematic parametric study of the various model constants could yield an explanation, though this is beyond the scope of the current work. In any case, given the simple nature of the model, the results are well representative of reality, and quite adequate for the purpose of interpreting the experimental heat release rates reported in Chapter 4.

5. 3 Phase I Simulation – Global Combustion Parameter Multipliers

The first phase of modeling focused on generating comparisons between the combustion of the pyrolysis oils and diesel fuel. This was accomplished by modeling the pyrolysis oil cases using baseline diesel fuel properties and adjusting the governing rate expressions using multipliers for ignition delay (M_i), combustion (M_c) , and vaporization (M_v) such that agreement was obtained between the model and the experimental heat release and ignition delay data. In this way, the differences between pyrolysis oil combustion and diesel fuel heat release profiles could be interpreted through some combination of longer or shorter ignition delay, and faster or slower vaporization or combustion kinetics than would be expected with diesel fuel. Figure 5.19 illustrates the interdependence of the three global fuel-side combustion parameters as formulated in the model.

Figures 5.20-22 illustrate the impact of independently varying the three parameters. As shown in Figure 5.20, increasing the ignition delay multiplier increases the peak heat release. This well-known phenomenon results from the fact that a greater fraction of the fuel is allowed to pre-mix prior to SOC, resulting in a more intense "pre-mixed" rapid heat release phase. Consistent with this picture, the in-cylinder liquid and total unburned fuel curves show a greater fuel vapor charge available at SOC with increasing delay. Note that with sufficiently long ignition delay, burning is characterized by a single rapid heat release phase.

In Figure 5.21, the combustion rate multiplier is shown to affect the heat release profile by shifting the magnitude and timing of the peak (at constant ignition delay), with slower combustion yielding later and lower peak heat release and cylinder pressure. While the in-cylinder liquid fuel mass profile is not significantly affected by changing the combustion rate, the amount of in-cylinder unburned fuel increases as the combustion rate multiplier is reduced, meaning that a greater fuel-vapor build-up occurs. Thus as the combustion chemical kinetics are slowed, the heat release profile essentially loses its "mixing controlled phase" and the entire combustion process becomes "pre-mixed." This can be seen by comparing the heat release of the 0.4 and 1.0 combustion multiplier cases. In the latter, and consistent with the classical DI combustion model, a rapid heat release phase (cause by the buildup of a fuel-air charge prior to SOC) is

followed by a second combustion phase with a lower characteristic heat release rate determined by the rate at which fuel-air charge is prepared. In the former case, however, because the chemical kinetics are slow, there is an abundance of fuel-air charge present during the bulk of the combustion process, and as a result the heat release profile never switches to a "mixing controlled" curve. As will be shown in the following sections, the experimental pyrolysis oils heat release data are consistent with this slow chemical kinetics combustion picture.

The impact of the vaporization rate multiplier on peak heat release and ignition delay is shown in Figure 5.22. As the vaporization rate is increased, the peak heat release rate and cylinder pressure are increased while the ignition delay is reduced. In addition, it is shown that as the vaporization multiplier is increased the heat release profile approaches a single rapid heat release phase, as a result of the increasing availability of fuel vapor for fuel-air charge preparation. This is not to say, however, that mixing controlled combustion is normally limited by vaporization alone, as it is limited by both fuel vaporization and air entrainment rates. This is illustrated in Figure 5.23, in which the effect of doubling the calculated air entrainment rate is shown to increase the heat release rate, even as the evaporation rate multiplier is held constant at a value of 5.0.

5.3.1 Cases simulated

For each pyrolysis oil, the three representative 100-cycle ensemble averaged pressure and needle lift traces identified in Chapter 4 were used for simulation. In Section 5.4, it will be shown that the simulation results obtained using these cases represent well the experimental data. They are listed again below for convenience.

TABLE 5.6 Pyrolysis oil cases modeled. Air inlet temperature varied from 55 to 89 °C, SOI varied from -3 to -8 DATC. Engine run at 2400 rpm at constant load. SOI temperature calculated from cylinder pressure.

FUEL/CASE	NREL I	II	III	ENSYN I	II	III
T_{cyl} at SOI [K]	870	920	950	850	920	950
Fueling [mg/cyc]	28	32	34	33	35	37
SOI [DATC]	-9	-4	-3	-13	-7	-4
Ignition delay [CAD]	9.9	6.2	4.9	12.1	7.9	6.2

5.3.2 Multiplier methodology

As noted above, it is possible to interpret the experimental pyrolysis oil heat release data through the manipulation of the vaporization, ignition delay, and combustion rate multipliers. In particular, it is possible to search for a combination of the three multipliers (ignition delay, vaporization, combustion) which would produce the same heat release profile (using diesel fuel properties) as the experimental data for each of the three conditions (cases I-III). In this way the experimental results can be interpreted using physical arguments, i.e. that in relation to diesel fuel, the pyrolysis oils vaporize faster, burn slower, and so on.

The multiplier methodology, illustrated in Figure 5.24, is an iterative procedure which begins with obtaining the correct ignition delay for the experimental case under question. Once the correct ignition delay is obtained with the ignition delay multiplier, the combustion multiplier is adjusted so that the peak heat release occurs at the proper timing. Finally, the vaporization multiplier is adjusted to provide the correct peak heat release. Since the vaporization multiplier affects the ignition delay, it is sometimes necessary to iterate by re-adjusting the ignition delay multiplier.

The method converges to a unique solution because only the combustion multiplier can significantly affect the location of the peak heat release relative to SOC. As shown in Figure 5.25, the impact of vaporization multiplier on peak heat release timing relative to SOC is negligible over a three order of magnitude variation. In contrast, varying the combustion rate multiplier from 1.0 to 0.2 increased the time to peak heat release by a factor of 2.5. Once the ignition delay and correct peak heat release timing are obtained, only the vaporization rate manipulation can yield the correct magnitude of the peak release. Physically, this is explained by the fact that the positive slope of the early combustion phase is dictated by chemical kinetics, since the fuel is already pre-mixed, while the maximum heat release is determined by the amount of fuel which has pre-mixed; it reaches a maximum and decreases as the pre-mixed charge is consumed.

Figures 5.26-28 illustrate the application of the multiplier method to NREL oil case II. When the ignition delay, vaporization, and combustion multipliers are equal to one (the baseline diesel case), the resulting heat

release profile does not match the experimental data (Figure 5.26). The peak heat release is approximately 20% less than, and the peak heat release timing relative to SOC 30% earlier than the experimental data. To match the experimental peak heat release timing and magnitude, the combustion rate multiplier was reduced to a value of 0.29, and the vaporization multiplier was increased to 8.0, respectively (Figure 5.27). This greater vaporization rate required that the ignition delay multiplier be increased from 1 to 1.4 to maintain the correct ignition delay of 5.5 CAD. As shown in Figure 5.28, the calculated heat release and pressure traces produced by this method agree well with the experimental data. Physically, the results mean that relative to diesel fuel at these cylinder conditions, the NREL oil vaporizes more rapidly, burns more slowly, and takes longer to ignite.

It should be noted that because the fuel properties used in the simulations are for diesel fuel, the multipliers required to match the predictions and experimental data will vary from case to case. For example, the ignition delay multiplier will vary with charge temperature because the default activation temperature (3500 K) may be very different from that of the pyrolysis oils. Thus each set of M_i, M_c, M_v which give agreement between the experimental data and model predictions are applicable for the condition modeled only.

5.3.3 Uncertainty analysis

The sensitivities of the ignition delay, and peak heat release magnitude and timing with respect to ignition delay, vaporization, and combustion rate multipliers were calculated in order to place uncertainty boundaries around the multipliers for each case simulated. The sensitivities were calculated by varying the multipliers and linearly fitting the resulting ignition delay and heat release parameters, as shown in Figures 5.29-31. The tolerances employed in the procedure were that

a) the ignition delay should agree to within 0.1 CAD of the experimental value, the model resolution,

b) the peak heat release magnitude should agree to within 5% of the experimental value,

c) the peak heat release timing relative to SOI should agree to within 5% of the experimental value.

Using these tolerances and the derived multiplier sensitivities, the multiplier uncertainties were calculated as the ratio of the tolerance and the calculated multiplier sensitivity with respect to the variable under question. For example, the uncertainty for the ignition delay multiplier, U_{ID}, was calculated as

$$U_{ID} = \pm \frac{0.1 \text{ CAD}}{2.5 \text{ CAD per unit change in multiplier magnitude}} = \pm 0.04$$

By similarly calculating combustion and vaporization multiplier uncertainties using characteristic peak heat release timing and magnitude of 10 DSOC and 0.10 1/deg, respectively, absolute uncertainties of ± 0.016 and ± 0.025 for corresponding vaporization and combustion rate multipliers. Thus for the baseline ignition delay, combustion, and vaporization multipliers of 1, the resulting uncertainties on the three multipliers are as follows:

1. M_i, ignition delay ± 4 %
2. M_c, combustion rate ± 2 %
3. M_v, vaporization rate ± 3 %

5.3.4 Phase I Results

Repeating the multiplier method for the remaining NREL and ENSYN cases yielded the rate equation multipliers given in Table 5.7. The corresponding peak heat release magnitudes and timings are listed in Table 5.8. It can be seen that the pyrolysis combustion kinetics are slower, the vaporization faster (except in one case), and the ignition delay longer than would be the case with diesel fuel. The results are notable in that under no circumstances does the ignition delay multiplier take a value of less than 1.0, even as the vaporization multiplier varies from 0.2 to 8.0.

TABLE 5.7 Phase I Multipliers.

FUEL/CASE	NREL I	II	III	ENSYN I	II	III
Combustion, M_c	0.25	0.29	0.39	0.23	0.18	0.17
Vaporization, M_v	1.0	8.0	10.0	0.2	2.0	2.0
Ignition, M_i	2.1	1.4	1.0	2.0	1.5	1.2

TABLE 5.8 Experimental and predicted instantaneous heat release magnitude and timing obtained using multipliers given in Table 5.7. Heat release magnitude normalized by fuel energy input per cycle.

FUEL/CASE	NREL I	II	III	ENSYN I	II	III
Peak magnitude [1/deg]	0.15	0.12	0.11	0.13	0.11	0.08
Model [1/deg]	0.15	0.12	0.11	0.13	0.11	0.08
Peak timing [DASI]	14.7	11.4	8.4	17.3	14.1	12.8
Model [DASI]	15.0	11.3	8.0	17.3	13.8	12.8

The fact that the ignition delay multiplier is greater than 1.0 even though the vaporization is as fast or faster (except in the low temperature ENSYN case) than with diesel fuel means that slower chemistry underlies the longer ignition delay of the pyrolysis oils examined. Even considering ENSYN Case I, in which the vaporization multiplier is 0.2 (the only instance in which the vaporization multiplier was found to be less than 1.0), the ignition delay multiplier is 2.0, meaning that the ignition chemistry of diesel fuel is so much faster than pyrolysis oil that even when the vaporization rate is reduced by 80%, the ignition delay calculated based on diesel fuel properties is still half that experimentally observed. This slower chemistry could result from lower local temperatures (due to a high heat of vaporization), or from the chemical structure of the oils.

It can also be demonstrated with the model that slow vaporization (whether due to atomization or volatility) cannot underlie the long ignition delay of the pyrolysis oils. By reducing vaporization rate to such a degree that the long ignition delay of the pyrolysis oils is replicated without reducing the delay multiplier from its default value of unity, it can be seen that the resulting heat release profiles become inconsistent with the experimental data; the calculations yield excessively low heat release rates. The simulation of NREL case I, where the vaporization rate multiplier has been reduced to a value of 0.07 in order to reproduce the experimental ignition delay is shown in Figure 5.32, where it can be seen that the calculated peak heat release is approximately half the experimental peak heat release. This remains true even if the combustion multiplier is increased because the combustion is now mixing limited. In sum, the experimentally observed heat release profiles are characteristic of much greater vaporization rates than would be required to

reproduce the longer experimentally observed ignition delays through slow vaporization alone. This is found to be true with both oils under all conditions tested.

As shown in Table 5.7, the ignition delay multipliers decrease with increasing cylinder temperature (from Case I to Case III), meaning that the ignition kinetics of both oils are more sensitive to temperature than is diesel fuel; i.e. that they have higher apparent global activation energies of ignition. It can also bee seen from Table 5.7 that for the NREL oil, the combustion multiplier increases by more than 50% from Case I to Case III, while with the ENSYN oil it decreases by 15% for the same range. This suggests that the apparent activation energy of combustion of the NREL oil is greater than, and that of the ENSYN oil less than that of diesel. In all cases the NREL oil combustion remains more rapid than ENSYN oil combustion, though both burn more slowly than diesel fuel.

Combustion characterization

Figures 5.33-35 show the normalized in-cylinder injected, unburned, and liquid fuel mass for three sets of rate equation multipliers:

(a) NREL case II given above,
(b) NREL case II, with a combustion multiplier of unity, and
(c) NREL case II with all multipliers set to unity (default diesel).

These plots capture the essential differences of diesel and pyrolysis oil combustion from a macro-perspective. For this purpose, NREL case II can be considered typical. First, considering only the impact of slow combustion kinetics, Figures 5.33 and 5.34 show that the greater buildup of fuel vapor in case (a) results from the fact that a combustible charge is prepared faster than it can be consumed by chemical processes. In contrast, the case (b) simulation shows that after the initial premixed combustion phase, the unburned fuel follows closely the liquid fuel curve, indicating that the combustion proceeds according to the availability of fuel-air charge.

Second, the effect of rapid vaporization can be seen by comparing cases (b) and (c) in Figures 5.34 and 5.35. The liquid fuel mass curves illustrate the more rapid vaporization of case (b), as well as a greater

build up of fuel vapor up to and during the premixed combustion phase. In both cases, following the early premixed phase, the unburned fuel mass follows the liquid fuel mass profile, consistent with a mixing controlled process. As expected, the overall burn rate is reduced in case (c).

Fuel vapor as a mass fraction of unburned fuel is plotted versus fuel burn fraction for the three cases in Figure 5.36. Whereas in case (a), the NREL simulation, the average fuel vapor fraction throughout the combustion event remains near 40%, in case (c), the diesel simulation, the average vapor fraction is near 20%. The fact that the curve (b) approaches curve (c) following the early premixed combustion phase indicates that the air entrainment and reaction rate is sufficient to allow most of the excess fuel vapor which results from the large vaporization multiplier to burn, and in fact that under these conditions the combustion is limited only by the rate at which fuel vaporizes, i.e. that the combustion is mixing controlled. Most importantly, this means that the excess fuel vapor built up in case (a) is actually mixed with enough air to burn, and that the combustion in this case is *always* kinetically limited, a result that holds for all the pyrolysis oil cases. *Apart from the longer ignition delay, this is the major characterizing difference between pyrolysis oil and diesel fuel combustion.*

Summary

In sum, phase I of the modeling points to the following conclusions:

- The combustion of both pyrolysis oils is always kinetically limited.
- The long ignition delay of both pyrolysis oils results from slow chemistry, not slow vaporization.
- With regard to the differences between the NREL and ENSYN oils, the rate multipliers indicate that the NREL oil vaporizes and burns more rapidly than the ENSYN.

5.4 Phase II Simulation – Mapping Combustion Behavior to Fuel Properties

The second phase of the modeling effort was undertaken mainly to separate the overlapping effects of thermal cracking severity (molecular weight) and water content on the combustion characteristics of the pyrolysis oils. In particular, by subtracting out the impact of water on the relevant fuel properties (such as latent heat of vaporization), it would be possible to then predict the combustion behavior of the "parent" fuels, and on this water-free basis to compare the NREL and ENSYN oils. This comparison would then yield a quantitative estimate of the importance of the different degrees of pyrolysis severity (as indicated by the differing molecular weights) undergone by the two pyrolysis oils. It would also give a quantitative estimate for the degree to which the ignition delays could be improved by removing water. Figure 5.37 illustrates the approach. Whereas Phase I utilized diesel fuel properties and a set of imposed rate equation multipliers to match the experimental data, Phase II looked into the particular fuel properties that underlied the imposed multipliers. For example, rather than using a varying ignition delay multiplier, what activation energy would give the same results? Three main questions were pursued:

1. How does water affect the vaporization versus chemical processes leading up to autoignition?
2. How do the pyrolysis oils' ignition delay and combustion rate compare to one another and to diesel fuel when the effect of water is removed? What is the importance of the difference in severity of thermal cracking indicated by the differing molecular weights?
3. Can water alone account for the slower observed heat release of the pyrolysis oils?

5.4.1 Approach

As shown in Figure 5.37, the water in the fuel can impact the droplet diameter (via viscosity, surface tension, and density), latent heat of vaporization, heating value, and specific heat of the combusting vapor phase mixture (and therefore the local gas temperatures). The modeling procedure therefore consisted of inputting the various fuel properties and systematically altering their values in accordance with "adding" or "removing" water from the base fuel. It was assumed that the water played no intrinsic role in the ignition or combustion chemistry apart from its impact on local temperature, though it should be noted that chemical

kinetic effects of water vapor via promotion of hydrogen-oxygen radical recombination have been reported [6].

The heating value, droplet diameter (correlating with viscosity, density, and surface tension), latent heat of vaporization, and volatility profiles were input according to the estimates given in Table 5.9 and Appendix D. Because the model does not include an option to input water as a species in the fuel, the elemental composition was adjusted as if the water were intrinsic to the fuel, such that the products of combustion would contain the correct concentration of water vapor. This allowed the model to more accurately compute the specific heat of the burned gases, which in turn affects the local temperatures. The Arrhenius constants for the ignition delay and combustion equations were obtained by fitting the ignition delay and heat release profiles to experimental data in the manner described in 5.3.1. In this case, however, there were two inputs available for adjustment in the ignition delay equation: the activation temperature, and pre-exponential term $\mathbf{A_i}$ (see Equation 5.4). The ignition delay constants were fit to the data by using the input activation temperature to match the slope of the experimental ignition delay curve (as a function of cylinder temperature at SOI), and then using the pre-exponential term to shift the entire predicted ignition delay curve up or down to match the data.

A preliminary set of calculations with the base fuel properties (Table 5.9, in bold) showed that the vaporization rate was under-predicted in all the experimental cases (I-III, both oils), which was expected given the large vaporization multipliers found in Phase I. That is, the combination of greatly increased heat of vaporization and the slightly increased volatility relative to diesel fuel could not reproduce the effect of the large vaporization multipliers using diesel fuel properties. This suggests that the vaporization of the pyrolysis oils proceeds faster than predicted by applying the quasi-equilibrium 1-D diffusion equations as formulated in the model.

[6] Dryer, F.L. "Water Addition to Practical Combustion Systems—Concepts and Applications," *Sixteenth Symposium (International) on Combustion*, the Combustion Institute, 1976, 279-295.

One possible explanation is the micro-explosion phenomenon observed in single droplet pyrolysis oil combustion experiments by previous researchers and observed in diesel engine combustion experiments with water-oil emulsions, as presented in Chapter 1. Depending on the particular pyrolysis oil, micro-explosive behavior was found to range from causing "complete atomization" of the parent droplet, to a less effective "eruption" causing only partial fragmentation. Microexplosions result from the build up and rapid expansion of volatile species within the droplet when the Lewis number is small (thermal diffusivity > mass diffusivity). Because the model assumes equilibrium vaporization typical of diesel fuel combustion (Le > 1), it is not capable of predicting microexplosive phenomena.

Apart from micro-explosions, the under-predicted vaporization rate could also arise from error in the estimated distillation curves (obtained from NREL), and from the model's equilibrium distillation assumption. The initial mean droplet diameter was therefore allowed vary so that the calculated vaporization rate gave the correct peak heat release with a vaporization multiplier of unity, according to the method discussed in section 5.3.1. From a physics perspective, it would have been preferable to use the vaporization multiplier to obtain the correct vaporization rates since it is not clear that the more rapid vaporization is due to droplet fragmentation, but, due to the model's upper limit of the input vaporization multiplier (a maximum value of 10), it was necessary to manipulate the droplet diameter to achieve sufficient vaporization rates. The impact on the simulation of varying initial droplet diameter or vaporization rate multiplier is identical. In any case, the fact that the experimental results are well matched even in the early combustion stage by simply adjusting the droplet diameter, indicates that the method is a fair approximation of reality.

In summary, then, the Phase II modeling procedure is the same as the multiplier method described in Section 5.3.1, with two exceptions. First, pyrolysis oil properties are used in the calculations instead of diesel properties. Second, whereas the vaporization and ignition rate equations were manipulated through multipliers to match the experimental results, the experimental results are now matched by changing the initial droplet diameter and Arrhenius constants in the ignition rate equation. The combustion rate multiplier is used as before, since there is no input in the model for the actual Arrhenius constants. Once

the correct ignition rate constants, droplet diameter, and combustion multipliers are obtained by comparison to experimental data from the base fuels, then the water content is "varied" to determine its impact on ignition delay.

Three levels of water content were chosen for modeling: 26, 17, and 0 wt %. The first two correspond to the water contents of the ENSYN and NREL fuels, respectively. Because experimental data was recorded for the NREL fuel at 17 and 26 % water content, it was possible to verify that the water content "variation" was properly represented. The fuel properties used are given in Table 5.9.

TABLE 5.9 Fuel properties. Bold represents base fuels as received; non-bold represent model fuels.

	ENSYN			NREL M2			Diesel
Water [wt %]	**26**	17	0	**17**	26	0	**0**
Carbon [wt %]	**42.9**	48.1	58.0	**48.1**	42.9	58.0	**87.0**
Hydrogen [wt %]	**8.4**	8.0	7.4	**7.9**	8.2	7.2	**13.0**
Nitrogen [wt %]	**1.1**	1.2	1.5	**1.3**	1.2	1.6	**0.0**
Oxygen [wt %]	**47.4**	42.3	32.8	**42.7**	47.7	33.2	**0.0**
Density [kg/m^3]	**1220**			**1200**			**850**
Latent heat [kJ/kg]	**1300**	900	400	**900**	1300	400	**280**
LHV [MJ/kg]	**16.3**	18.4	22.5	**17.0**	15.0	20.8	**42.5**
10% distillation temp [K]	**420**			**420**			**490**
50% distillation temp [K]	**540**			**540**			**540**
Average mol. Weight	**550**			**370**			**184**

5.4.2 Baseline ignition, combustion, and vaporization

The equivalent droplet diameter and ignition constants obtained by matching the model's predictions to the experimental data for the NREL and ENSYN cases at their baseline water contents (17% and 26%, respectively) are given in Table 5.10. Note that the pre-exponential term, $\mathbf{A_I^*}$, in the ignition rate expression and the Sauter mean diameter, $\mathbf{SMD^*}$, are both normalized by the diesel fuel default value. The corresponding predicted and experimental ignition delay data for these values are shown to agree well in Figure 5.38, and Table 5.11 shows the good agreement between the calculated and experimental heat release data. Also shown in Figure 5.38 are the predicted and experimental ignition delay data for the NREL case with 26% water, where the good agreement between the two indicates that the method of

"varying" the water content in the model is adequate, and that the ignition rate constants obtained with the baseline case (17% water) can be used to make predictions at other conditions. Note that the model correctly predicts the decreasing importance of water content with increasing cylinder temperature at SOI, as the 17% and 26% curves merge.

TABLE 5.10 Fuel properties implied by matching experimental data and model parameters.

	NREL	ENSYN	Diesel
Ignition A_i*	0.7	1	1
Ignition E_a/R [K]	4300	4200	3500

TABLE 5.11 Phase II experimental and predicted heat release magnitude and timing and combustion multiplier. Case numbers as defined in Table 5.6.

FUEL/CASE	NREL I	II	III	ENSYN I	II	III
SMD*	0.9	0.6	0.2	0.9	0.7	0.9
Combustion M_c	0.39	0.36	1.00	0.31	0.26	0.24
Peak magnitude [1/deg]	0.15	0.12	0.11	0.13	0.11	0.084
Model [1/deg]	0.15	0.12	0.11	0.13	0.11	0.084
Peak timing [DASI]	14.7	11.4	8.4	17.3	14.1	12.8
Model [DASI]	15.0	10.5	8.5	17.5	14.0	12.8

5.4.3 Impact of water and molecular weight on ignition delay

Using the fuel properties given in Table 5.10, the impact of water on ignition delay was assessed by varying the water content from 26% to 0%. The results are plotted in Figures 5.39 and 5.40. By comparing the 0% water curves to the baseline curves for the NREL and ENSYN oils, it can be seen that according to the model, water accounts for 15% and 20%, respectively, of the ignition delay at T_{SOI} = 870 K.

The 0% curve represent the best possible ignition delay that could be obtained if the water were entirely removed from the oils, assuming that the atomization characteristics are unchanged (in reality, they would worsen as removing water increases the viscosity, as discussed in Chapter 3). The 0% curve thus represents the inherent ignition quality of the 'parent oil,' and by comparing that of the NREL and ENSYN oils, the significance of the remaining process variable under question, the thermal cracking severity (quantified by the differing average molecular weights of the two oils, 370 g/mol NREL vs. 550 g/mol ENSYN, as

presented in Chapter 3), can be assessed as in Figure 5.41, where both curves are plotted with the diesel fuel data.

The differences between the two pyrolysis oils remain significant when water is removed; the greater molecular weight of the ENSYN oil appears to increase the disparity between the pyrolysis and diesel fuel ignition delay by an additional 1.4 CAD at T_{SOI} = 870 K (3.8 vs. 2.4 CAD excess delay over diesel). This is a result of changes in chemistry and vaporization, as shown in Figure 5.41, where the predicted ignition delay for the ENSYN oil which has been assigned the same ignition chemistry constants as the NREL oil is plotted (dotted line). As shown, the chemical difference account for approximately half the increased ignition delay of the ENSYN oil.

Thus it can be concluded that *both* the water content and the pyrolysis severity are important factors in the long ignition delays. In particular, the poor ignition quality of the pyrolysis oils is inherent to the molecular structure, and is exacerbated by the presence of water.

Turning now to the nature of the impact of water on the ignition delay, it can be seen from Figure 5.42 that the primary effect is on the vaporization (via the latent heat). The middle curve was obtained by forcing the 0% water case to have that same vaporization rate as the case with 17% water. This was accomplished by reducing the vaporization multiplier such that the in-cylinder liquid fuel mass history of both cases was the same. Thus, when controlling for the impact of water on vaporization, the residual difference in ignition delay is minimal. It can be concluded that even with the higher activation temperatures of the pyrolysis oils, the role of water in reducing the reaction rates via local temperature reduction is small compared to its impact on vaporization rate.

5.4.4 Impact of water and molecular weight on combustion rate

By comparing the combustion multipliers of phase I and II of the modeling (Tables 5.7 and 5.11), it can be seen that when the water is accounted for in the fuel properties, a portion of the combustion multiplier is recovered. That is, when diesel fuel properties are assumed (Table 5.7), a combustion multiplier of 0.25 is

found for NREL Case I; when the water is accounted for (Table 5.11), however, the combustion multiplier increases to 0.39. In physical terms this means that the average combustion rate of the NREL oil is 0.39 times as fast as diesel fuel carrying the same water content. This trend holds true for all the cases. The fact that the combustion rate multiplier increases when the water is accounted for means that water is indeed partly responsible for the slower combustion rates of the pyrolysis oils, but the fact that the multiplier remains significantly lower than one even when accounting for water means that the slow combustion chemistry is inherent to the fuel structure.

Table 5.11 also shows that the combustion multipliers of the NREL oil are significantly greater than those of the ENSYN oil, implying that the combustion chemistry of the former is more rapid. Because the water is accounted for already, the difference in combustion rates is due to the inherent structural differences of the fuels implied by the different molecular weights. Figure 5.43 summarizes the differences, showing the relative combustion rates of the pyrolysis oils with respect to straight diesel fuel and diesel fuel with equivalent water content.

5.5 Summary

With respect to diesel fuel combustion, it has been shown that the pyrolysis oils are characterized by relatively rapid vaporization, and slow ignition and combustion kinetics which are exacerbated by the presence of water. With respect to one another, it was found that, subject to the caveats given in Section 5.4.1, the increased pyrolysis severity of the NREL oil gave it faster vaporization, ignition, and combustion kinetics than the ENSYN oil. It would thus appear that for the pyrolysis oils, average molecular weight can be used as an indicator of expected combustion quality, with lower molecular weight yielding better combustion quality.

Returning to the questions posed at the outset:

1. Slow vaporization cannot account for the longer ignition delay of the pyrolysis oils, which is not to say that faster vaporization would not reduce ignition delay.
2. Water impacts ignition delay mainly by reducing the vaporization rate.
3. Even if all the water could be removed without adversely affecting the atomization quality, both pyrolysis oils would nevertheless exhibit long ignition delays due to the inherent fuel structure.
4. Water accounts only partially for the slow observed combustion rates of the pyrolysis oils.

These are quantitatively summarized in Chapter 6.

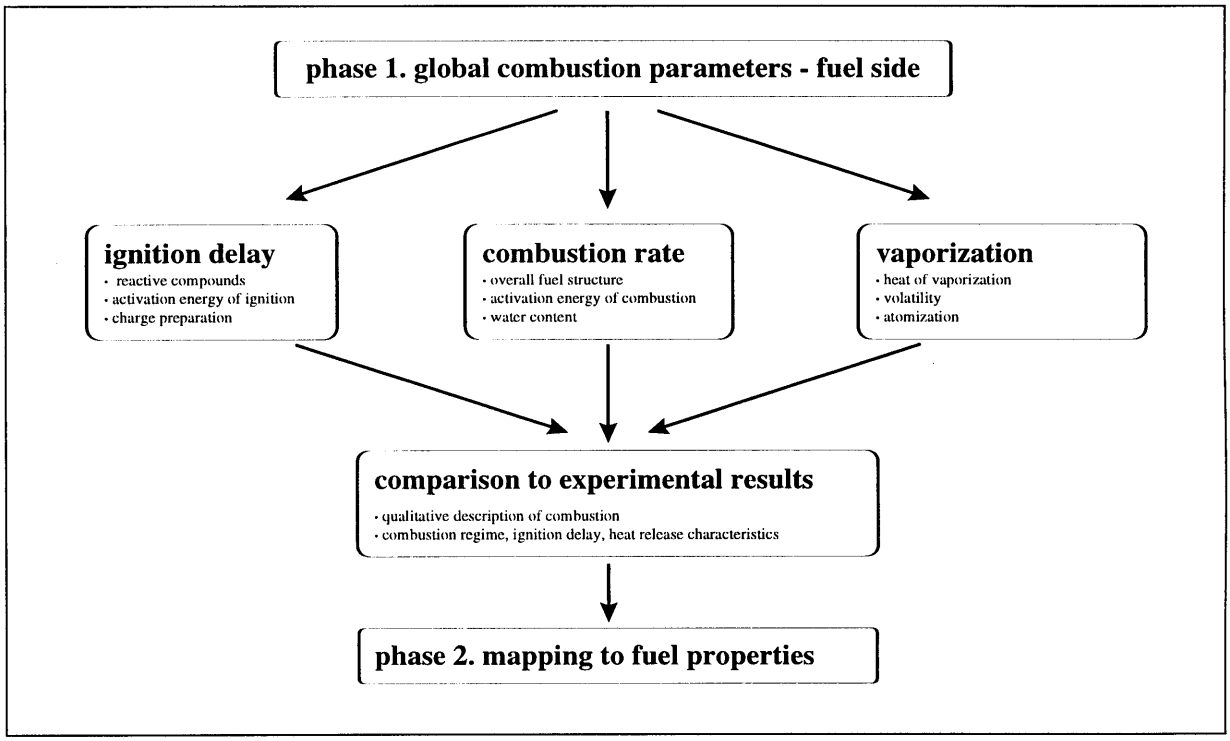

Figure 5.1 Modeling overview.

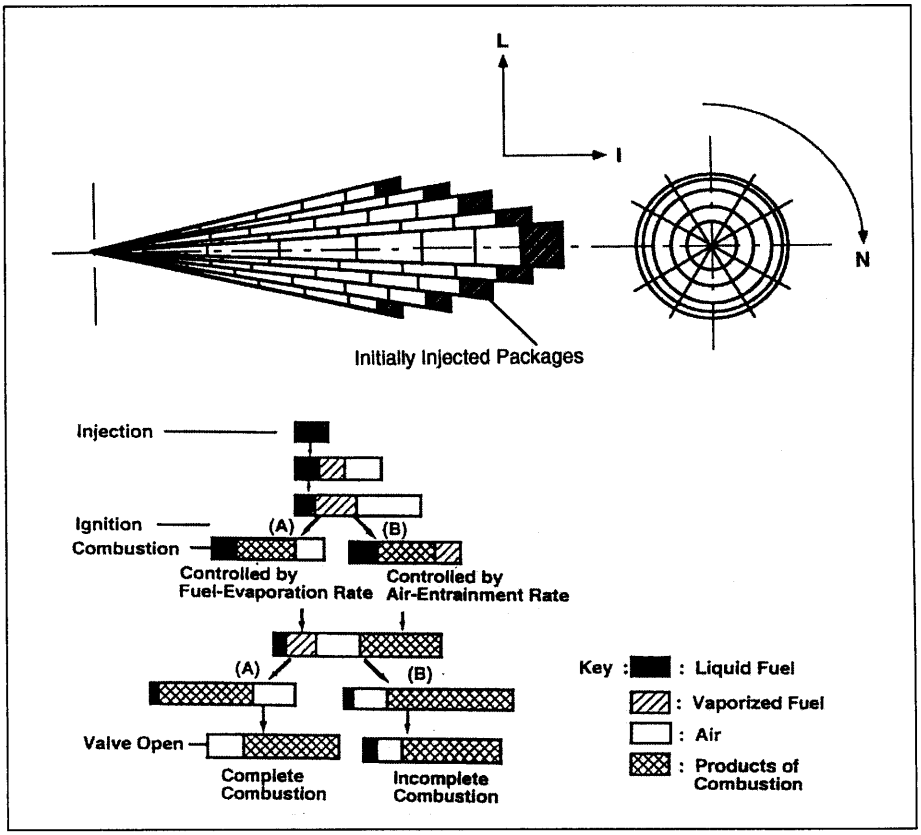

Figure 5.2 Modeling concept. Fuel jet represented by 5 radial X 100 axial zones. Each zone initially contains fuel only and proceeds as a fuel column until break up, at which time air entrainment and droplet vaporization begins. Combustion starts after ignition criteria are met, and proceeds at a rate determined by chemical kinetics, fuel vaporization, or air entrainment. From Hiroyasu [2].

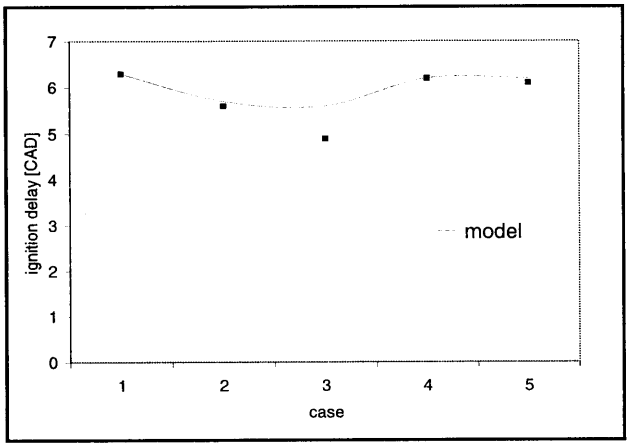

Figure 5.3 Experimental and predicted ignition delay for Cases 1 through 5. 4.8-4.9 bar IMEP, 55-89 deg C air inlet, -3 to -8 DATC SOI. Experimental delay determined by averaging data over 100 cycles.

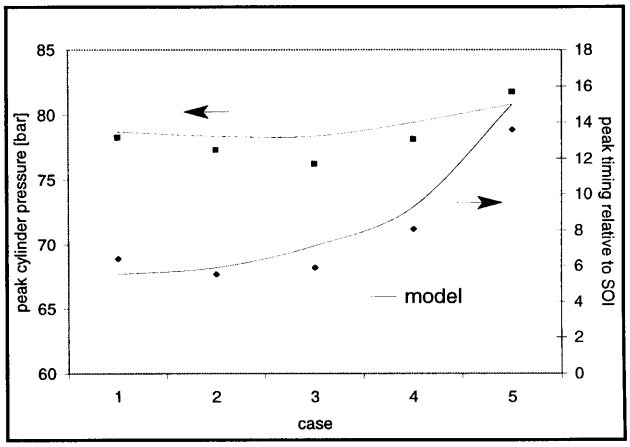

Figure 5.4 Experimental and predicted peak cylinder pressure and timing relative to SOI for the 5 cases.

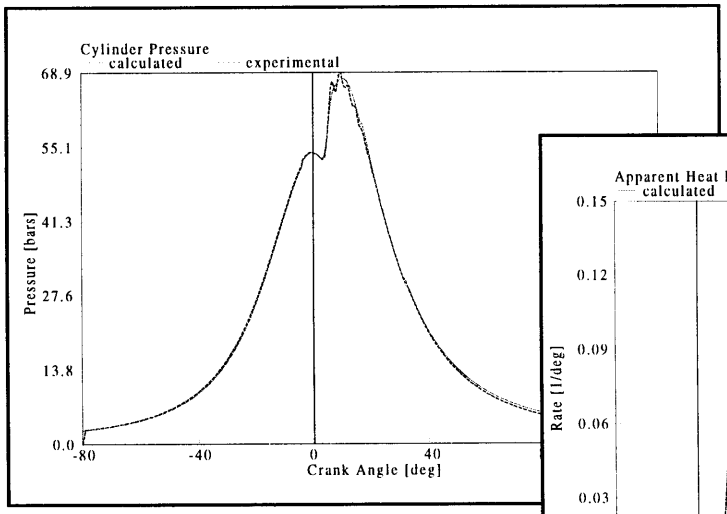

Figure 5.5 Experimental and predicted cylinder pressure for Case 1.

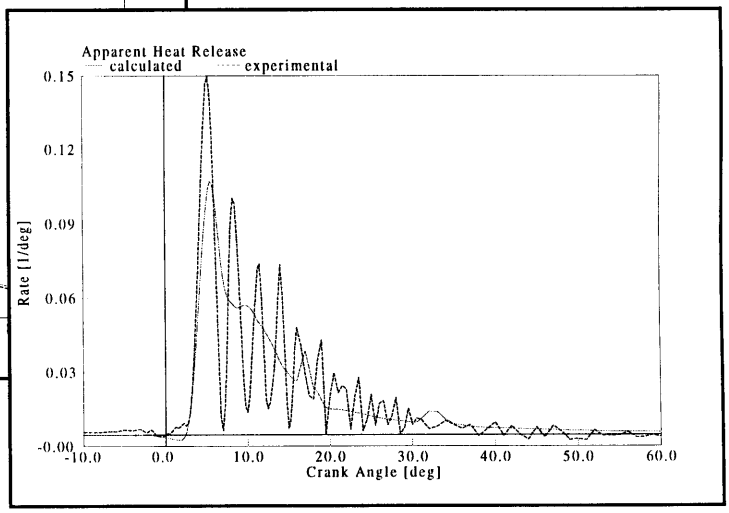

Figure 5.6 Experimental and predicted normalized heat release rate for Case 1.

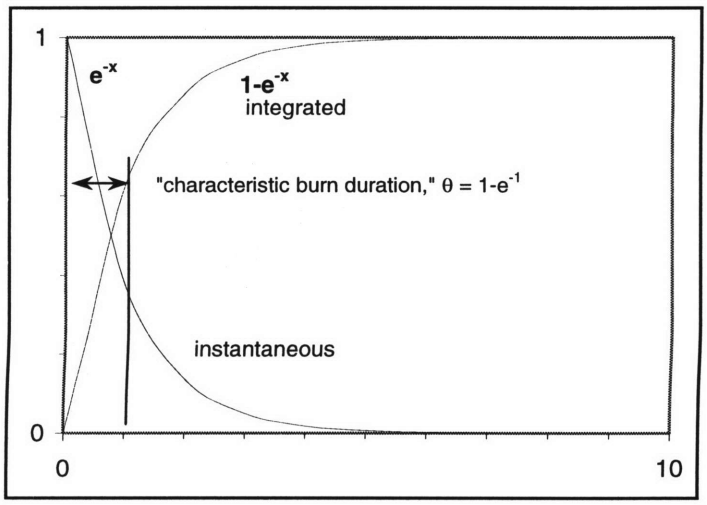

Figure 5.7 Characteristic burn duration defined.

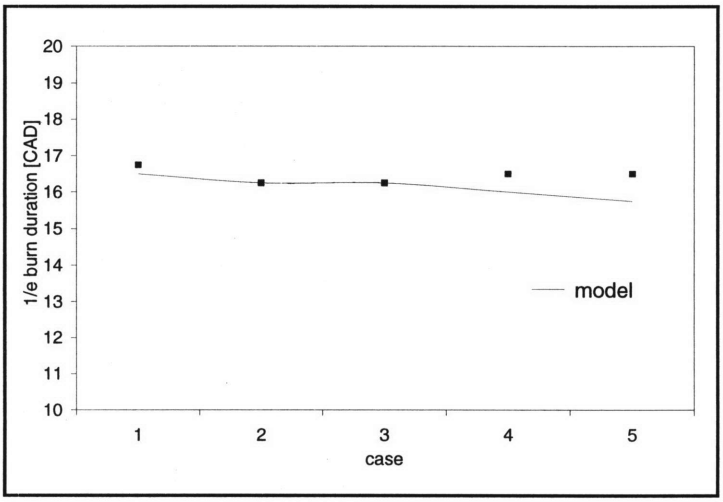

Figure 5.8 Experimental and predicted burn duration for Cases 1 through 5.

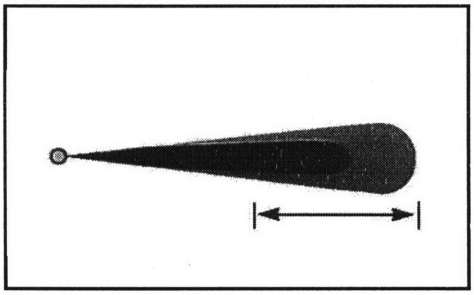

Figure 5.9 Fuel jet at 4 DSOI (-7.5 DATC). Dark area represents liquid-containing region, light color represents region containing fuel in vapor phase only. Arrow represents chemiluminescent region. From Dec [4].

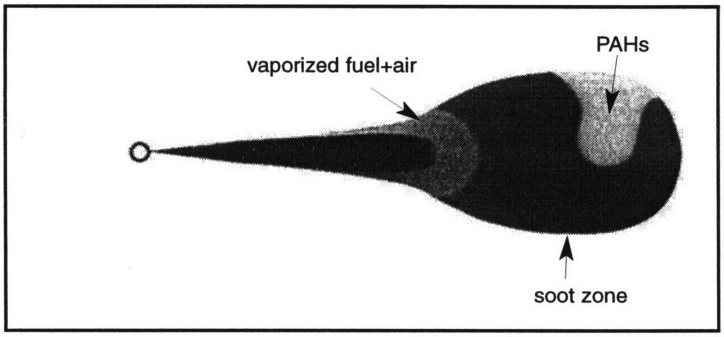

Figure 5.10 Fuel jet at 6 DSOI (-5.5 DATC). Dark bulb-shaped region represents area containing soot. Bright area indicates PAHs. From Dec [4].

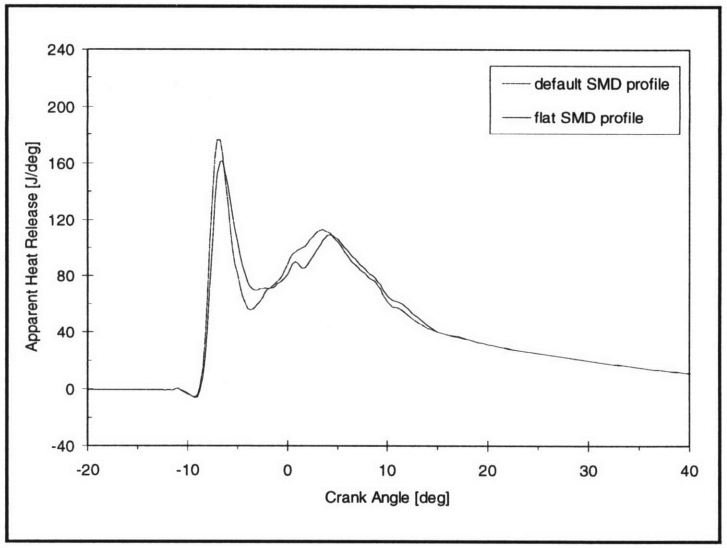

Figure 5.11 Predicted heat release for experimental conditions given.

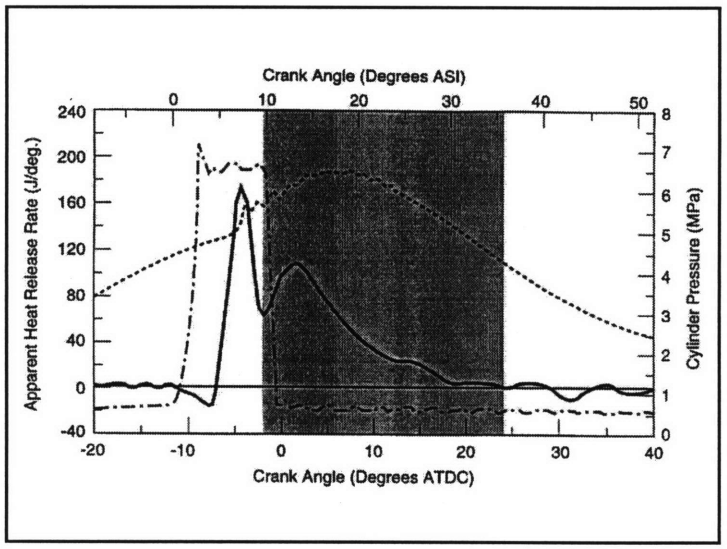

Figure 5.12 Experimental heat release [4].

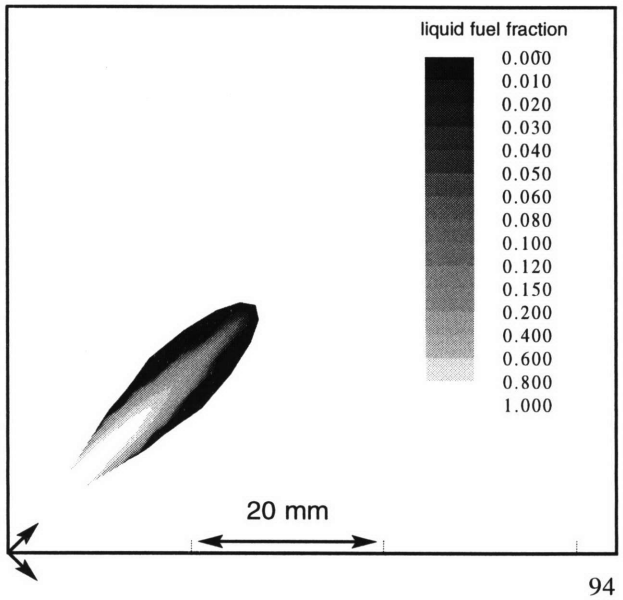

Figure 5.13 Typical fuel jet penetration for default SMD radial distribution profile. Contours are plotted as the ratio of liquid to total fuel, with darkest shading corresponding to zero liquid fuel (100% vapor).

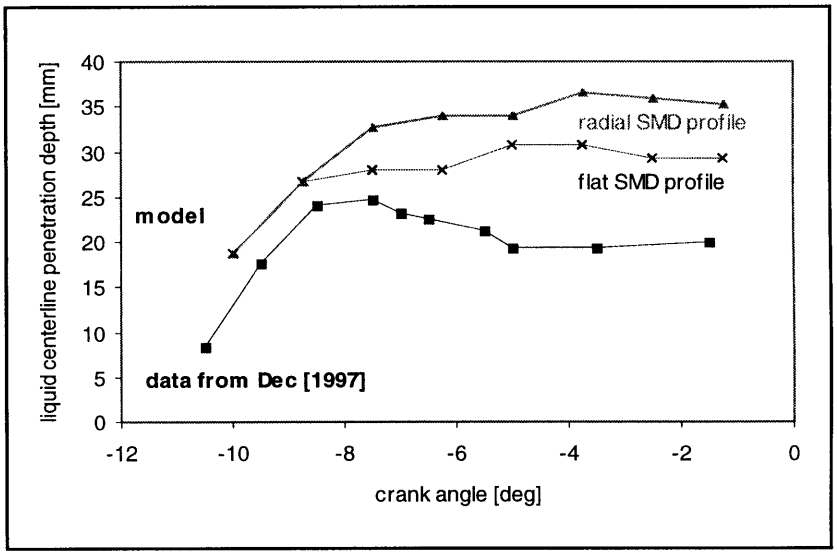

Figure 5.14 Experimental and predicted liquid fuel penetration. Flat SMD profile corresponds to a uniform initial droplet diameter distribution radially across the jet, while radial SMD profile corressponds to the default radial distribution function placing smaller droplets at the jet periphery.

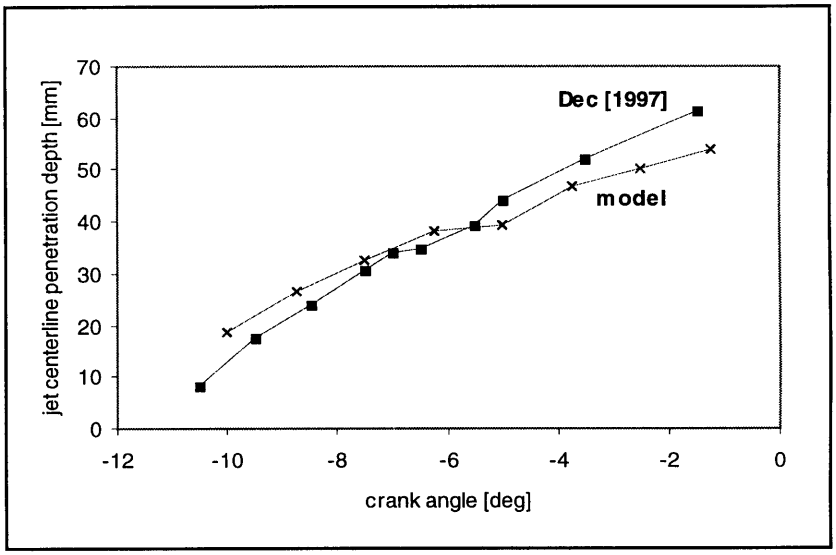

Figure 5.15 Experimental and predicted jet penetration depth.

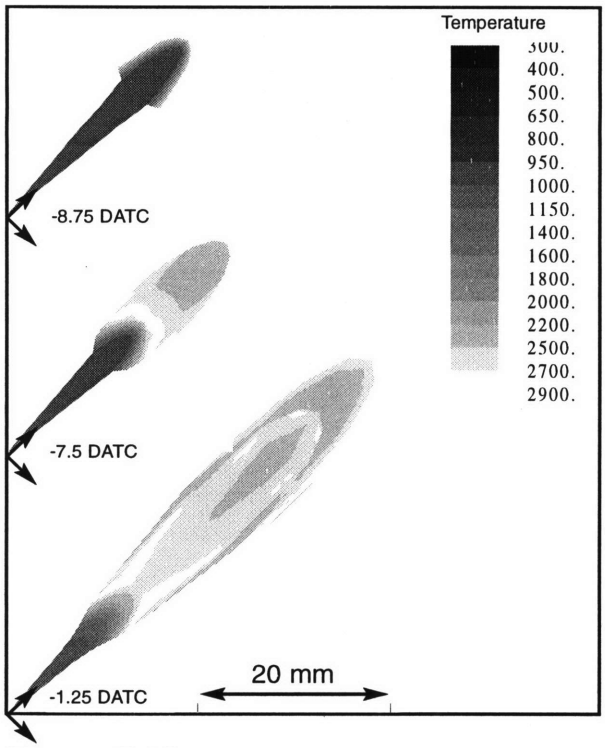

Figure 5.16 Temperature contours at three points in time during ignition, pre-mixed, and mixing controlled phases, respectively.

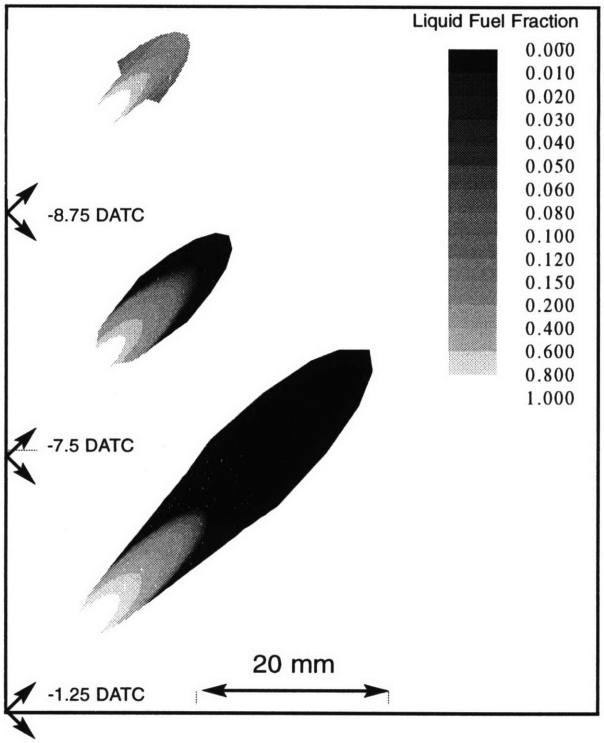

Figure 5.17 Liquid fuel fraction contours at three points in time during ignition, pre-mixed, and mixing controlled phases, respectively. Note contour corresponding to fraction of 1 (100% liquid) not shown here.

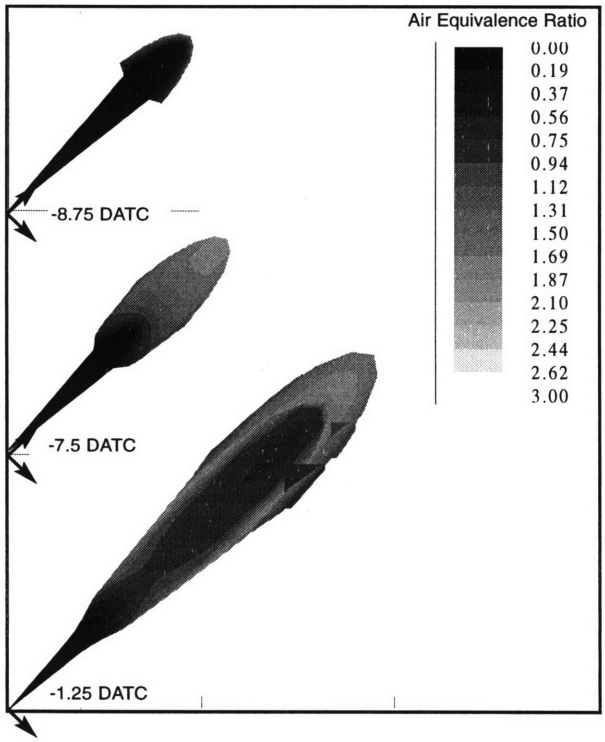

Figure 5.18 Equivalence ratio contours at three points in time during ignition, pre-mixed, and mixing controlled phases, respectively.

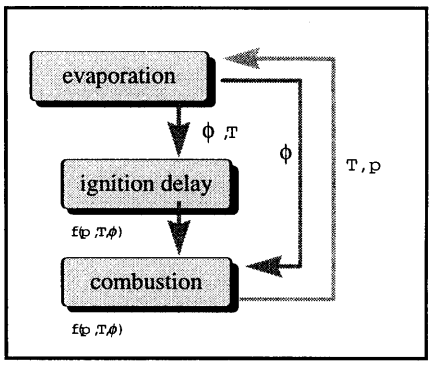

Figure 5.19 Modeled process interdependencies. T, p, ϕ, represent local temperature, pressure, and equivalence ratio.

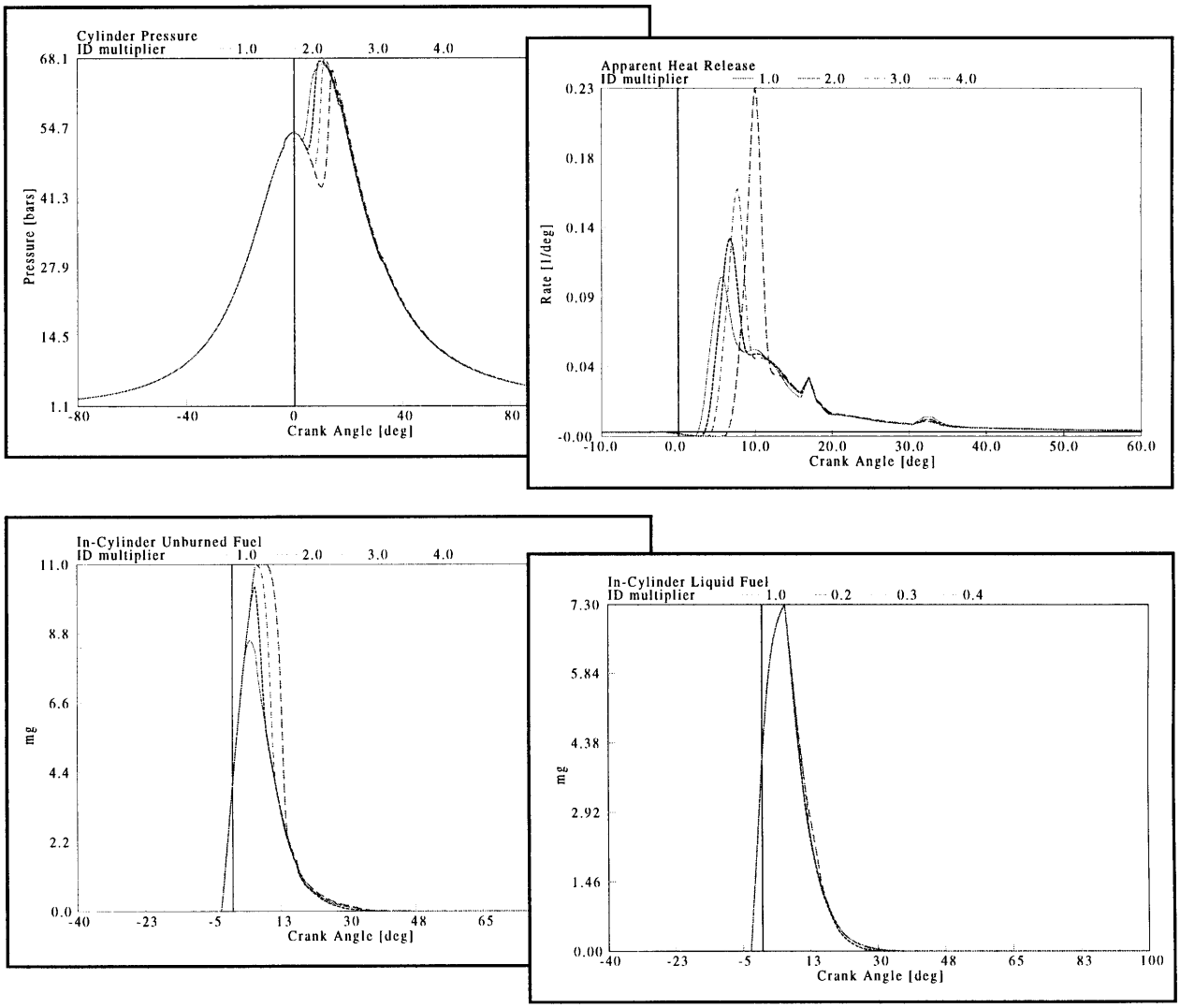

Figure 5.20 Impact of **ignition delay multiplier** on pressure, heat release, unburned, and liquid fuel traces. ID multiplier varied from varied from 1 to 4. M_c, M_v = 1.

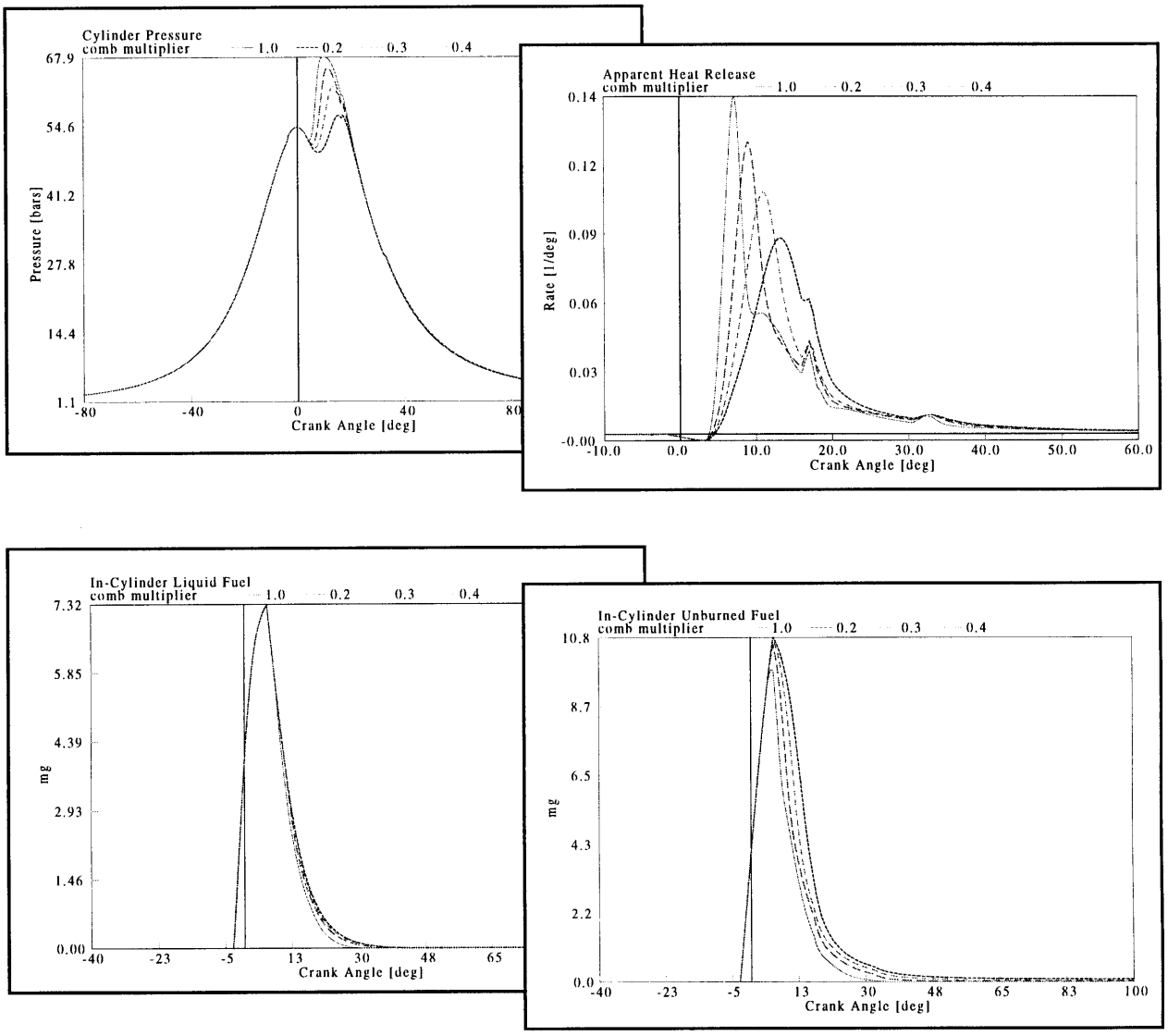

Figure 5.21 Impact of **combustion multiplier**; varied from 0.2 to 1.0. M_i, M_V = 1.

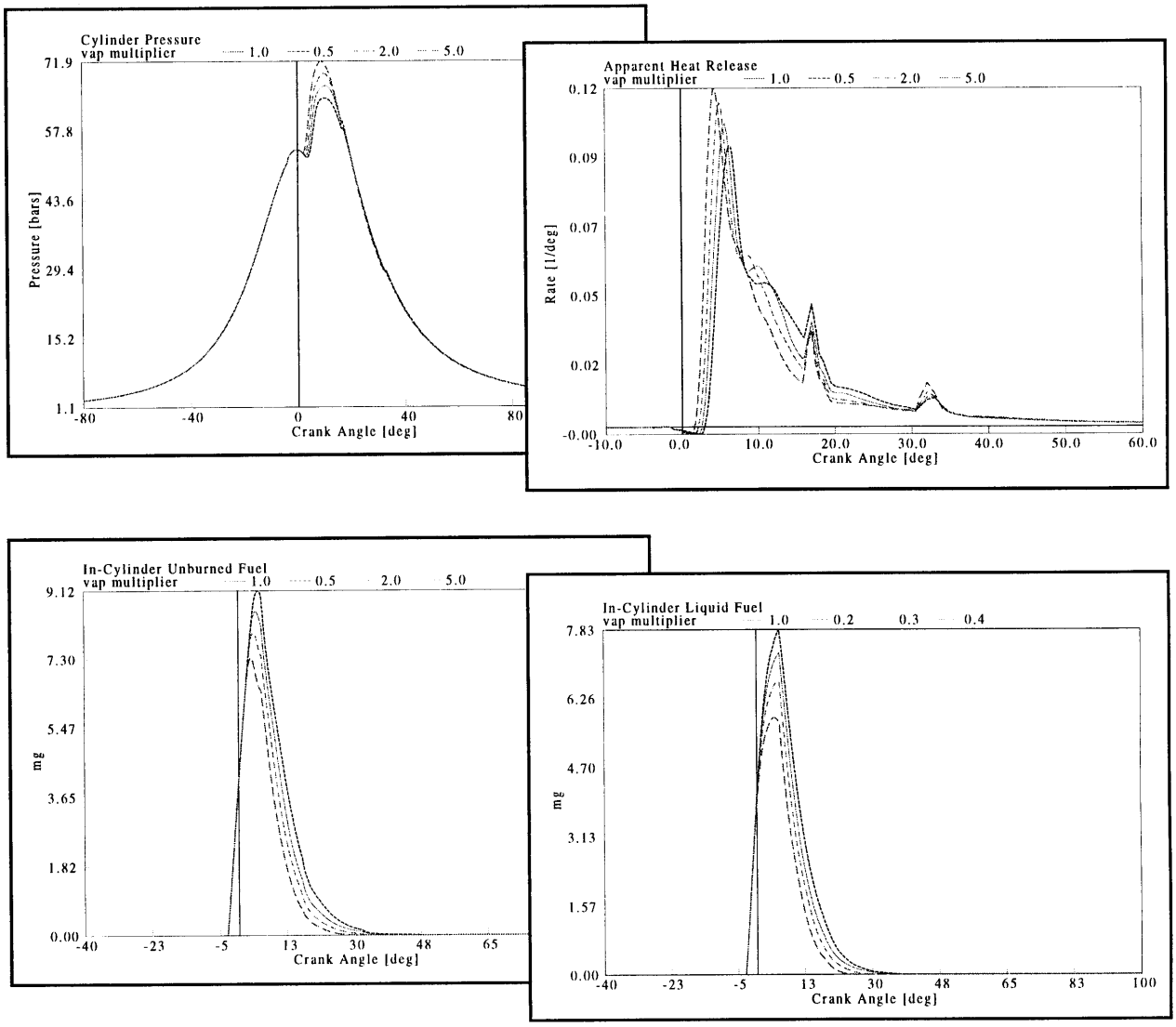

Figure 5.22 Impact of **vaporization multiplier**; varied from 0.5 to 5. M_c, M_i = 1.

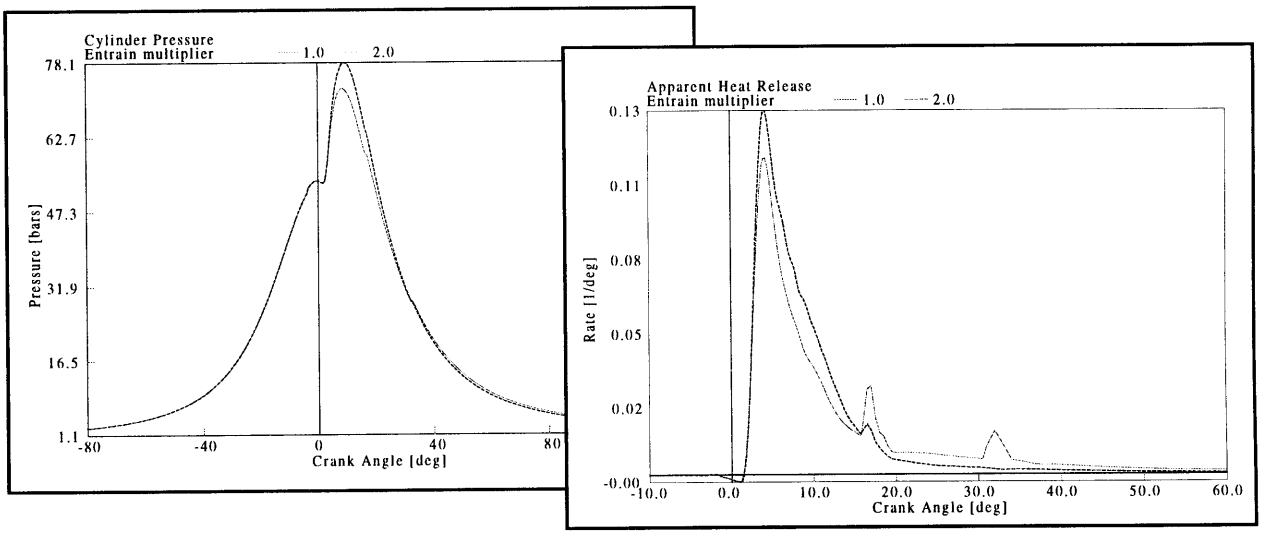

Figure 5.23 Impact of entrainment rate multiplier. Mv = 5; M_j, M_c = 1.

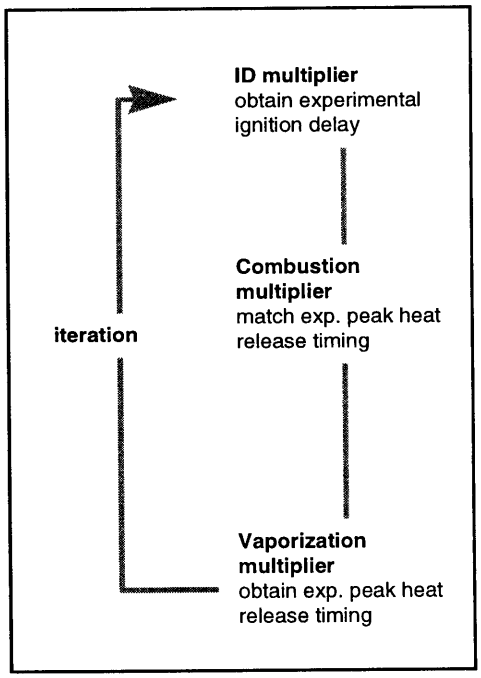

Figure 5.24 Multiplier method for Phase I modeling.

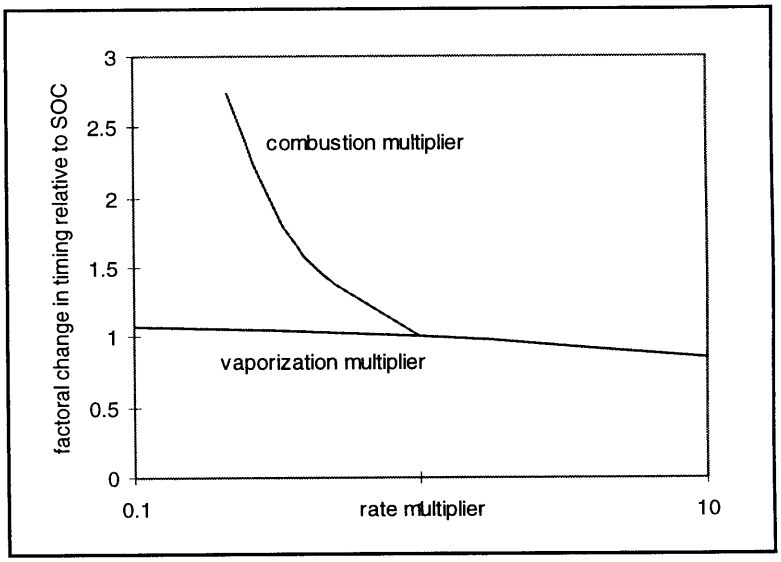

Figure 5.25 Impact of vaporization and combustion rate multipliers on peak heat release timing relative to SOC. (Case I operating conditions.)

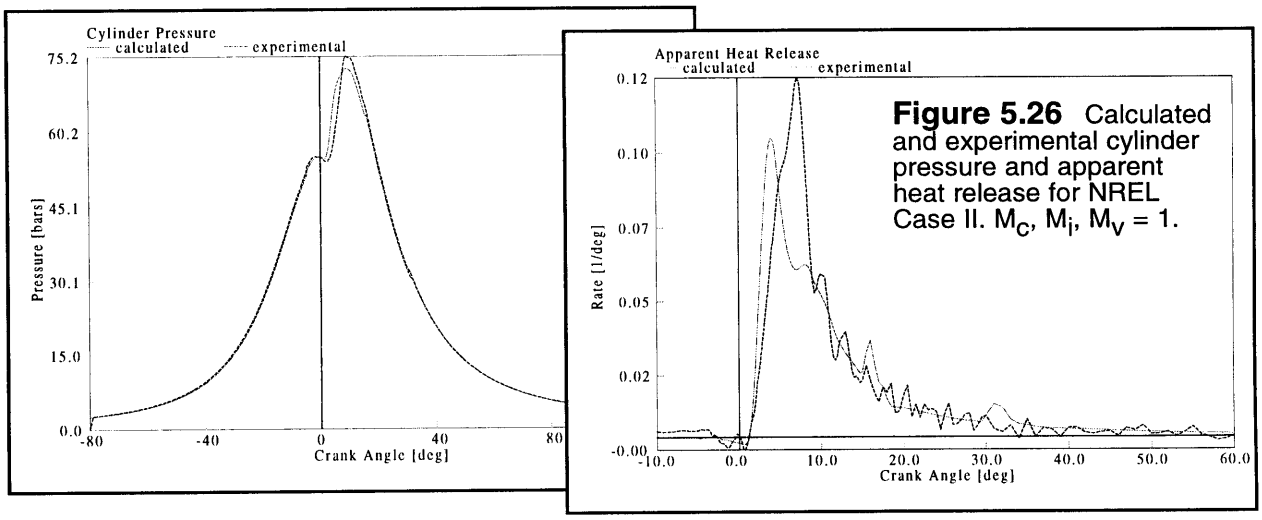

Figure 5.26 Calculated and experimental cylinder pressure and apparent heat release for NREL Case II. M_c, M_i, M_v = 1.

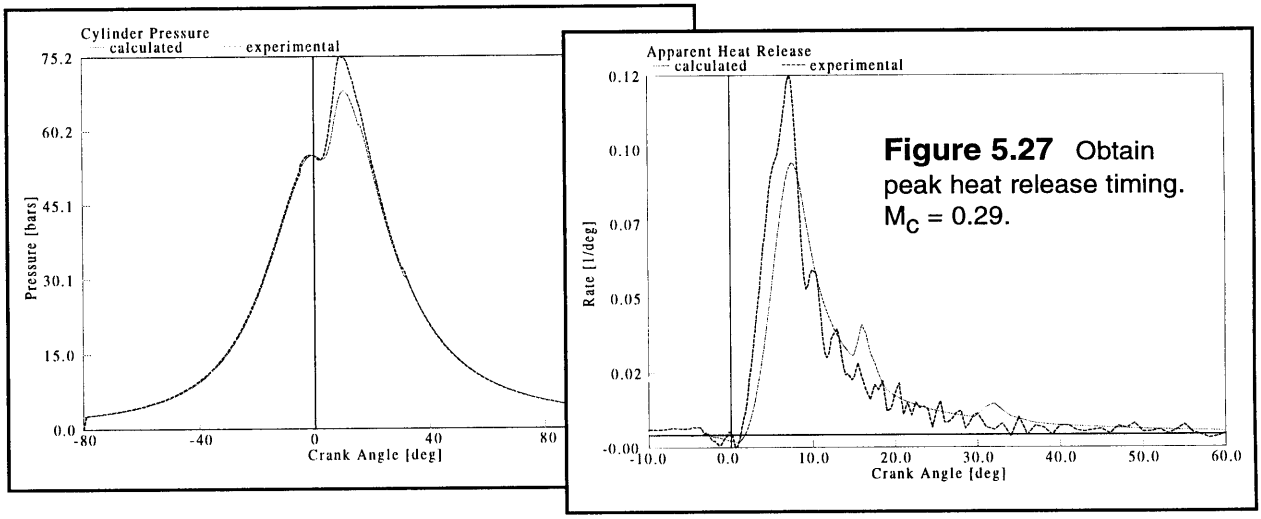

Figure 5.27 Obtain peak heat release timing. M_c = 0.29.

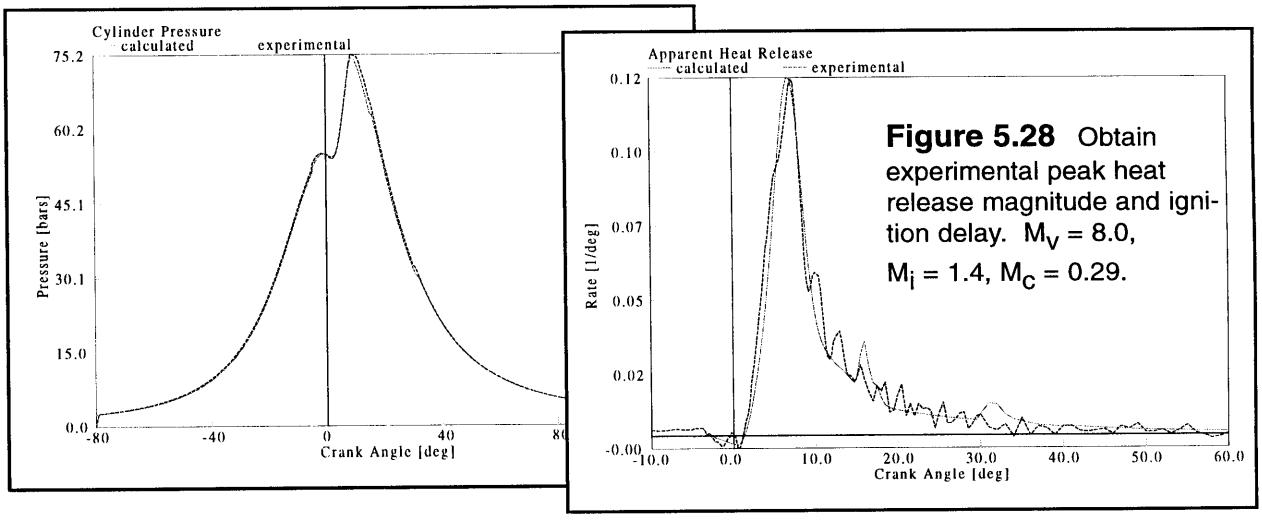

Figure 5.28 Obtain experimental peak heat release magnitude and ignition delay. M_v = 8.0, M_i = 1.4, M_c = 0.29.

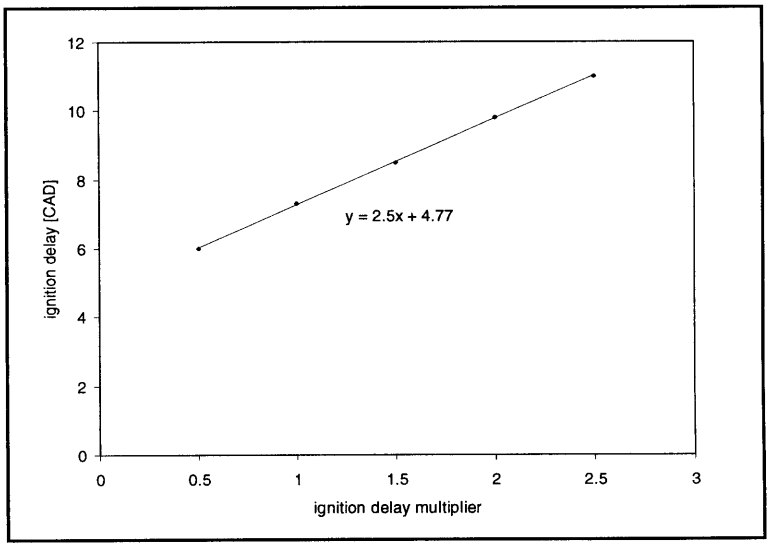

Figure 5.29 Impact of ignition delay multiplier on peak heat release. ENSYN Case I conditions.

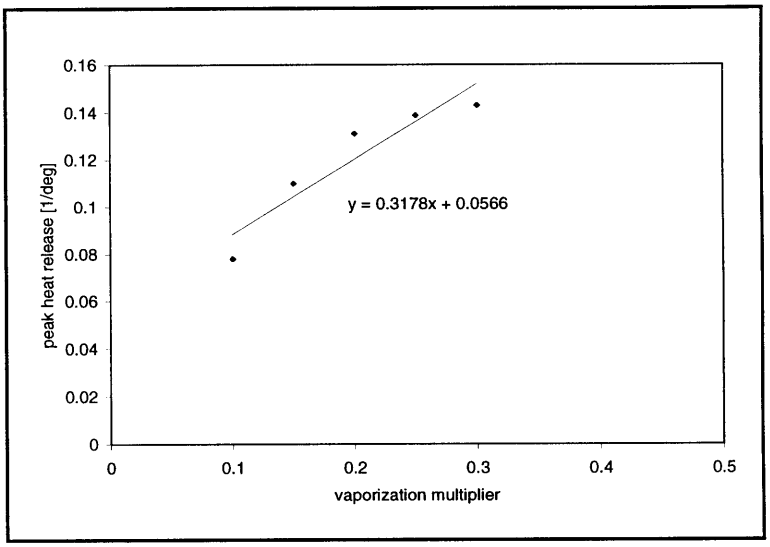

Figure 5.30 Impact of vaporization multiplier on peak heat release. ENSYN Case I conditions.

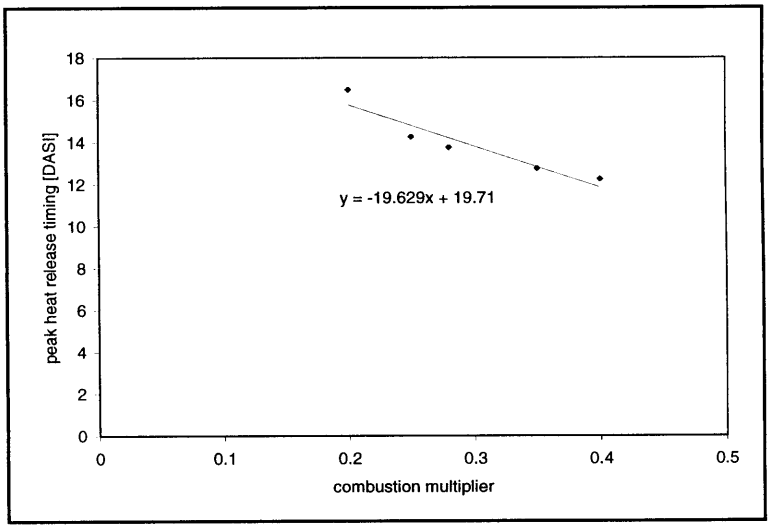

Figure 5.31 Impact of combustion multiplier on peak heat release timing relative to SOI. ENSYN Case I conditions.

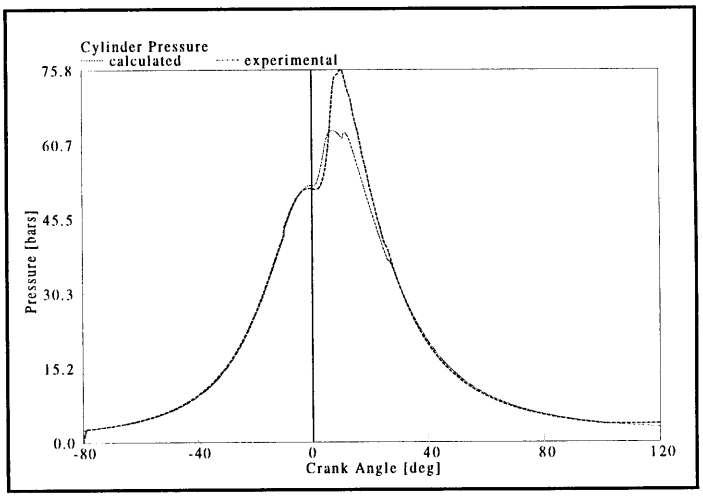

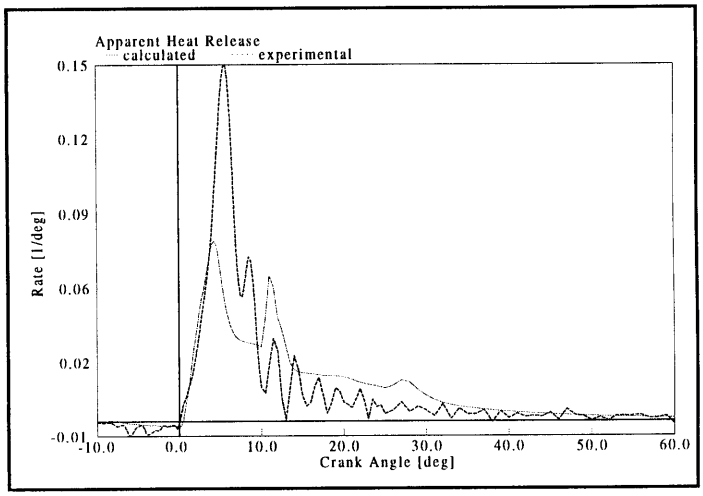

Figure 5.32 Predicted and experimental cylinder pressure and heat release rate when correct ignition delay is obtained by reducing vaporization. NREL Case I; $M_V = 0.07$; M_C, $M_i = 1$.

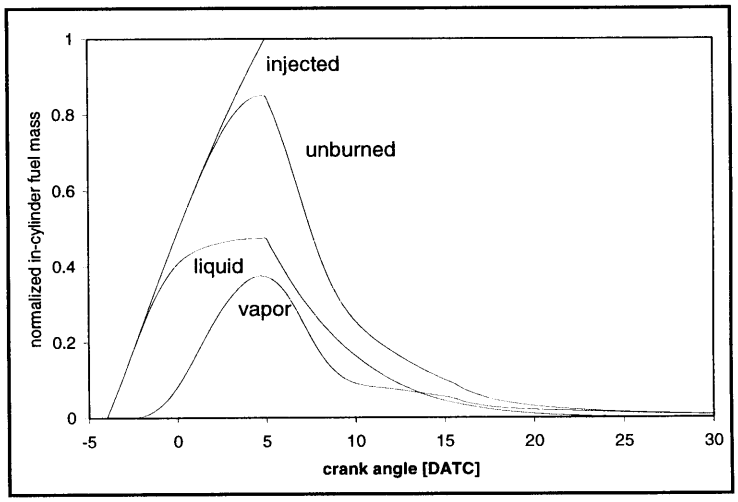

Figure 5.33 Case (a) calculated in-cylinder fuel distribution versus crank angle for NREL case II. $M_c = 0.29$, $M_v = 8.0$, $M_i = 1.5$. All curves normalized by total fuel injected per cycle.

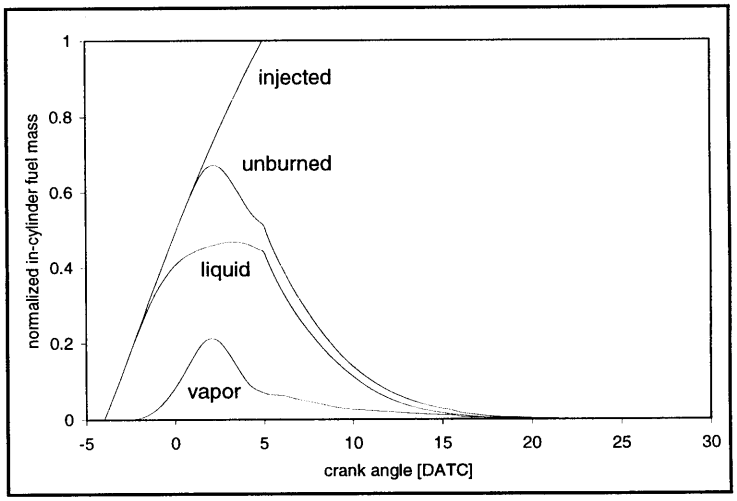

Figure 5.34 Case (b), $M_c = 1$, $M_v = 8.0$, $M_i = 1.5$. Represents NREL II hypothetical case where combustion rate equals that of diesel.

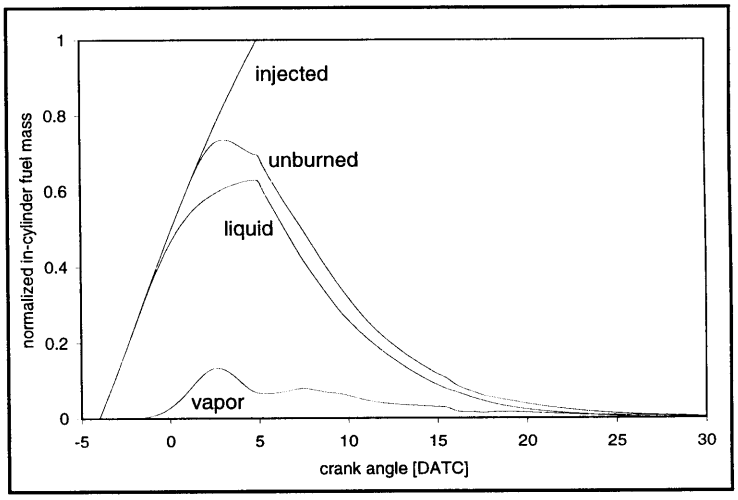

Figure 5.35 Case (c), all multipliers equal to one, representative of diesel combustion with experimental set up.

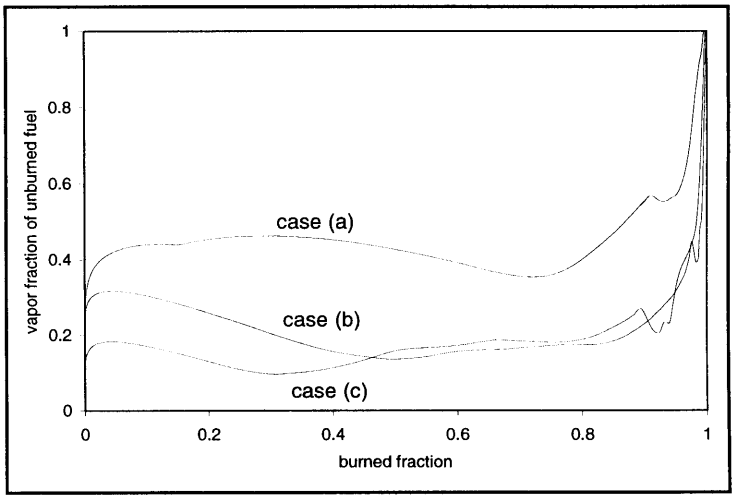

Figure 5.36 Fuel vapor fraction of unburned fuel versus burned fraction. Burned fraction of 0+ corresponds to SOC, 1 corresponds to EOC.

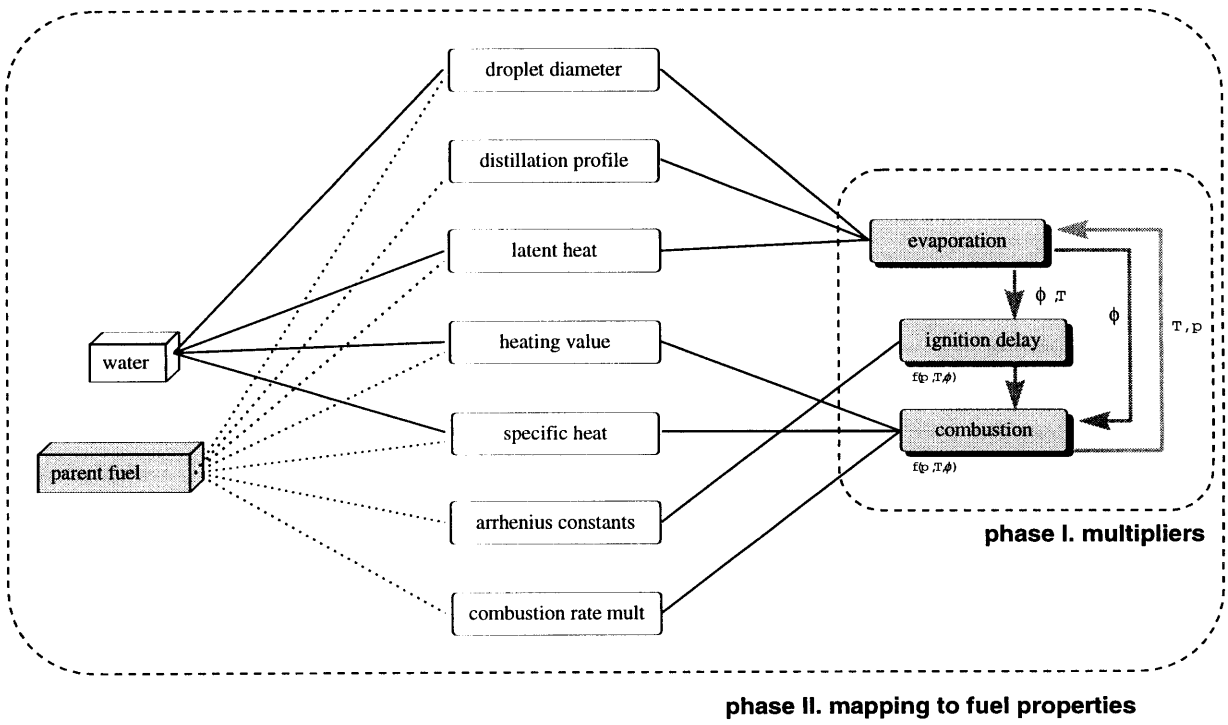

Figure 5.37 Phase II modeling and related fuel properties. Gas specific heat is calculated internal to the model based on input fuel composition and JANAF data. Arrhenius and combustion rate multipliers obtained via fit to experimental data as in Phase I. Distillation profile input on water-free basis.

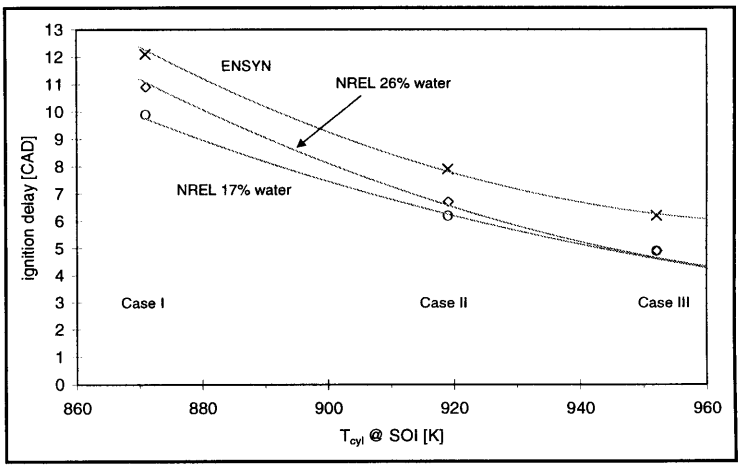

Figure 5.38 Predicted and experimental ignition delay for ENSYN and NREL oils. Experimental data represented by solid lines (obtained by regression, per Chapter 3). NREL 26% water content prediction based on constants obtained from 17% case.

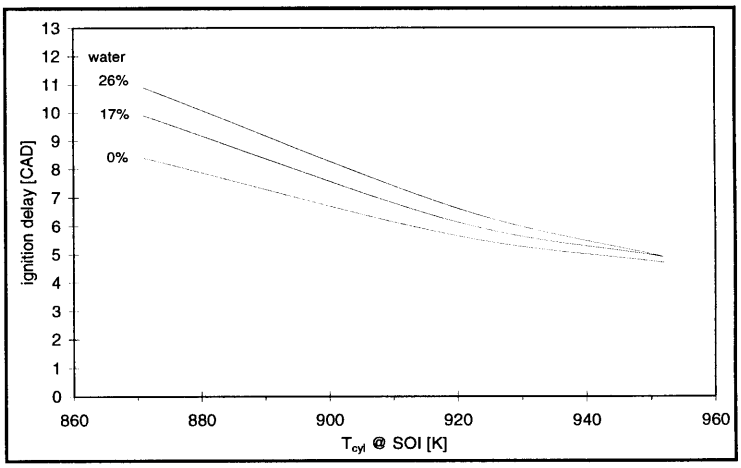

Figure 5.39 Impact of water content on ignition delay for NREL oil. (simulation)

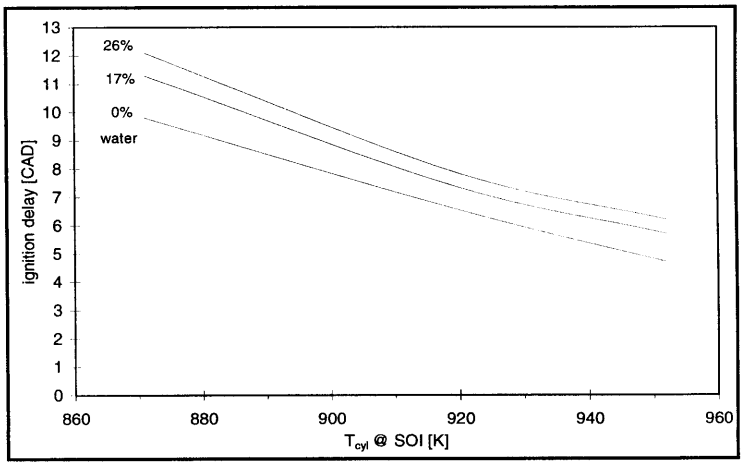

Figure 5.40 Impact of water content on ignition delay for ENSYN oil. (simulation)

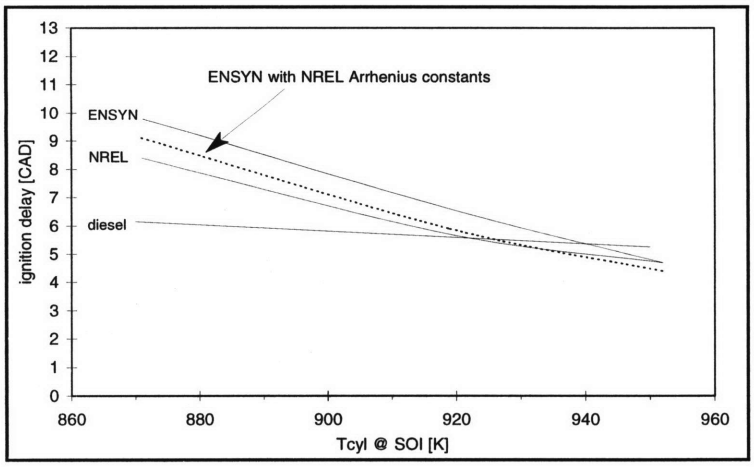

Figure 5.41 "Parent fuel" (water free) predicted ignition delay. Measured diesel delay plotted for reference. Dotted line represents ENSYN fuel prediction using NREL chemistry constants. Residual difference from NREL due to slower vaporizaton.

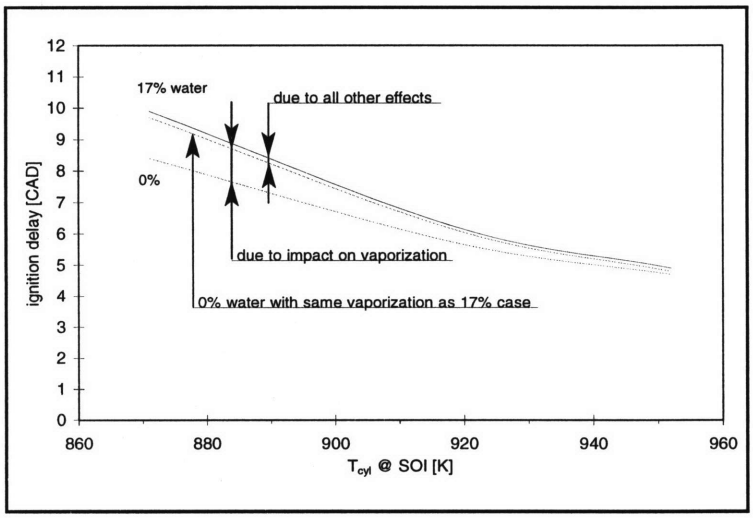

Figure 5.42 Impact of water on ignition delay for NREL oil. Estimated effect due to reduced vaporization rate versus all other effects. Intermediate curve represents 0% case forced to have the same vaporization vaporization profile as 17% case.

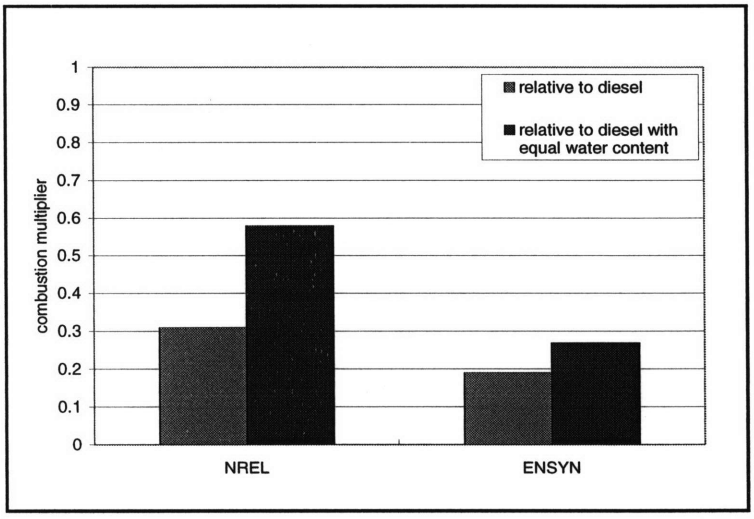

Figure 5.43 Relative combustion rate of NREL and ENSYN oils with respect to diesel fuel (combustion rate = 1). Averaged combustion multipliers of Cases I-III.

Chapter 6 Summary, Conclusions and Recommendations

6.1 Summary

The purpose of this work was to characterize how the combustion of biomass pyrolysis oils in a high speed diesel engine differs from that of No. 2 fuel oil, and to elucidate connections between various pyrolysis process parameters and resulting combustion properties. This objective was pursued by comparing the ignition delay and heat release data of diesel fuel and two wood pyrolysis oils made using the ENSYN Rapid Thermal Process, and NREL Vortex Ablative Pyrolysis, which differ in reactor configuration, hot gas residence time, condensation train temperature, and extent of feedstock drying. The ENSYN process is the most widely implemented commercial process, while the NREL process represents a more elaborate laboratory controlled system which utilizes hot gas filtration and careful collection of volatile species.

Combustion experiments demonstrated that while the pyrolysis oils exhibited similar indicated thermal efficiencies to diesel fuel, they were characterized by much greater apparent ignition activation energies, longer delays, shorter burn duration, and lower peak heat release and pressure rise rates. Most problematic was that neither pyrolysis oil could ignite without combustion air preheating. It was also found that the

NREL oil consistently exhibited shorter ignition delay times and characteristic burn durations than the ENSYN oil, leading to an examination of the possible reasons for the better performance of the NREL oil. Based on what was known about the ENSYN and NREL pyrolysis processes, four parameters which could be responsible for the differing performance were selected for investigation: average molecular weight (an indicator of the severity of thermal cracking), volatiles profile (a measure of volatiles collection efficiency), water content (a measure of the extent of feedstock drying and other process variables), and physical properties which were derivative of these.

Physico-chemical analysis showed that of the four parameters, only the water content and the average molecular weight were significantly different across the two oils; the ENSYN oil contained more water (26.3 versus 16.9 wt %) and had a greater average molecular weight (550 versus 370 g/mol) than the NREL oil. Therefore additional combustion experiments were carried out with a hydrated NREL oil whose water content equaled that of the ENSYN oil. By comparing the experimental results to those of the base NREL and ENSYN oils, it was possible to ascertain the combustion significance of the differing water content, and molecular weight.

While water addition to the NREL oil increased its ignition delay, it remained significantly lower than that of the ENSYN oil, accounting for approximately half the difference in ignition delay times at lower charge temperatures. Therefore, while water content is an important parameter with respect to combustion, the lower water content cannot fully account for the better ignition characteristics of the NREL oil, suggesting that the difference in thermal cracking is also important.

A modeling study was undertaken to interpret the experimental heat release and ignition delay data in terms of particular in-cylinder physical and chemical processes, and to relate these to particular fuel properties. In this way, pyrolysis combustion was characterized in relation to diesel fuel combustion, and the physics underlying the role of water in the pyrolysis oils could be accounted for, allowing a simulated comparison of "water free" NREL and ENSYN oils, whose differences presumably would be due solely to the differing extent of thermal cracking.

6.2 Conclusions

The results showed that

1. The indicated thermal efficiency of both the pyrolysis oils equaled that of the diesel fuel, though they exhibited excessively long ignition delay and required a moderate degree of combustion air preheating (55 deg C) to ignite reliably.

2. Apart from longer ignition delay, the major difference characterizing pyrolysis oil combustion is that it is always kinetically limited. This is due to a combination of rapid vaporization and slow chemistry. In contrast, diesel combustion is predominantly mixing limited.

3. The longer ignition delay of both pyrolysis oils results from slower chemistry, not slower mixing, though increasing mixing rates would nonetheless reduce ignition delay. The greater surface tension and viscosity of the pyrolysis oils do not appear to cause poor atomization; in general, the heat release profiles were consistent with greater fuel vaporization rates than with diesel fuel.

4. Water significantly affects the ignition delay of pyrolysis oils, predominantly through its impact on the heat of vaporization, which in turn reduces the vaporization rate. It respectively accounts for approximately 15% and 20% of the ignition delay at low charge temperatures, for the NREL and ENSYN oils, assuming that physical properties remain the same when water content is removed.

5. Long ignition delay is inherent to the chemical makeup of both pyrolysis oils; even on a water-free basis, the oils exhibit longer ignition delays due to high overall ignition activation energies (circa 4300 K, versus 3500 K for the diesel fuel).

6. The better performance of the NREL oil derives from its lower water content *and* its lower molecular weight. The additional thermal cracking undergone by the NREL oil appears to have upgraded it by improving its chemical and vaporization characteristics, in approximately equal proportions relative to affect on ignition delay, accounting *in toto* for approximately 50% of the difference in ignition delay times at low charge temperatures between the NREL and ENSYN oils. The differing water content of the two oils accounts for the remainder.

7. The slow combustion chemistry exhibited by both oils is due to the water content and the inherent fuel chemistry of the oils. After taking water into account, the characteristic combustion rates of the NREL and ENSYN oils are on average approximately 60% and 25% of diesel fuel, respectively. Without accounting for the water, the corresponding rates drop to 30% and 20% of diesel fuel, respectively.

6.3 Recommendations

Increasing the severity of thermal cracking and reducing water content has yielded better performing pyrolysis oils. While the effect of water content is well characterized, the impact of thermal cracking is not. Having identified it as an important parameter with respect to combustion, it is worthwhile to examine to what extent manipulating the thermal cracking severity can impact the combustion behavior of the oil produced using a particular method. This can be pursued by investigating the combustion characteristics of a series of oils whose only difference is the pyrolysis residence time. Furthermore, molecular weight is

only a quantitative surrogate indicator of the extent of thermal cracking, and lumps together a variety of effects on chemical makeup. To understand the true impact of the extent of thermal cracking on pyrolysis oil properties, the pyrolytic lignin fraction of the oils must be chemically analyzed in addition to the aqueous fraction. Finally, the greater vaporization rates characteristic of the pyrolysis oils cannot be accounted for using a quasi-steady equilibrium distillation model; it appears that the disruptive processes observed in atmospheric single-droplet combustion experiments of high Lewis number drops may also occur within the combustion chamber. Visualization studies in a combustion bomb apparatus could yield insight into this phenomenon under diesel-engine ambient conditions.

Apart from the unacceptably long ignition delay, which appears to be potentially tractable with adjustments to existing pyrolysis methods, the corrosivity and deposit buildup of the pyrolysis oils must be addressed before they can be utilized in any practical diesel combustion system. While the hot gas filtration of the NREL oil appears to have reduced its coking tendency relative to the ENSYN oil, further improvements in char removal will be required. Improvements in fuel injection equipment materials and methods borrowing from equipment developed for coal-water slurry combustion can also be pursued as a partial solution.

In sum, pyrolysis oils show promise as utilizable diesel engine fuels from a combustion perspective, but will require advances in char removal efficiency and coking tendencies before they can be widely implemented in existing equipment.

Appendix A Gas chromatograms

Analysis by J. Piskorz at RTI, Ltd. (6/4/98)
DB 1701 capillary column, FID detector.
Initial temperature 45 C for 3min
Ramp rate 10 deg/min up to 195 C
Final temperature 195 C for 5 min.

NREL M2-10 oil

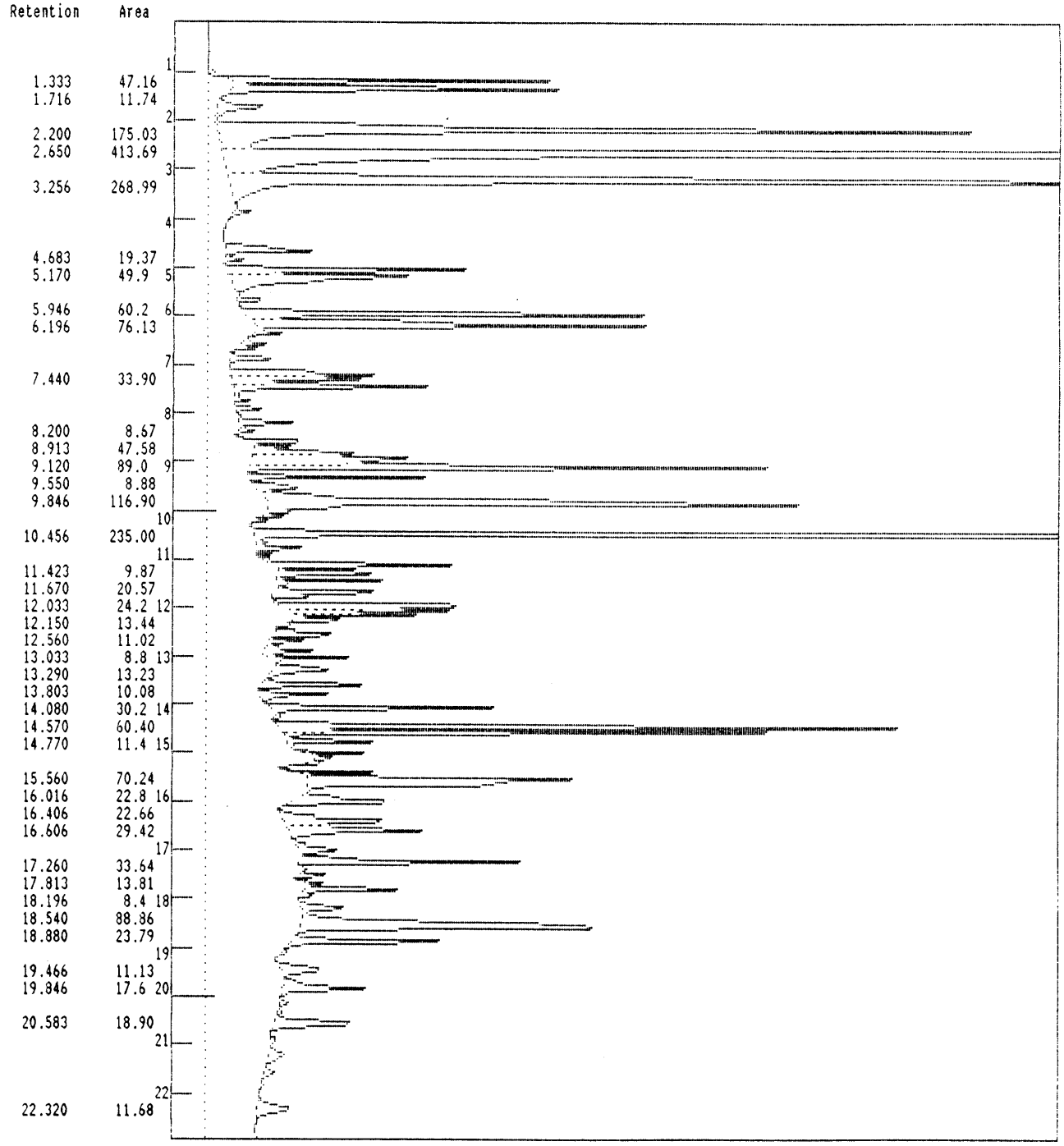

ENSYN RTP 15 TPD

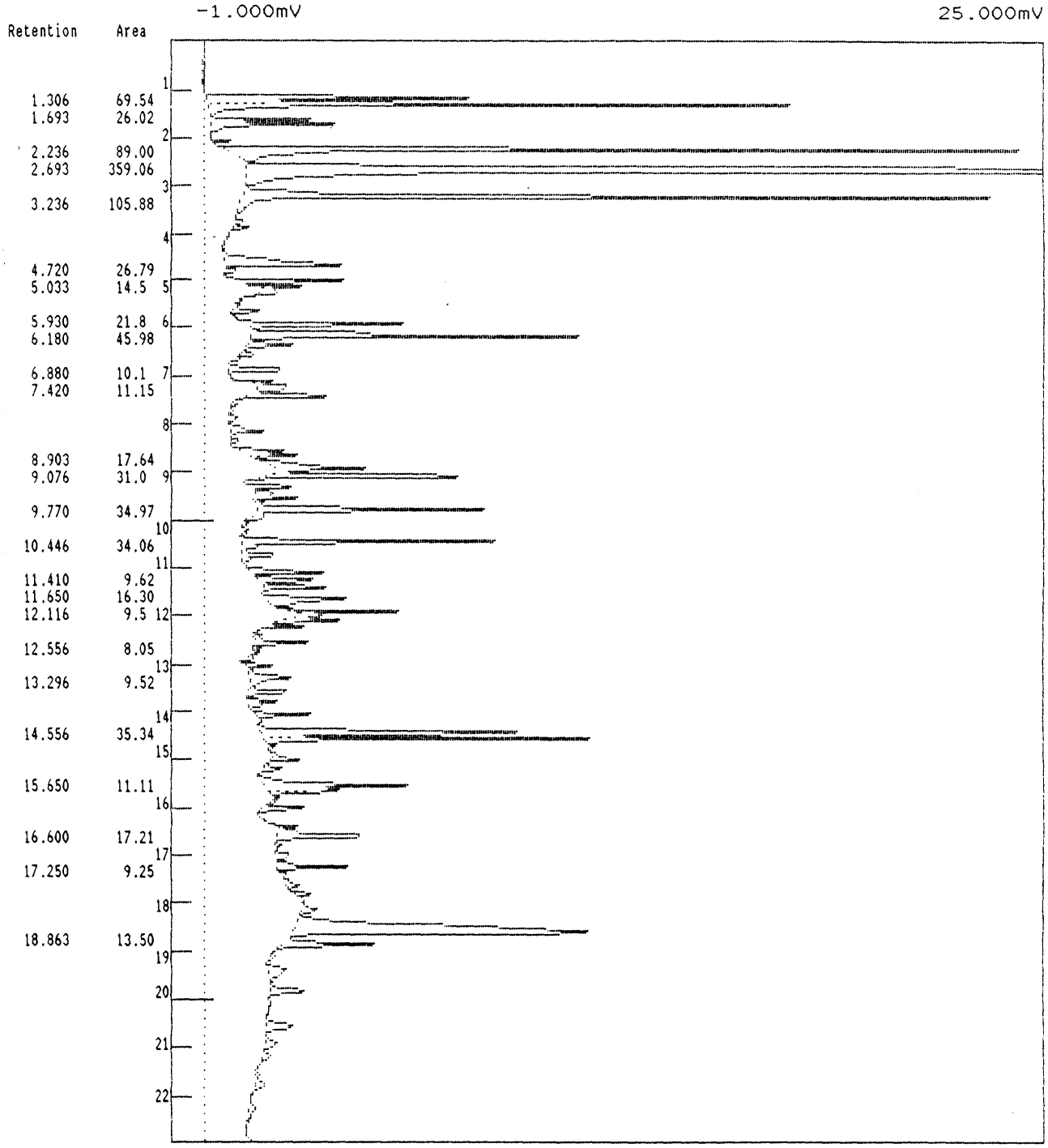

Appendix B Estimation of fuel temperature exiting injector nozzle

volume of fuel passages in nozzle (measured)

$$Vol \approx 0.215 \ cc$$

average residence time in nozzle

$$t = \frac{\dot{Q}}{Vol} \approx 0.5sec$$

average velocity

$$v = \frac{l}{t} \approx 8\text{cm/sec}$$

model as a simple pipe

$$A = \frac{\dot{Q}}{v} \quad D_{eff} \approx 0.0.28\text{cm}$$

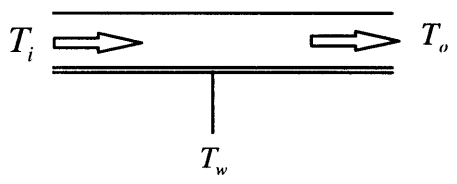

assume constant wall temperature

$$q = \dot{m}C_p(T_o - T_i) = hA\Delta T_{lm}$$

where $\Delta T_{lm} = \dfrac{T_o - T_i}{\dfrac{\Delta T_o - \Delta T_i}{\ln \Delta T_o / \Delta T_i}}$

after some algebra

$$\Delta T_o = T_w - T_o = (T_w - T_i)\exp(-hA/\dot{m}C_p)$$

where $40 < (hA/\dot{m}C_p)$ for any reasonable range of properties

$$\therefore T_o = T_w$$

Appendix C Sample model input file

```
!===DATA FILE for GTpowerS [Version 4.2.1]=====================================
! PROJECT: modelverify :GTpowerS
! DATE:   Wednesday, July 22, 1998
! TIME:   16:38:33
! CREATOR: GT-ISE [Version 4.2.1]

!===RUN SPECIFICATIONS=========================================================
TimeControl-----------------------------------------------------------[4.2.1]
 Periodic [ncyc] New 1 AutoStep 1 [edriver] !TIMCYC DURATN ISTATE TSMAX TSFIX SSTOL MAINDRV
 None None ign !IRESTR IRESTW IRESTINC
FlowControl-----------------------------------------------------------[4.2.1]
 def Off Ign ign Off off !TSMULT HTFLAG HTSS DTHT FLFLAG REALGAS

!===PLOT SPECIFICATIONS========================================================
PlotData--------------------------------------------------------------------
!I/O CMPTYP CMP VARIABLES XLOC
 p  cyl {65544} {temp}

!===REFERENCE OBJECTS==========================================================

Driver----------------------------------------------------------------[4.2.0]
!NAME TYPE CYCDEG DRVFREQ DRVPROF THETAB THETAE
 partc frequency 720.0 [rpm] ign [ic-eo] 0

EngCylCombDIJet-------------------------------------------------------[4.2.0]
!NAME OVIMEP CMBEND AXZONE
 cmb1 1.7 130 100
 5 !ASPECT
 [breakup-mult] [entmultbe] [entmultaf] [entmultimp] 1 1 1 !TBMULT CBAIR CAAIR CWALL WALLJT ENTAMP
ENTEXP
 [smd-mult] !SMDMULT
 def [drop-evap-mult] [tboil10] [tboil50] [tboil75] !TDRAG DVMULT TMP10 TMP50 TMP75
 [comb-mult] !CMBMULT
 [delay-mult] [delay-press-exp] [activa-temp] !CIGN1 CIGN2 CIGN4
 1.35 1.19 1.01 0.85 0.74 !SMD1 SMD2 SMD3 SMD4 SMD5
 model3 1 1 1 !SOOTMDL SFMULT SCMULT NOXMULT

EngCylDataComp--------------------------------------------------------[4.0.6]
 DataComp 1 on {pres htrl} {ign ign} !NAME NCDCOMP COMPARE EXT_DATA FACT_NORM
 THET1> [file1] <
 DATA1> [file2] <
 THET2> [file4] <
 DATA2> [file3] <

EngCylFlow------------------------------------------------------------[4.1.1]
!NAME FLWTYPE DOHEAD DCHEAD HHEAD SWLRAT TMBRAT UPRIME LRATIO PCUPNAME
 flw1 basic def 0 1e-020 [rswirl] def def def pcup

EngCylGeom------------------------------------------------------------[4.0.6]
!NAME BORE STROKE RODLEN PINOFF COMPRAT HCLEAR
 cylg1 80.26 88.9 155.6 0 [CRatio] 0.5

EngCylHeatTr----------------------------------------------------------[4.2.0]
!NAME HTRTYP HTMULT AHEAD APIST MULTRAD HGFILE
 htr1 woschni 1 1 1.21 ign ign
```

```
EngCylJetOutput-------------------------------------------------------------[4.0.6]
 jetout 1 off {smd} !NAME NCJPLOT XYPLOT XY_PLOTS
 0.1 0.3 0.5 0.7 0.9 !AXIP1 AXIP2 AXIP3 AXIP4 AXIP5
 0.5 0.5 0.5 0.5 0.5 !RADIP1 RADIP2 RADIP3 RADIP4 RADIP5
 off 5 {phb liqfue tzb} !CONTOUR DUMPFREQ XYZ_PLOTS
 off 0.5 zone {phb} !SPATIAL RADLOC XAXIS SPAT_PLOTS

EngCylPistCup---------------------------------------------------------------[4.2.0]
!NAME DCPIST HCPIST DOPIST HHPIST
 pcup 32 15.2 32 7.6

EngCylTWall-----------------------------------------------------------------[4.0.3]
!NAME THEAD TPIST TCYL
 tw1 520 520 400

EngFrictionCF---------------------------------------------------------------[4.2.0]
!NAME CFA CFB CFC CFD
 fric1 0.32 0.001 0.08665 0.0009

FPropBasic------------------------------------------------------------------[4.2.1]
!NAME FILENAME EVAPFLUID
 h2o <h2og.prp> ign
 o2 <o2.prp> ign
 n2 <n2.prp> ign
 fuelli [fuelli] ign
 fuelg [fuelg] ign

FPropMixture----------------------------------------------------------------[4.2.1]
!NAME STBURN FLBASIC FMI
 resi1 burn {air 0.97 fuelli 0.03}
 air noburn {n2 [n2] o2 [o2] h2o [h2o]}

FStateInit------------------------------------------------------------------[4.2.1]
!NAME PRES TEMP FLUID FMI
 ptvolef 1.01 298 {air 1}
 ptambint [imap] [imat] {air 0.97 resi1 0.03}
 ptivc [imap] [imat] {air 0.97 resi1 0.03}
 ptambexh 1.5 1000 {air 1}

InjectionProfile------------------------------------------------------------[4.0.6]
 injprf 0.21 4 0.7 !NAME DNOZZ NHOLES CNOZZ
 presprof [SOI] [fuelmass] !TYPE THINJ FUELMG
 THET> 0 [inj-mid1] [inj-mid2] [inj-duration] <
 PROF> [inj-open-press] [inj-mid-press1] [inj-mid-press2] [inj-close-press] <

ValveCam--------------------------------------------------------------------[4.2.1]
 val1 44 1 2.3341 0 180 !NAME VDIA VSTRAN VSTRLF VLASH VTMNG
 THET> -18 0 50 90 <
 LIFT> 0 3.6 3.6 0 <
 L/DI> 0 0.0866 0.2887 <
 CD11> 0 0.2809 0.5231 <
 CD22> 0 0.2809 0.5231 <
 CSWL> ign <
 CTMB> ign <
!++++++++++++++++++++++++++++++++++++++++
 val2 40 1 2.5667 0 180 !NAME VDIA VSTRAN VSTRLF VLASH VTMNG
 THET> -90 -60 0 30 <
 LIFT> 0 2.63 2.63 0 <
 L/DI> 0 0.1155 0.2887 <
 CD11> 0 0.2948 0.5497 <
 CD22> 0 0.2948 0.5497 <
```

```
CSWL> ign <
CTMB> ign <

|===COMPONENT OBJECTS=====================================================================

EndEnvFixed-----------------------------------------------------------[4.2.0]
|NAME PTCini PTYPE
 exh-env ptambexh total
 int-env ptambint total

EngCylinder-----------------------------------------------------------[4.2.1]
|NAME CYLSTART CYLGEOM PTCini PTCvolef FLOW HEATTR TWAL COMB COMBcopy SCAV OUTPUT
 cylinder [ivc] cylg1 ptivc ptvolef flw1 htr1 tw1 cmb1 ign ign last
Engine----------------------------------------------------------------[4.2.0]
|NAME ENGTYP NCYLS CONFIG VANGLE SPLDOPT RPM LOADTRQ FWINER INSTTRQ FRIC ANGSTRT
 engn1 4-stroke 1 in-line ign speed [rpm] ign ign off fric1 [ivc]
|CYLINDER# FINTRVL CYLGEOM CYLCSLD
 1 0 cylg1 ign

Pipe------------------------------------------------------------------[4.2.0]
|NAME D1 D2 PIPEL DXP CFR CHT CP1 CP2 HEATC FLEXW PTCini TWAL UI PNUM
 pepipe 32 32 76 80 0 2 0 0 ign ign ptambexh 470 0 1
 pipipe 36 36 60 50 0 2 0 0 ign ign ptambint 350 0 1

|===CONNECTION OBJECTS====================================================================

InjectorConn----------------------------------------------------------[4.2.0]
|NAME TYPE PRFNAME DRIVER ENGINE DIST1 DIST2 #INJ MRATIO TEMPINJ FUELLIQ FUELVAP FVAP
LCONTROL SMOKELIM
 injector proffx injprf * engn1 ign ign ign ign [tfuel] fuelli fuelg 0 ign ign
OrificeConn-----------------------------------------------------------[4.2.0]
|NAME ONUM PLUG DIA CD1 CD2 LCONTROL HEATCC
ValveConn-------------------------------------------------------------[4.2.1]
|NAME ONUM VALNAME CMPCAM CMPENG PAIR# HEATCC
 vi1 1 val1 * engn1 ign ign
 ve1 1 val2 * engn1 ign ign

|===PARTS/MAP=============================================================================

PartsList-------------------------------------------------------------------
|PART# TEMPLATE OBJECT NAME OVERRIDES
 65544 EngCylinder cylinder cylinder
 65545 Engine engn1 engine
 65556 EndEnvFixed exh-env exh-en1
 65548 EndEnvFixed exh-env exh-en2
 65549 EndEnvFixed int-env int-en1
 65547 EndEnvFixed int-env int-en2
 65554 Pipe pepipe pepipe1
 65539 Pipe pepipe pepipe2
 65551 Pipe pipipe pipipe1
 65540 Pipe pipipe pipipe2

 SystemMap-------------------------------------------------------------------
|PART# TEMPLATE OBJECT CMP1 CMP2 NAME OVERRIDES
 65550 OrificeConn def 65549.1 65551.1 1
 65538 OrificeConn def 65547.1 65540.1 2
 65555 OrificeConn def 65554.2 65556.1 4
 65541 OrificeConn def 65539.2 65548.1 5
 65546 EngCylConn ign 65544.5 65545.1 crnk
 65553 ValveConn ve1 65544.4 65554.1 eval1 CMPCAM=1
 65542 ValveConn ve1 65544.3 65539.1 eval2 CMPCAM=1
```

65557 InjectorConn injector 65544.0 ign injector DRIVER=1
65552 ValveConn vi1 65551.2 65544.1 ival1 CMPCAM=1
65543 ValveConn vi1 65540.2 65544.2 ival2 CMPCAM=1

|===RUN CASES==========

Parameters----------

activa-temp=3500 breakup-mult=0.8 comb-mult=1.4 CRatio=20 delay-mult=1 delay-press-exp=-1.25
drop-evap-mult=1 edriver=partc entmultaf=0.5 entmultbe=1.2 entmultimp=1.2 file1=<0909#5.prn>
file2=<0909#5.prn> file3=<0909#5h.prn> file4=<0909#5h.prn> fuelg=<dieselg.prp> fuelli=<dieselli.prp>
fuelmass=11.5
h2o=0 ic-eo=442 imap=1.14 imat=355 inj-close-press=250 inj-duration=9
inj-mid-press1=500 inj-mid-press2=500 inj-mid1=2 inj-mid2=2.1 inj-open-press=400 ivc=-139
n2=0.767 ncyc=1 o2=0.233 rpm=2400 rswirl=1 smd-mult=0.7
SOI=-3 tboil10=490 tboil50=542 tboil75=562 tfuel=340

End----------

Appendix D Pyrolysis oil heat of vaporization estimate

For modeling purposes presented in Chapter 5, an estimate of the heat of vaporization was needed, particularly to examine the impact of water on vaporization, ignition, and combustion. Because the composition of the oils is unknown beyond broad classifications of compounds—acids, aldehydes and ketones, alcohols, hydrocarbons, furans—heats of vaporization of representative compounds within each of these classes were arithmetically averaged, as given in the table below. This procedure was adequate for the purpose at hand because the heat of vaporization of water is many times greater than that of most liquids, and as a result it dominates the heat of vaporization of the mixture for the quantities of water present in the pyrolysis oils. The heat of vaporization versus water content is plotted below, with +/- the standard deviation of the averaged heats of vaporization. Note that this is an "effective" heat of vaporization which will give the correct net energy balance for a packet of fuel once vaporization is complete. The instantaneous value actually varies over the droplet lifetime.

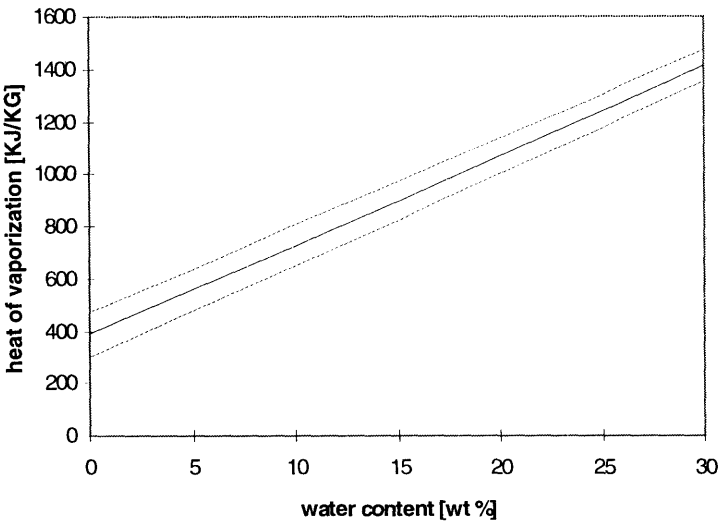

Compound	Heat of Vaporiz cal/g	KJ/KG
Acids		
acetic	96	402
butryic	114	477
formic	119	498
acetal	66	276
Aldehydes and Ketones		
acetaldehyde	136	569
benzaldehyde	86	360
salicylaldhyde	75	314
butyl methyl keto	82	343
diethylamine	91	381
ethyl methyl	105	439
isopropyl methyl	89	372
methyl amyl	83	347
methyl hexyl	74	310
Alcohols		
ethanol		
Hydrocarbons		
min		200
max		400
Furans		
furfaral	107	448
furane	95	397
Phenols		
phenol	103	431
Average		387
Standard Deviation		86